Spring 3-28-2013

Optimal Control of Weakly Forced Nonlinear Oscillators

Isuru Sammana Dasanayake
Washington University in St. Louis

WASHINGTON UNIVERSITY IN ST. LOUIS

School of Engineering and Applied Science

Department of Electrical and Systems Engineering

Thesis Examination Committee:
Jr-Shin Li, Chair
Dennis Barbour
Humberto Gonzalez
Istvan Kiss
Hiro Mukai
Heinz Schaettler

Optimal Control of Weakly Forced Nonlinear Oscillators

by

Isuru Sammana Dasanayake

A dissertation presented to the Graduate School of Art and Sciences
of Washington University in partial fulfillment of the
requirements for the degree of

DOCTOR OF PHILOSOPHY

May 2013
Saint Louis, Missouri

Contents

List of Figures

List of Tables

Acknowledgments

I would like to take this opportunity to express my gratitude to my advisor Professor Jr-Shin Li for his invaluable guidance, advice, and support. Throughout this work he was consistently provided me the opportunities, encouragement and support what grow my interest in researcher. Without his academic and financial support, this dissertation would not been possible.

I would like to thank my dissertation committee members for their time and effort as well as the rest of the Electrical and Systems Engineering faculty. It is a privilege to have studied under such talented teachers and researches. I thank our collaborators, Dr. Istvan Kiss and his team, at Saint Louis University for valuable experiment that he did in this labs to demonstrate our theoretical results and for fruitful discussions.

I also like to thank former and present members of our research group, in particular Justin Ruths, Anatoly Zlotnik, Ji Qi, Nathan Selling, Wei Zhang, Dionisis Stefanatos and Daniel McGibney for their support and helpful discussion. My special thanks goes to the Engineering Communication Center at Washington University for their helpful comments in editing this dissertation.

Last but not least, I express my heartfelt gratitude to my wife, daughter, parents, brothers, relatives and friends for their guidance, support and encouragement.

Isuru Sammana Dasanayake

Washington University in Saint Louis
May 2013

Dedicated to my family.

ABSTRACT OF THE DISSERTATION

Optimal Control of Weakly Forced Nonlinear Oscillators

by

Isuru Sammana Dasanayake

Doctor of Philosophy in Electrical Engineering

Washington University in St. Louis, 2013

Research Advisor: Professor Jr-Shin Li

Optimal control of nonlinear oscillatory systems poses numerous theoretical and computational challenges. Motivated by applications in neuroscience, we develop tools and methods to synthesize optimal controls for nonlinear oscillators described by reduced order dynamical systems. Control of neural oscillations by external stimuli has a broad range of applications, ranging from design of oscillatory neurocomputers to deep brain stimulation for Parkinsons disease. In this dissertation, we investigate fundamental limits on how neuron spiking behavior can be altered by the use of an external stimulus (control). Pontryagins maximum principle is employed to derive optimal controls that lead to desired spiking times of a neuron oscillator, which include minimum-power and time-optimal controls. In particular, we consider practical constraints in such optimal control designs including a bound on the control amplitude and the charge-balance constraint. The latter is important in neural stimulations used to avoid from the undesirable effects caused by accumulation of electric charge due to external stimuli. Furthermore, we extend the results in controlling a single neuron and

consider a neuron ensemble. We specifically, derive and synthesize time-optimal controls that elicit simultaneous spikes for two neuron oscillators. Robust computational methods based on homotopy perturbation techniques and pseudospectral approximations are developed and implemented to construct optimal controls for spiking and synchronizing a neuron ensemble, for which analytical solutions are intractable. We finally validate the optimal control strategies derived using the models of phase reduction by applying them to the corresponding original full state-space models. This validation is largely missing in the literature. Moreover, the derived optimal controls have been experimentally applied to control the synchronization of electrochemical oscillators. The methodology developed in this dissertation work is not limited to the control of neural oscillators and can be applied to a broad class of nonlinear oscillatory systems that have smooth dynamics.

Chapter 1

Introduction

Oscillation is a phenomenon that can be observed in various natural and engineered complex systems. Control of oscillatory dynamics has numerous applications in different fields ranging from systems biology to quantum physics. These complex systems often require an optimal hierarchical organization and dynamical structure, such as synchrony, for normal operation and are extensively studied in science and engineering [123]. Examples include neural circuitry in the brain [132], sleep cycles and metabolic chemical reaction systems in biology [48, 89, 30, 99], semiconductor lasers in physics [34], and vibrating systems in mechanical engineering [5]. Cutting-edge technologies in science and engineering rely on modeling, analyzing, controlling and optimizing these increasingly complex dynamical systems. The complexity of these systems has reached a level that is beyond human comprehension, and hence, existing control theory has been pushed to the limits of its facility for analyzing and designing these complicated dynamical systems. The large scale and nonlinearity of these systems poses serious theoretical and computational challenges. Therefore, development of new theoretical and computational methods that are capable of dealing with these complex systems are essential in many of today's practical applications such as neurological treatment of Parkinson's disease and epilepsy in neuroscience [3, 4, 117], application of optimal waveforms for the entrainment of weakly forced oscillators that maximize the locking range for a given frequency entrainment range in electrochemistry [50, 139], and control of the time-scale adjustment of the circadian systems to light in biology [136].

In this dissertation, we focus on the optimal control of nonlinear oscillatory systems motivated by emerging applications in neuroscience, electrochemistry, and biology.

We capture the dynamics of nonlinear oscillators by the phase models and derive the optimal inputs for driving them between desired initial and final conditions using the optimal control theory. The dissertation is organized as follows. In Chapter 1, we give some motivating applications for optimal control of neurological oscillators and a brief introduction to oscillatory neurological systems. In the latter part of the chapter, we present how phase models are constructed and reduced from full state-space dynamical models. In Chapter 2, we derive minimum-power controls for spiking neuron oscillators, based on phase models, at specified time instances with both bounded and unbounded controls. In Chapter 3 and 4, we derive charge-balanced minimum-power and time-optimal controls for generic phase oscillators and present several examples to validate our results. The charge-balanced constraint which eliminates the net electrical charge accumulation due to external stimuli, is important in neurological applications to avoid harmful side effects. In Chapter 5, we present more challenging optimal control problems that involve both coupled and uncoupled ensembles of neuron oscillators. We start with a two-neuron system and use geometric techniques to synthesize optimal control inputs. We develop a robust computational method based on homotopy perturbation [51] for construction of optimal controls that elicit simultaneous spiking of a neuron ensemble, which is analytically intractable. We compare the derived optimal controls with pseudospectral method. Finally in Chapter 6, we give concluding remarks for this work and point out some future research directions.

1.0.1 Motivating Remarks

Control of neurons by external current stimuli has received increased scientific attention in recent years for its wide range of applications, from the design of oscillatory neurocomputers to Deep Brain Stimulation (DBS). In these applications efficient manipulation of the dynamics of neuron population such as synchrony and desynchrony is compelling.

Deep Brain Stimulation

DBS is a widely practiced therapeutical procedure for several neurological disorders such as Parkinson's disease, essential tremor, and dystonia [4, 87]. Involuntary tremors in head and limbs, which is caused by the pathological synchronization of motor control neurons in the basal ganglia and thalamus regions, are common symptoms in these diseases [18]. In DBS, a series of electrical pulses are applied to inhibit pathological synchrony among these neurons through surgically implanted electrodes [85, 93]. In recent years researchers have extensively studied the engineering problems in DBS, especially the problems related to synchronization and desynchronization phenomena. For example, a system of noisy coupled phase oscillators are studied, and a demand-controlled deep-brain double-pulse stimulation has been suggested to desynchronize when synchronization occurs [128]. As an alternative approach, nonlinear delay feedback control has been used to achieve desynchronization or synchronization for systems of globally coupled limit-cycle oscillators [69].

Motivated by DBS, we employ the control theory to investigate the optimal strategies of controlling a neural population with the least possible side-effects. Power minimization of the neurological stimulus is performed for several reasons and benefits. Minimum energy is desired in all biological applications to minimize the effects to sensitive biological organs. At the same time, utilization of the minimum-power signals can increase the battery lifetime of the neurological implant. Hence, it has a huge advantage from the patient point of view. Patients do not want to go through the regular surgeries to replace the batteries of the surgical implants, where as they can use the same units for a longer time due to less power consumption.

Cardiac Pacemaker and Electrical Stimulators for Paralyzed Individuals

The cardiac pacemaker and electrical stimulators for generation of motion in paralyzed individuals are other applications which employ electric pulses to stimulate nervous tissues [61]. In cardiac pacemakers design, electric pulses are used to regulate a patient's heart rate [71, 72]. In these applications, neurons among a population are considered as a single oscillator and an external stimulus is used to maintain its

periodic behavior in prescribed tolerance, where power and charge minimization of the external stimulus is critical.

Neurocomputer

The study of thalamo-cortical systems suggests a new architecture for a neurocomputer that consists of oscillators having different frequencies and connected weakly via a common medium forced by an external input [56]. This architecture can be synthesized using voltage control oscillators, optical oscillators, and many other oscillatory systems. The main difference in the neurocomputer over an ordinary computer is its ability to perform simple nonlinear transformations in parallel. This feature enables it to do tasks, such as pattern recognition, that cannot be done efficiently with ordinary computers. Weak thalamic input, having appropriate frequencies in its power spectrum, can dynamically connect any two oscillators, including those that have different frequencies and would be unlinked otherwise [56]. This property gives a mechanism to construct a neurocomputer with required interconnections. Therefore the study of the optimal control of a cluster of neurons gives a systematic way to synthesize neurocomputers with required inter-connections.

Study of the optimal control of neural oscillators also reflect the role of intrinsic neural dynamics in determining the time course of synaptic inputs to which a neuron is optimally tuned to respond [90]. Therefore optimal currents of neural oscillators address the question of how the dynamics of individual neurons determine the processing of synaptic inputs to produce spikes.

Chemical Computing Devices

Similar to neurocomputers, new generation of chemical computing devices that mimics the operation of human brain can be constructed with a network of electrochemical oscillators. A fundamental question in constructing a chemical-computer is how to bring individual chemical oscillators in a small network to a desired condition by global control without destroying their local behavior. Since various network topologies are

easy to construct with electrochemical oscillators, they can be used to experimentally verify the optimal control strategies that we drive for the networks.

Circadian Systems

The design of optimal control on subsequent light exposure may provide a noninvasive method to control rhythms in physiology [89]. This method also can provide a therapeutic approach to time related disorders such as insomnia and bipolar disorder. Finding the optimal control (light schedule) for human circadian rhythm can enhance protocols that are practiced in mitigating jet-lag and improving cognitive functions.

1.0.2 Literature Review of Neural Control

Modeling, analysis and control of neural dynamics have drawn significant attention in scientific community around the world. The early work dates back to the early 1900's, when Lapicque introduced a model for the frog nerve to compare the data he obtained from frog nerve stimulation [77]. This model, based on a simple electrical circuit, lay the foundation for later models of neurons and nervous systems [12]. In the 1950's Hodgkin and Huxley developed a mathematical description of the giant squid axon [52], for which they received the Nobel prize in 1963. Followed by Hodgkin and Huxley's breakthrough discovery, many researchers have come up with different descriptions for neural dynamics. Among them, the work done by Rose and Hindmarsh [109], Fitzhugh and Nagumo [35, 98] and Morris and Lecar [92] are highly cited in the scientific literature and greatly appreciated by the research community. Model reduction techniques such as phase model reduction [86, 76, 11] have been developed to further simplify these models especially when modeling populations of neurons.

These formulations of neurons as dynamical systems enable researchers to identify neuron properties by systems theory. For example, properties such as stability and the existence of periodic solutions for both single neuron oscillators and neural networks have been extensively studied. Also identification of the neural characteristics to ensure asymptotically stable oscillations is made possible by exploring the local stability of a homogeneous network of spiking neurons [40]. Phase models have

been used to analyze the dynamics of coupled and uncoupled neurons. For example, existence, stability, and degeneracy of solutions have been studied for a class of permutation-symmetric globally-coupled phase oscillator networks on N-dimensional tori [10]. Researchers have also perform a probabilistic analysis of repetitively-firing neural populations' responses to simple pulselike stimuli to compute the Phase Response Curve (PRC) associated with various neuron models [11]. A generic three-dimensional bursting neuron model was adapted to model central pattern generator interneurons and slow and fast motoneurons in insect locomotory systems [41]. The phase dynamics of weakly coupled Hodgkin-Huxley neurons that exhibit bistability and out-of-phase locking have been used to show that excitatory coupling can result in an effective inhibition [47]. Phase models have been used to investigate a chain of weakly coupled oscillators and to identify the effects of local changes in frequencies, coupling strengths, and different kind of anisotropy [73].

In recent years, control techniques have been applied to neural systems to perform various tasks. Brain chaos has been controlled by suppressing unstable fixed points in bursting neural networks, which increases the periodicity of the neural population [117]. Scientists have converted chaotic orbits into desired periodic orbits by using temporally programmed small controls to improve the systems performance against some general classes of criteria [24]. Using multilinear feedback techniques, researchers have controlled the individual phase relationship between coupled oscillators [63]. The singular perturbation method and averaging theory have been used to show the difficulty of achieving synchrony in type I neuron models, which have strictly positive PRCs [28]. Optimal controls of neuronal spiking activity for neurons receiving a class of random synaptic inputs and optimal variances are found for the diffusion process approximating an integrate and fire model such as Hodgkin-Huxley model [33]. The optimal variance obtained by this method sets the lowest possible bound in controlling the stochasticity of neuronal activity [33]. The influence of the spiking rate and the stimulus duration on noraderneric neurons has also been explored [11]. Synchronization engineering techniques have been applied to tune complex dynamical structures in phase models of oscillators [69]. Optimal control theory such as Euler-Lagrange equations has been applied for phase model dynamics to synthesize minimum-power controls to change the rate of their periodic behavior [90].

1.1 Neurological Oscillators

Neurons are biological cells that are capable of generating, transmitting and processing electrical signals. There are about 10^{11} neurons in human brain that are responsible for all of the brain functions such as vision, hearing and motor control. Neurons exhibit short-lasting voltage spikes known as action potentials, which are sensitive to external current stimuli [60]. The inter-spike time interval of a neuron characterizes its properties and can be controlled by an external current stimuli. A neuron often fires periodically when it is injected with a constant current [31]. Spiking behavior of neurons are captured by various mathematical models. Here we present two well-popular neuron models namely Hodgkin-Huxley and Morris-Lecar that we used in our calculations. We choose the parameter values of these neuron models to exhibit stable periodic motions.

1.1.1 Hodgkin-Huxley Model

The Hodgkin-Huxley model is a four dimensional system that describes the propagation and initiation of the action potential in squid axon [52]. The dynamics of the Hodgkin-Huxley neuron are described by a set of differential equations

$$
\begin{aligned}
C\dot{V} - I &= -g_{Na}h(V - V_{Na})m^3 - g_k(V - V_K)n^4 - g_L(V - V_L) \\
\dot{m} &= a_m(V)(1 - m) - b_m(V)m \\
\dot{h} &= a_h(V)(1 - h) - b_h(V)h \\
\dot{n} &= a_n(V)(1 - n) - b_n(V)n \\
a_m(V) &= 0.1(V + 40)/[1 - \exp(-(V + 40)/10)] \\
b_m(V) &= 4\exp[-(V + 65)/18] \\
a_h(V) &= 0.07\exp[-(V + 65)/20] \\
b_h(V) &= 1/(1 + \exp[-(V + 35)/10)] \\
a_n(V) &= 0.01(V + 55)/[1 - \exp(-(V + 55)/10)] \\
b_n(V) &= 0.125\exp[-(V + 65)/80],
\end{aligned}
$$

where V, I and C are the membrane voltage, current and capacitance per unit area respectively. Parameters g_{Na}, g_k and g_l denote the potassium, sodium and leak conductance per unite area, and V_K, V_{Na} and V_l denote the potassium, sodium and leak reversal potentials respectively. Variables m, h and n are called gating variables which determine the propagation rate of the action potential. We choose the following parameter values for this system which give rise to stable periodic orbit.

$$\begin{array}{lll} V_{Na} = 50\ mV, & V_k = -77\ mV, & v_L = -54.4\ mV, \\ g_{Na} = 120\ mS/cm^2, & g_k = 36\ mS/cm^2, & g_L = 0.3\ mS/cm^2, \\ C = 1\ \mu F/cm^2, & I = 10\ \mu A/cm^2. & \end{array}$$

1.1.2 Morris-Lecar Model

The Morris-Lecar model was originally proposed to capture the oscillating voltage behavior of giant barnacle muscle fibers [92]. Over the past years this model has been extensively studied and used as a standard model for representing many different real neurons that are experimentally observable. The dynamics of the Morris-Lecar neuron is described by

$$\begin{aligned} C\dot{V} - I &= g_{Ca} m_\infty (V_{Ca} - V) + g_K \omega (V_k - V) + g_L (V_L - V) \\ \dot{\omega} &= \phi(\omega_\infty - w)/\tau_\omega(V) \\ m_\infty &= 0.5[1 + \tanh((V - V_1)/V_2)] \\ \omega_\infty &= 0.5[1 + \tanh((V - V_3)/V_4)] \\ \tau_\omega &= 1/\cosh[(V - V_3)/(2V_4)], \end{aligned}$$

where V and C represent the membrane voltage and conductance per unit area. I is the applied current. Parameters g_L, g_{Ca} and g_K are the maximum or instantaneous conductance value for leak, Ca, and K pathways respectively. V_K, V_{Ca} and V_L denotes the potassium, sodium and leak reversal potentials and ω is the recovery variable, which is almost equal to the normalized K ion conductance. Parameters m_∞ and ω_∞ are the faction of open Ca and K channels at steady state. V_1 and V_3 are potential at which $m_\infty = \omega_\infty = 0.5\ mV$. V_2 and V_3 are the reciprocal of slope of voltage dependence of m_∞ and ω_∞. The time constant for the K channel relaxation in response to changes of voltage is given by τ_ω. We consider the following parameter

values for our calculations in proceeding chapters.

$$\begin{array}{lll} \phi = 0.5, & I^b = 0.09\ \mu A/cm^2, & V_L = -0.01\ mV, \\ v_2 = 0.15\ mV, & V_3 = 0.1\ mV, & v_4 = 0.145\ mV, \\ g_{Ca} = 1\ mS/cm^2, & V_k = -0.7\ mV, & V_L = -0.5\ mV, \\ g_k = 2\ mS/cm^2, & g_L = 0.5\ mS/cm^2, & C = 1\ \mu F/cm^2. \end{array}$$

1.2 Phase Models for Oscillatory Systems

In systems theory, a nonlinear oscillator is described by a set of ordinary differential equations that have a stable periodic orbit. This system of equations can be reduced to a single first order differential equation, which is valid, while the state of the full system remains in a neighborhood of its unforced periodic orbit [11]. This reduction allows us to represent the dynamics of a weakly forced oscillator by a single phase variable that defines the evolution of the oscillation. Consider a time-invariant system $\dot{x} = f(x, I)$, where $x(t) \in \mathbb{R}^n$ is the state and $I(t) \in \mathbb{R}$ is the control, which has an unforced stable attractive periodic orbit $\gamma(t) = \gamma(t + T)$ homeomorphic to a circle, satisfying $\dot{\gamma} = f(\gamma, 0)$. We can represent this system in a phase-reduced form as

$$\dot{\theta} = f(\theta) + Z(\theta)I(t), \tag{1.1}$$

where θ is the phase variable, f and Z are real-valued functions, and $I(t) \in \mathbb{R}$ is the control [11, 60]. One complete oscillation of the system corresponds to $\theta \in [0, 2\pi)$. The function f gives system's baseline dynamics and Z is known as the PRC, which describes the infinitesimal sensitivity of the phase to an external control input. In the case of neural oscillators, I represents an external current stimulus and f is referred to the instantaneous oscillation frequency in the absence of any external input, i.e., $I = 0$. Neuron spiking occurs when the oscillator evolves through one complete cycle. As a convention, the occurrence of spikes takes place at $\theta = 2n\pi$, where $n = 0, 1, 2, \ldots$.

1.2.1 Phase Model Reduction of Nonlinear Oscillator

By definition, phase is an abstract variable used to define the evolution of the oscillation. Many types of physical, chemical, and biological oscillators can be described by a phase dynamics. Generally, the phase of the neural oscillator is defined by the time since the last spike. Phase map maps one period of the oscillation $i.e.[0, T)$ to the interval $[0, 2\pi)$. Figure 1.1 illustrates the phase map for the Hodgkin-Huxley neuron model given in Section 1.1.1.

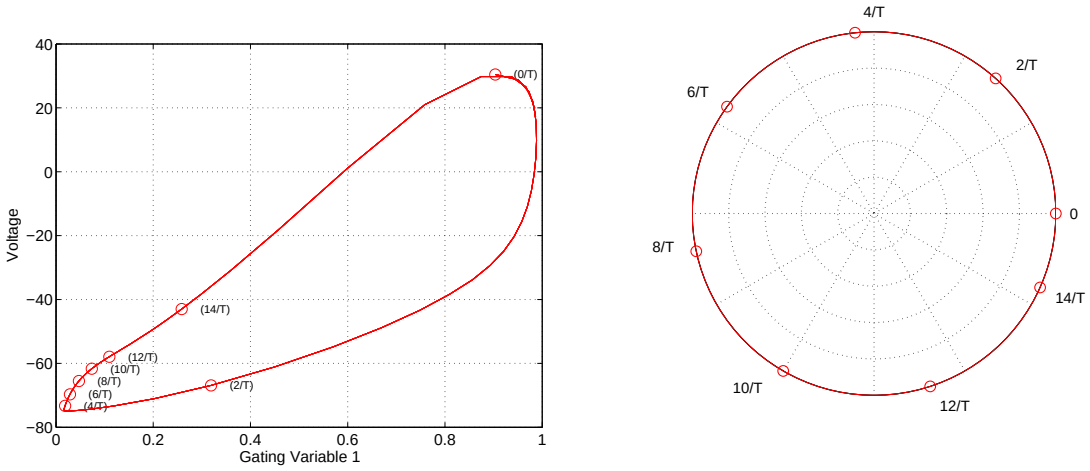

(a) (b)

Figure 1.1: (a) Periodic orbit of the Hodgkin-Huxley model, (b) Phase map of the Hodgkin-Huxley model

1.2.2 Isochrons

The definition of the phase given in 1.2.1 works for oscillators when their state is in the periodic orbit, but when controlling the oscillations, it is necessary to define the phase of the oscillation in the neighborhood of the periodic orbit. This is done by defining the isochrons. Isochrons characterize the points in the state-space which have same asymptotic phase. We denote the isochron through a point $x \in \gamma$ as $N(x)$. Isochrons are local invariant sections; that is, for a point $y \in N(x)$, $x(T, y) = y' \in N(x)$. The map $y \to y'$ is a Poincare map for the limit cycle which takes time exactly T to return. The existence of isochrons allows us to define the phase of any point in

the neighborhood of the limit cycle [31]. In practice isochrons are usually calculated numerically.

1.2.3 Phase Response Curve

Phase response curve describes the infinitesimal sensitivity of the phase to an external control input. This function can be calculated by applying weak stimulus to perturb the state of the system at selected points on the periodic orbit. Application of a stimulus at phase ϕ of a the oscillator perturb its vector field and assign a new phase ϕ'. This new phase value can be calculated by using isochrons. For each phase ϕ at which the stimulus is applied, we get a new phase ϕ'. The change of the phase at each point as function of the phase, that the stimulus has been applied, is given by

$$\Delta(\phi) = \phi' - \phi.$$

This function defines the phase response curve or phase resetting curve. Typically, for neurons, both in experiments and in numerical simulation, the phase change is measured by the time of the next event. Suppose at phase ϕ, we give an external stimulus which changes the time for the next spike form T to T'. Then the PRC can be defined as $\Delta(\phi) = T' - T$. Usually, phase is normalized to be in the range of 0 to 2π. Therefore, we multiply the PRC by factor $2\pi/T$. Figure 1.2 and 1.3 shows the numerically calculated PRCs for Hodgkin-Huxley and Morris-Lecar neuron models given in Section 1.1.1 and 1.1.2. There exist some analytical methods to calculate PRC developed By Kuramato and Malkins. It has been shown that the PRC is the solution to the adjoint equation obtained from linearizing the state-space oscillatory system in its periodic orbit[86].

1.2.4 Canonical Phase Models

In this section, we introduce both analytically derived and numerically calculated phase models for some commonly used neural oscillatory models. These models are used throughout the dissertation to synthesize different optimal control strategies.

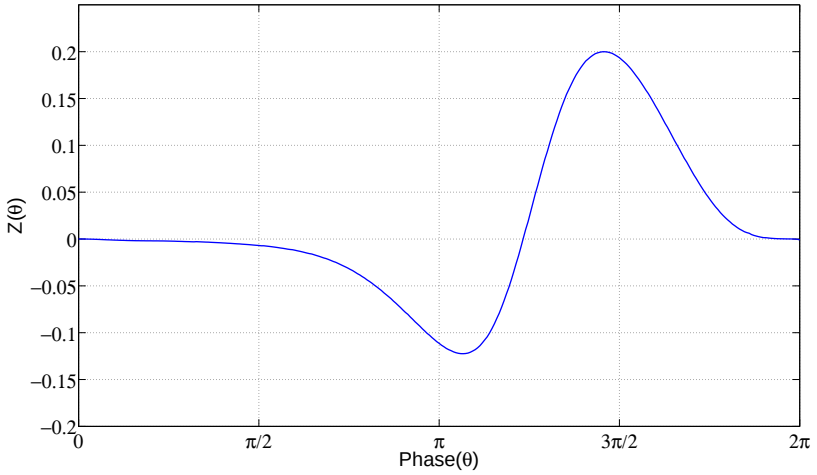

Figure 1.2: The Hodgkin Huxley PRC for the parameters given in Section 1.1.1

Sinusoidal Phase Model

Consider the nondimensionalized following system with sinusoidal PRC,

$$\dot{\theta} = \omega + z_d \sin\theta \cdot I(t), \tag{1.2}$$

where ω is the natural oscillation frequency of the neuron and z_d is a model-dependent constant. The neuron described by this phase model spikes periodically with the period $T = 2\pi/\omega$ in the absence of any external input, i.e., $I(t) = 0$. Note that this type of PRC's with both positive and negative regions can be obtained by periodic orbits near the super critical Hopf bifurcation[11]. This type of bifurcation occurs for Type II neuron models like the Fitzhugh-Nagumo model [64].

SNIPER Phase Model

The SNIPER PRC is derived for neurons near a SNIPER bifurcation (i.e., a saddle-node bifurcation of a fixed point on a periodic orbit) which is found for Type I neurons [28] like the Hindmarsh-Rose model [109]. Similar to sinusoidal phase model, the SNIPER phase model is given by

$$\dot{\theta} = \omega + z_d(1 - \cos\theta)I(t). \tag{1.3}$$

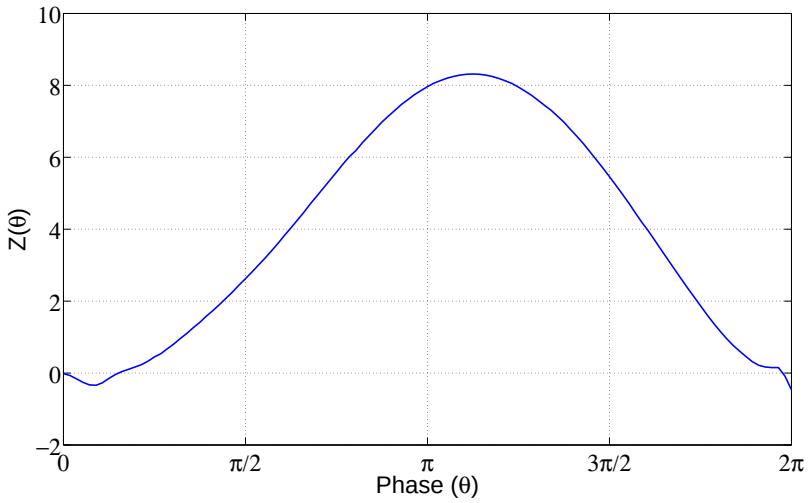

Figure 1.3: The Morris-Lecar PRC for the parameters given in Section 1.1.2

where $\omega > 0$ is the natural frequency of the oscillation and $z_d > 0$ is a model-depended constant.

Theta Phase Model

The theta neuron phase model is defined by $f(\theta) = 1 + \cos\theta + (1 - \cos\theta)I_b$ and $g(\theta) = (1 - \cos\theta)$, where I_b is the neuron baseline current [90]. If $I_b > 0$, then the neuron spikes periodically with the period $T_0 = \pi/\sqrt{I_b}$ in the absence of any external current $I(t)$. When $I_b \leq 0$, the neuron does not spike autonomously but it can be fired by the use of an input $I(t)$. Note that when $I_b > 0$, this neuron model can be transformed to the SNIPER phase model by a coordinate transformation [90].

Hodgkin-Huxley Phase Model

For the set of parameter values given in Section 1.1.1, the Hodgkin-Huxley neuron system exhibits periodic motion with natural frequency $\omega = 0.43\, rad/ms$. The phase model of the Hodgkin-Huxley neuron model is given by

$$\dot{\theta} = \omega + Z(\theta)I(t) \tag{1.4}$$

where ω is the natural frequency of the oscillation and the PRC, $Z(\theta)$ is given in Figure 1.1.1.

Morris-Lecar Phase Model

Similar to Hodking-Huxley phase model, the phase model of the Morris-Lecar neuron [92] is given by (1.4). It has the natural frequency of 0.283 rad/ms for the parameters given in Section 1.1.2 and its PRC is depicted in Figure 1.3. It has been observed through experiments that the PRC for an Aplysia motoneuron is extremely similar to that of a Morris-Lecar PRC [38].

Chapter 2

Minimum-Power Controls for Spiking Neuron Oscillators

In this chapter, we study optimal control problems of spiking neurons whose dynamics are described by a phase model. We design minimum-power current stimuli (controls) that lead to targeted spiking times. In particular, we consider bounded control amplitude and characterize the range of possible spiking times determined by the bound which can be chosen sufficiently small within the range that the phase model is valid. We show that for a given bound, the corresponding feasible spiking times are optimally achieved by piecewise continuous controls. We present analytic expressions with numerical simulations of the minimum-power stimuli for several phase models. We demonstrate the applicability of our method by experimentally verifying the derived control laws with chemical oscillators.

2.1 Introduction

Control of neurons and hence the nervous system by external current stimuli (controls) has received increased scientific attention in recent years for its wide range of applications from deep brain stimulation to oscillatory neurocomputers [132, 101, 56]. Conventionally, neuron oscillators are represented by phase-reduced models, which form a standard nonlinear system [11, 135]. Intensive studies using phase models have been carried out, for example, on the investigation of the patterns of synchrony that result from the type and architecture of coupling [3, 130] and on the response of large groups of oscillators to external stimuli [90, 128], where the inputs to the neuron

systems were initially defined and the dynamics of neural populations were analyzed in detail.

Recently, control theoretic approaches have been employed to design external stimuli that drive neurons to behave in a desired way. For example, a multilinear feedback control technique has been used to control the individual phase relation between coupled oscillators [63] and geometric control theory has been adopted to study controllability and optimal control of a network of neurons with different natural oscillation frequencies [84]. There has been an increase in the demand for controlling not only the collective behavior of a network of oscillators but also the behavior of each individual oscillator. It is feasible to change the spiking periods of oscillators or tune the individual phase relationship between coupled oscillators by the use of electric stimuli [117, 63]. Minimum-power stimuli that elicit spikes of a neuron at specified times close to the natural spiking time were analyzed [90]. Optimal waveforms for the entrainment of weakly forced oscillators that maximize the locking range have been calculated, where first and second harmonics were used to approximate the phase response curve (PRC) [49]. These optimal controls were found mainly based on the calculus of variations, which restricts the optimal solutions to the class of smooth controls and the bound of the control amplitude was not taken into account.

In this chapter, we apply techniques from optimal control theory to derive minimum-power controls that spike a neuron at desired time instants. We consider bounded control amplitude and fully characterize the range of feasible spiking times determined by the bound. In particular, our optimal control strategies are general so that the bound can be chosen sufficiently small within the range that the PRC is valid. The design of such minimum-power stimuli to elicit spikes of neuron oscillators is also of clinical importance, notably in deep brain stimulation therapy for Parkinson's disease and essential tremor [4], where mild stimulations are required. In addition, interest of reducing the energy consumption in neurological implants such as cardiac pacemakers makes such optimal designs imperative.

This chapter is organized as follows. In Section 1.2, we introduce the phase model for spiking neurons and formulate the related optimal control problem. In Section 2.3, we derive minimum-power controls associated with specified spiking times in the absence and presence of control amplitude constraints, in which various phase models,

including sinusoidal PRC, SNIPER PRC, and Morris-Lecar PRC, are considered. In addition, we present examples and simulations to demonstrate the resulting optimal control strategies. Finally in Section 2.4, we experimentally apply the derived control laws to chemical oscillators to change their frequency to desired value.

2.2 Optimal Control Problem Formulation

A periodically spiking or firing neuron can be considered as a periodic oscillator governed by the nonlinear dynamical equation of the form (1.1) This nonlinear dynamical system is referred to as the phase model for the oscillation. The assumption that $Z(\theta)$ vanishes only on isolated points and that $f(\theta) > 0$ are made so that a full revolution of the phase is possible. By convention, neuron spikes occur when $\theta = 2n\pi$, where $n \in \mathbb{N}$, e.g., $\theta = 0$ or 2π. In the absence of any input $I(t)$, the neuron spikes periodically with period T at its natural frequency, while the spiking time can be advanced or delayed in a desired manner by an appropriate choice of $I(t)$.

In this chapter, we study optimal design of neural inputs that lead to the spiking of neurons at a specified time T_f after spiking at time $t = 0$. In particular, we find the bounded stimulus that fires a neuron with minimum power, which is formulated as the following optimal control problem,

$$\begin{aligned} \min_{I(t)} \quad & \int_0^{T_f} I(t)^2 \, dt \\ \text{s.t.} \quad & \dot{\theta} = f(\theta) + Z(\theta) I(t), \\ & \theta(0) = 0, \quad \theta(T_f) = 2\pi \\ & |I(t)| \leq M, \quad \forall \; t \in [0, T_f], \end{aligned} \tag{2.1}$$

where $M > 0$ is the amplitude bound of the current stimulus $I(t)$. Here, we consider both hyper-polarizing and depolarizing inputs, i.e., $I(t)$ can be positive or negative. If T_f is equal to the natural spiking time, then no input is needed. We first investigate the case when the control amplitude is unbounded, upon which the optimal control with bounded amplitude can be constructed. Note that by applying the control $I(t)$ repetitively we can obtain 1:1 phase locking pattern with specified spiking time.

2.3 Derivation of Minimum-Power Controls

We consider the minimum-power optimal control problem of spiking neurons as formulated in (2.1) for various phase models including both models for type I and type II neurons. Specifically, we examine the examples of sinusoidal PRC, SNIPER PRC, and Morris-Lecar PRC.

2.3.1 Sinusoidal Phase Model

Consider the following system with sinusoidal PRC as described in Section 1.2.4,

$$\dot{\theta} = \omega + z_d \sin\theta \cdot I(t), \tag{2.2}$$

where ω is the natural oscillation frequency of the neuron and z_d is a model-dependent constant.

Spiking Sinusoidal Neurons with Unbounded Controls

The optimal current profile can be derived by Pontryagin's maximum principle [107, 121] (See Appendix A). Given the optimal control problem as in (2.1), we form the control Hamiltonian

$$H = I^2 + \lambda(\omega + z_d \sin\theta \cdot I), \tag{2.3}$$

where λ is the Lagrange multiplier. The necessary optimality conditions give

$$\dot{\lambda} = -\frac{\partial H}{\partial \theta} = -\lambda z_d I \cos\theta, \tag{2.4}$$

and $\frac{\partial H}{\partial I} = 2I + \lambda z_d \sin\theta = 0$. Hence, the optimal current I satisfies

$$I = -\frac{1}{2}\lambda z_d \sin\theta. \tag{2.5}$$

The optimal control problem is then transformed to a boundary value problem, which characterizes the optimal trajectories of $\theta(t)$ and $\lambda(t)$,

$$\dot{\theta} = \omega - \frac{z_d^2 \lambda}{2} \sin^2 \theta, \tag{2.6}$$

$$\dot{\lambda} = \frac{z_d^2 \lambda^2}{2} \sin \theta \cos \theta, \tag{2.7}$$

with boundary conditions $\theta(0) = 0$ and $\theta(T_f) = 2\pi$ while $\lambda(0)$ and $\lambda(T_f)$ are unspecified.

Additionally, since the Hamiltonian is not explicitly dependent on time, the optimal triple (λ, θ, I) satisfies $H(\lambda, \theta, I) = c$, $\forall\, 0 \leq t \leq T_f$, where c is a constant. Together with (2.5), this yields

$$-\frac{z_d^2}{4} \sin^2 \theta \lambda^2 + \omega \lambda = c. \tag{2.8}$$

Since $\theta(0) = 0$, $c = \omega \lambda_0$, where $\lambda_0 = \lambda(0)$, which is undetermined. The optimal multiplier can be found by solving the above quadratic equation (2.8), which gives

$$\lambda = \frac{2\omega \pm 2\sqrt{\omega^2 - \omega \lambda_0 z_d^2 \sin^2 \theta}}{z_d^2 \sin^2 \theta}, \tag{2.9}$$

and then, from (2.6), the optimal trajectory of θ follows

$$\dot{\theta} = \mp \sqrt{\omega^2 - \omega \lambda_0 z_d^2 \sin^2 \theta}. \tag{2.10}$$

Integrating the equation (2.10), we find the spiking time T_f in terms of the initial condition λ_0,

$$T_f = \int_0^{2\pi} \frac{1}{\sqrt{\omega^2 - \omega \lambda_0 z_d^2 \sin^2 \theta}} d\theta. \tag{2.11}$$

Note that we choose the positive sign in (2.10), which corresponds to forward phase evolution. Therefore, given a desired spiking time T_f of the neuron, the initial value, λ_0, corresponding to the optimal trajectory of the multiplier can be found via the one-to-one relation in (2.11). Consequently, the optimal trajectories of θ and λ can be easily computed by evolving (2.6) and (2.7) forward in time. Plugging (2.9) into (2.5), we obtain the optimal feedback law for spiking the neuron at time T_f of the

form

$$I^* = \frac{-\omega + \sqrt{\omega^2 - \omega\lambda_0 z_d^2 \sin^2\theta}}{z_d \sin\theta}, \tag{2.12}$$

where λ_0 is to be calculated according to (2.11).

The feasibility of spiking the neuron at a desired time T_f largely depends on the initial value of the multiplier, λ_0. It is not feasible to have a 2π revolution if $\lambda_0 \geq \omega/z_d^2$. This fact can be seen from Figure 2.1, where the system evolution defined by (2.6) and (2.7) for $z_d = 1$ rad/nC and $\omega = 1$ rad/ms with respect to different λ_0 values ($\theta = 0$ axis) is illustrated. When $\lambda_0 = 0$, the spiking period is equal to the natural spiking period, $2\pi/\omega$, and no external stimulus needs to be applied, i.e., $I^*(t) = 0$, $\forall t \in [0, 2\pi/\omega]$. T_f is a monotonically increasing function of λ_0 for fixed ω and z_d and, the average phase velocity decreases when λ_0 increases, the spiking time $T_f > 2\pi/\omega$ for $\lambda_0 > 0$ and $T_f < 2\pi/\omega$ for $\lambda_0 < 0$. Figure 2.2 shows variation of the spiking time T_f with the λ_0 corresponding to the optimal trajectories for different ω values with $z_d = 1$ rad/nC.

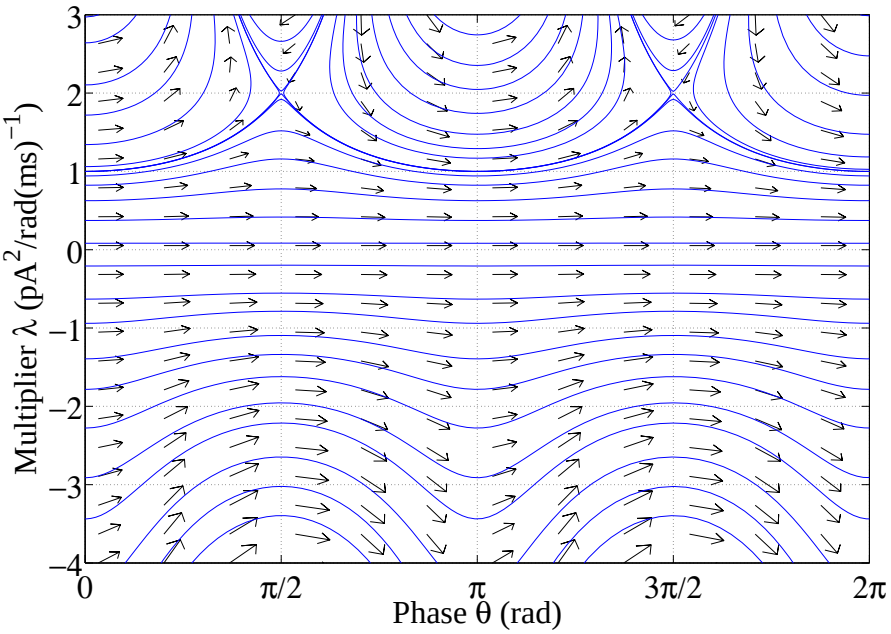

Figure 2.1: Extremals of sinusoidal PRC model with $z_d = 1$ rad/nC and $\omega = 1$ rad/ms

The relation between the spiking time T_f and required minimum energy $E = \min \int_0^{T_f} I^2(t)dt$ is evident via a simple sensitivity analysis [13]. Since a small change

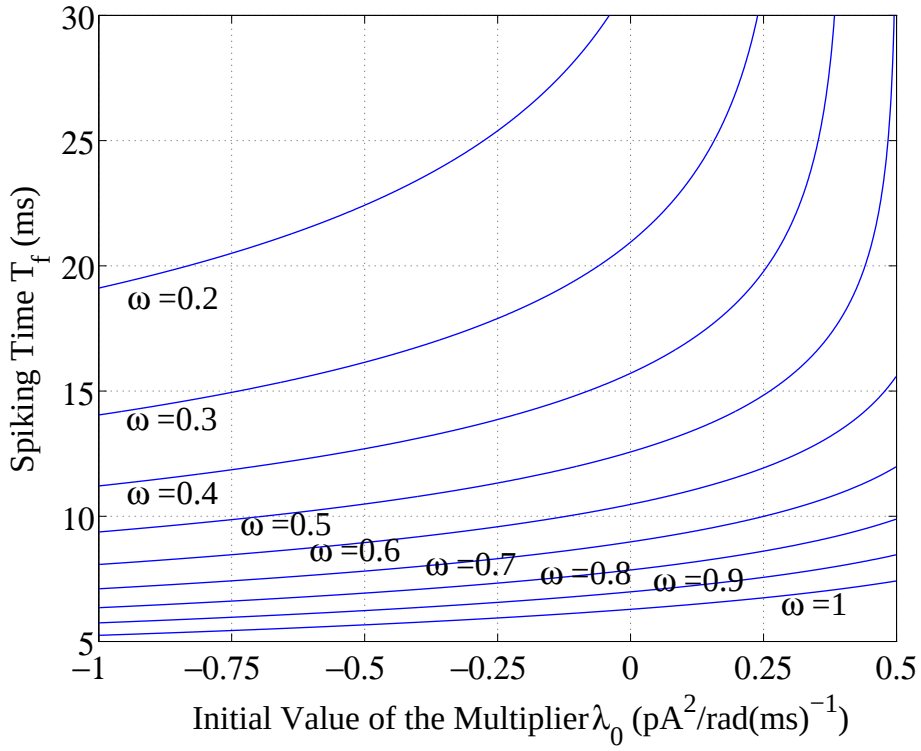

Figure 2.2: Variation of the spiking time, T_f, with respect to the initial multiplier value, λ_0, leading to optimal trajectories, with different values of ω (rad/ms) and $z_d = 1$ rad/nC for sinusoidal PRC model.

in the initial condition, $d\theta$, and a small change in the initial time, dt, result in a small change in power according to $dE = \lambda(t)d\theta - H(t)dt$, it follows that $-\frac{\partial E}{\partial t} = H = c = \omega\lambda_0$ [13]. This implies that E increases with initial time t for $\lambda_0 < 0$ and decreases for $\lambda_0 > 0$. Since the increment of the initial time is equivalent to the decrement of spiking time T_f, $\partial E/\partial T_f = \omega\lambda_0$. Since $\lambda_0 < 0$ ($\lambda_0 > 0$) corresponds to $T_f < 2\pi/\omega$ ($T_f > 2\pi/\omega$), we see that the required minimum energy increases if we move away from the natural spiking time.

The minimum-power stimulus I^* as in (2.12) plotted with respect to time and the phase for various spiking times $T_f = 3, 5, 10, 12$ ms with $\omega = 1$ rad/ms and $z_d = 1$ rad/nC are shown in Figure 2.3(a) and 2.3(b), respectively. The respective optimal trajectories of $\lambda(\theta)$ and $\theta(t)$ for these spiking times are illustrated in Figure 2.4(a) and 2.4(b).

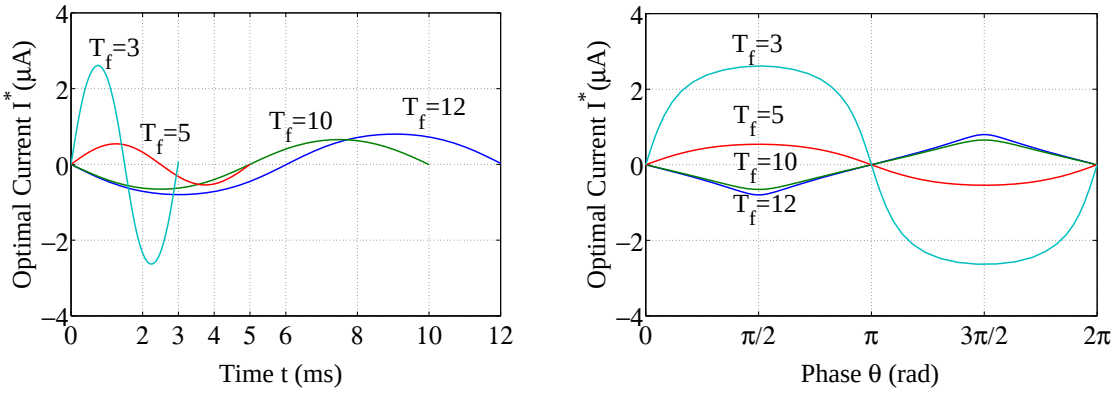

(a) (b)

Figure 2.3: (a) Optimal control for spiking times $T_f = 3, 5, 10, 12$ ms for sinusoidal PRC model with $z_d = 1$ rad/nC and $\omega = 1$ rad/ms, and (b) variation of the optimal control with phase θ for the same spiking times.

Spiking Sinusoidal Neurons with Bounded Controls

In practice, the amplitude of stimuli in physical systems are limited and phase models are valid for weak inputs, hence we consider spiking the sinusoidal neuron with bounded control amplitude, namely, in the optimal control problem (2.1), $|I(t)| \leq M < \infty$ for all $t \in [0, T_f]$, where T_f is the desired spiking time. In this case, there exists a range of feasible spiking periods depending on the value of M, in contrast to the previous case where any desired spiking time is feasible. We first observe that given this bound M, the minimum time it takes to spike a neuron can be achieved by choosing the control that keeps the phase velocity $\dot{\theta}$ maximum over $t \in [0, T_f]$. Such a time-optimal control, for $z_d > 0$, can be characterized by a switching, i.e.,

$$I^*_{Tmin} = \begin{cases} M & \text{for} \quad 0 \leq \theta < \pi \\ -M & \text{for} \quad \pi \leq \theta < 2\pi \end{cases} . \tag{2.13}$$

Consequently, the spiking time with I^*_{Tmin} for $\omega \neq z_d M$ can be computed using (2.2) and (2.13), which yields

$$T^M_{min} = 2\pi \sqrt{\frac{1}{-z_d^2 M^2 + \omega^2}} - \frac{4 \tan^{-1}\left\{ z_d M / \sqrt{-z_d^2 M^2 + \omega^2} \right\}}{\sqrt{-z_d^2 M^2 + \omega^2}}. \tag{2.14}$$

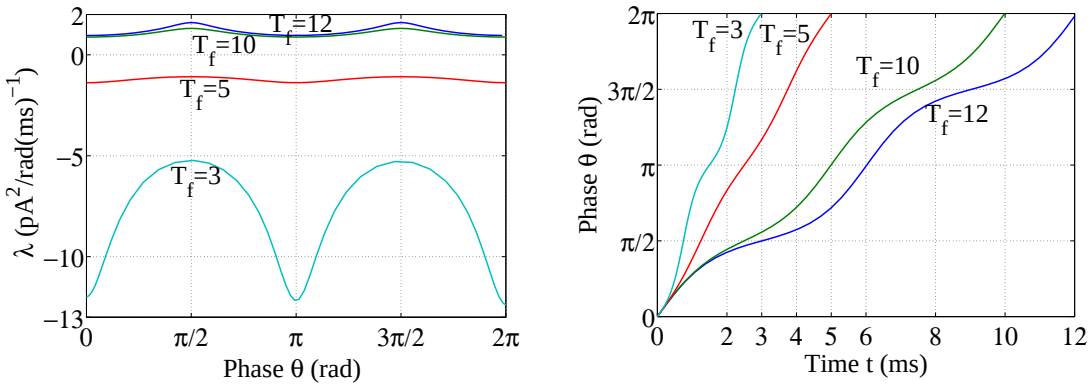

(a) (b)

Figure 2.4: (a) Variation of the optimal multiplier, λ^*, with θ, and (b) optimal phase trajectories following the optimal control for spiking times $T_f = 3, 5, 10, 12$ ms for sinusoidal PRC model with $z_d = 1$ rad/nC and $\omega = 1$ rad/ms.

It follows that I^*, given in (2.12), is the minimum-power stimulus that spikes the neuron at a desired spiking time T_f if $|I^*| \leq M$ for all $t \in [0, T_f]$. However, there exists a shortest possible spiking time by I^* given the bound M.

Simple first and second order optimality conditions applied to (2.12) find that the maximum value of I^* occurs at $\theta = \pi/2$ for $\lambda_0 < 0$ and at $\theta = 3\pi/2$ for $\lambda_0 > 0$ (see Figure.2.5(a)) . According to (2.11), $\lambda_0 = 0$ corresponds to $T = 2\pi/\omega$ and $\lambda_0 < 0$ ($\lambda_0 > 0$) corresponds to $T < 2\pi/\omega$ ($T > 2\pi/\omega$). Therefore, the λ_0 for the shortest spiking time with control I^* satisfying $|I^*(t)| \leq M$ can be calculated by substituting $I^* = M$ and $\theta = \pi/2$ to the equation (2.12), and then from (2.11) we obtain this shortest spiking period $T^{I^*}_{min}$.

$$T^{I^*}_{min} = \int_0^{2\pi} \frac{1}{\sqrt{\omega^2 + z_d M(z_d M + 2\omega)\sin^2(\theta)}} d\theta. \tag{2.15}$$

Since I^* takes the maximum value at $\theta = 3\pi/2$ for $\lambda_0 > 0$, we have $|I^*| \leq (\omega - \sqrt{\omega^2 - \omega\lambda_0 z_d^2})/z_d$, which leads to $|I^*| < \omega/z_d \leq M$ for $\lambda_0 > 0$. This implies that I^* is the minimum-power control for any desired spiking time $T_f > 2\pi/\omega$ when $M \geq \omega/z_d$, and hence for any spiking time $T_f \geq T^{I^*}_{min}$. Shorter spiking times $T_f \in [T^M_{min}, T^{I^*}_{min})$ are feasible but can not be achieved by I^*. Let $T_f \in [T^M_{min}, T^{I^*}_{min})$, then there exist

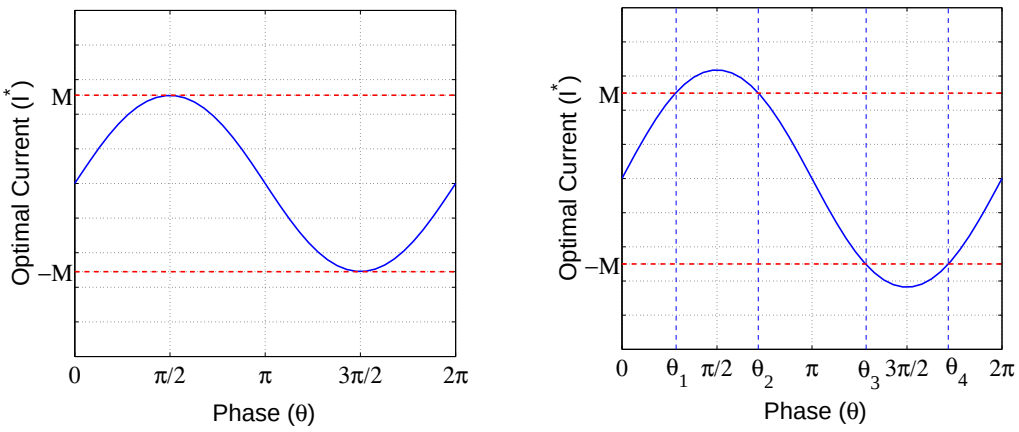

Figure 2.5: (a) An illustration of the optimal control I^* with its maximum value occurring at $\theta = \pi/2$ for $c > 0$, which gives the shortest possible spiking time subject to the control bound M. (b) An illustration of the case when $I^* > M$ with intersections at θ_1, θ_2, θ_3, and θ_4.

two angles $\theta_1 = \sin^{-1}[-2M\omega/(z_d M^2 + z_d\omega\lambda_0)]$ and $\theta_2 = \pi - \theta_1$ where I^* meets the bound M, illustrated in Figure 2.5(b). When $\theta \in (\theta_1, \theta_2)$, $I^* > M$ and we take $I(\theta) = M$ for $\theta \in [\theta_1, \theta_2]$. The Hamiltonian of the system when $\theta \in [\theta_1, \theta_2]$ is, from (2.3), $H = M^2 + \lambda(\omega + z_d \sin\theta\, M)$. If the triple (λ, θ, M) is optimal, then H is a constant, which gives $\lambda = (H - M^2)/(\omega + z_d M \sin\theta)$. This multiplier satisfies the adjoint equation (2.4), and therefore $I(\theta) = M$ is optimal for $\theta \in [\theta_1, \theta_2]$. Similarly, by symmetry, $I^* < -M$ when $\theta \in [\theta_3, \theta_4]$, where $\theta_3 = \pi + \theta_1$ and $\theta_4 = 2\pi - \theta_1$, if the desired spiking time $T \in [T^M_{min}, T^{I^*}_{min})$. It can be easily shown by the same fashion that $I(\theta) = -M$ is optimal in the interval $\theta \in [\theta_3, \theta_4]$. Therefore, the minimum-power optimal control that spikes the neuron at $T_f \in [T^M_{min}, T^{I^*}_{min})$ can be characterized by four switchings between I^* and M as shown in (2.16).

Note that $T^M_{min} < T^{I^*}_{min}$. According to (2.2) when $M \geq \omega/z_d$, arbitrarily large spiking times can be achieved by making $\dot{\theta}$ arbitrary close to zero. Therefore we consider two cases for $M \geq \omega/z_d$ and $M < \omega/z_d$.

Case I: $M \geq \omega/z_d$. Since $|I^*| < \omega/z_d \leq M$ for $\lambda_0 > 0$, I^* is the minimum-power control for any desired spiking time $T_f > 2\pi/\omega$, and hence for any spiking time $T_f \geq T^{I^*}_{min}$. Variation of the maximum value of the control I^* with spiking time T_f

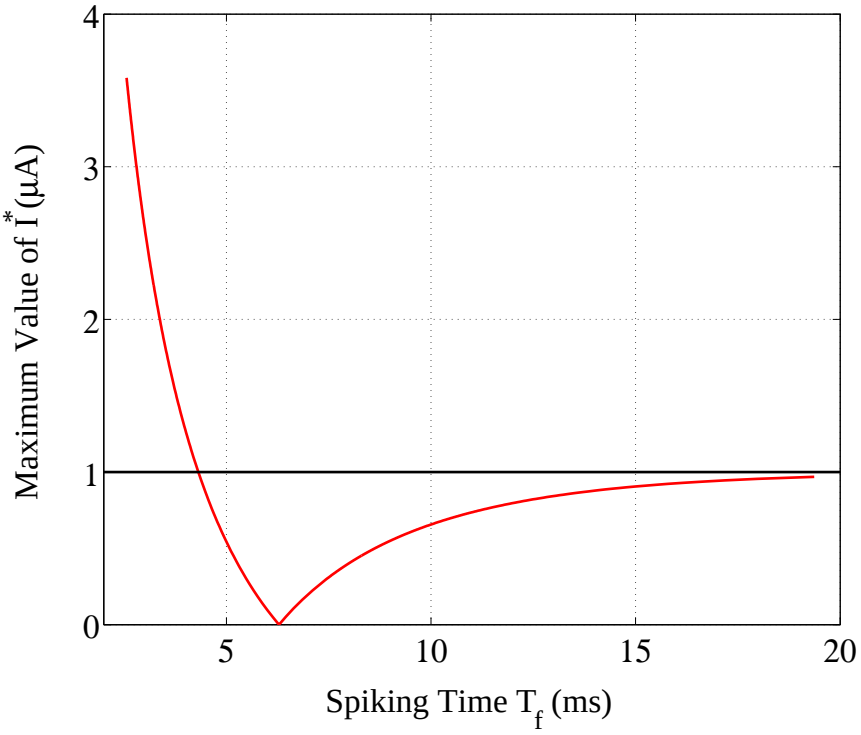

Figure 2.6: Variation of the maximum value of I^* with spiking time T_f for sinusoidal PRC model with $\omega = 1$ rad/ms and $z_d = 1$ rad/nC.

for $\omega = 1$ rad/ms and $z_d = 1$ rad/nC is depicted in Figure 2.6. Shorter spiking times $T_f \in [T^M_{min}, T^{I^*}_{min})$ are feasible but, due to the bound M, can not be achieved by I^* since it requires a control with amplitude greater than M for some $t \in [0, T_f]$. However, these spiking times can be optimally achieved by applying controls switching between I^* and I^*_{Tmin}.

The minimum-power optimal control that spikes the neuron at $T_f \in [T^M_{min}, T^{I^*}_{min})$ is characterized by four switchings between I^* and M, i.e.,

$$I^*_{M,T_f<T} = \begin{cases} I^* & 0 \le \theta < \theta_1 \\ M & \theta_1 \le \theta \le \theta_2 \\ I^* & \theta_2 < \theta < \theta_3 \\ -M & \theta_3 \le \theta \le \theta_4 \\ I^* & \theta_4 < \theta \le 2\pi, \end{cases} \tag{2.16}$$

in which $\theta_1 = \sin^{-1}[-2M\omega/(z_d M^2 + z_d\omega\lambda_0)]$ and $\theta_2 = \pi - \theta_1$ are the phases where I^* meets the bound M, $\theta_3 = \pi + \theta_1$ and $\theta_4 = 2\pi - \theta_1$. The initial value of the multiplier, λ_0, resulting in the optimal trajectory, can then be found according to the desired $T_f \in [T^M_{min}, T^{I^*}_{min})$ through the relation

$$T_f = \int_0^{\theta_1} \frac{4}{\sqrt{\omega^2 - \omega\lambda_0 z_d^2 \sin^2\theta}} d\theta + \int_{\theta_1}^{\frac{\pi}{2}} \frac{4}{\omega + z_d M \sin(\theta)} d\theta.$$

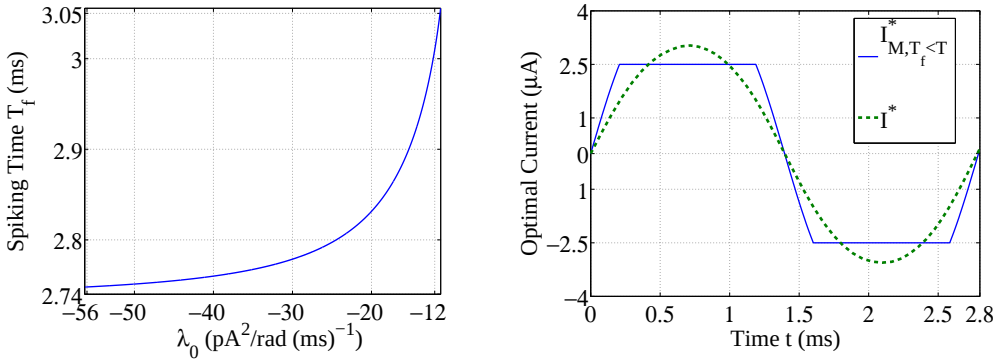

(a) (b)

Figure 2.7: (a) Variation of the spiking time $T_f \in [T^M_{min}, T^{I^*}_{min})$ for sinusoidal PRC model with initial multiplier value, λ_0, for the bound of control amplitude $M = 2.5\mu A$ (b) Minimum-power controls with ($M = 2.5\mu A$) and without a constraint on the control amplitude of sinusoidal PRC model for $T_f = 2.8$ ms, $z_d = 1$ rad/nC, and $\omega = 1$ rad/ms.

Figure 2.7(a) shows the relation between λ_0 and T_f by $I^*_{M,T_f<T}$ for $M = 2.5$, $z_d = 1$, and $\omega = 1$. From (2.14) the minimum possible spiking time with this control bound $M = 2.5\mu A$ is $T^M_{min} = 2.735$ ms and from (2.15) the minimum spiking time by I^* is $T^{I^*}_{min} = 3.056$ ms. Thus, in this example, any desired spiking time $T_f > 3.056$ ms can be optimally achieved by I^* whereas any $T_f \in [2.735, 3.056)$ ms can be optimally obtained by $I^*_{M,T_f<T}$ as in (2.16). Figure 2.7(b) illustrates the bounded and unbounded optimal controls that fire the neuron at $T_f = 2.8$ ms, where I^* is the minimum-power stimulus when the control amplitude is not limited and $I^*_{M,T_f<T}$ is the minimum-power stimulus when the bound $M = 2.5\mu A$. I^* drives the neuron from $\theta(0) = 0$ to $\theta(2.8) = 2\pi$ with 13.54 $\times 10^{-15} A^2 s$ of energy whereas $I^*_{M,T_f<T}$ requires 14.13 $\times 10^{-15} A^2 s$.

Case II : $M < \omega/z_d$. In contrast with Case I in the previous section, achieving arbitrarily large spiking times is not feasible with a bound $M < \omega/z_d$. In this case,

the longest possible spiking time is achieved by

$$I^*_{Tmax} = \begin{cases} -M & \text{for } 0 \le \theta < \pi, \\ M & \text{for } \pi \le \theta < 2\pi. \end{cases}$$

The spiking time of the neuron under this control is,

$$T^M_{max} = 2\pi\sqrt{\frac{1}{-z_d^2M^2+\omega^2}} + \frac{4\tan^{-1}\left\{z_dM/\sqrt{-z_d^2M^2+\omega^2}\right\}}{\sqrt{-z_d^2M^2+\omega^2}}, \tag{2.17}$$

and the longest spiking time feasible with control I^* is given by

$$T^{I^*}_{max} = \int_0^{2\pi} \frac{1}{\sqrt{\omega^2 + z_dM(z_dM-2\omega)\sin^2(\theta)}} d\theta. \tag{2.18}$$

Then, by similar analysis for Case I, any spiking time $T_f \in [T^M_{min}, T^{I^*}_{min})$ for a given $M < \omega/z_d$ can be achieved with the minimum-power control $I^*_{M,T_f<T}$ as given in (2.16), any $T_f \in [T^{I^*}_{min}, T^{I^*}_{max}]$ can be achieved with minimum power by I^* in (2.12), and moreover any $T_f \in (T^{I^*}_{max}, T^M_{max}]$ can be obtained by switching between I^* and I^*_{max}. The corresponding switching angles are $\theta_5 = \sin^{-1}[2M\omega/(z_dM^2 + z_d\omega\lambda_0)], \theta_6 = \pi - \theta_5, \theta_7 = \pi + \theta_5$ and $\theta_8 = 2\pi - \theta_5$, and the minimum-power optimal control for $T_f \in (T^{I^*}_{max}, T^M_{max}]$ is characterized by

$$I^*_{M,T_f>T} = \begin{cases} I^* & 0 \le \theta < \theta_5 \\ -M & \theta_5 \le \theta \le \theta_6 \\ I^* & \theta_6 < \theta < \theta_7 \\ M & \theta_7 \le \theta \le \theta_8 \\ I^* & \theta_8 < \theta \le 2\pi. \end{cases}$$

The λ_0 resulting in the optimal trajectory by $I^*_{M,T_f>T}$ can be calculated according to the given $T_f \in (T^{I^*}_{max}, T^M_{max}]$ via the relation

$$T_f = \int_0^{\theta_5} \frac{4}{\sqrt{\omega^2 - \omega\lambda_0 z_d^2 \sin^2\theta}} d\theta + \int_{\theta_5}^{\frac{\pi}{2}} \frac{4}{\omega - z_dM\sin\theta} d\theta.$$

Figure 2.8(a) shows the relation between λ_0 and T_f by $I^*_{M,T_f>T}$ for $M = 0.55\mu A$, $z_d = 1$ rad/nC, and $\omega = 1$ rad/ms. From (2.17) the maximum possible spiking time

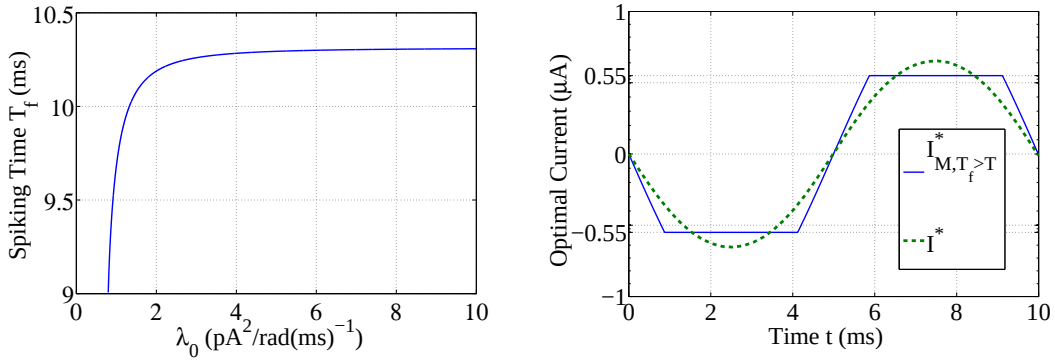

(a) (b)

Figure 2.8: (a) Variation of the spiking time $T_f \in (T_{max}^{I^*}, T_{max}^{M}]$ with the initial value of the multiplier, λ_0, for sinusoidal PRC model when $M = 0.55\mu A$. (b) Minimum-power controls with ($M = 0.55\mu A$) and without a constraint on the control amplitude for sinusoidal PRC model with $T_f = 10$ ms, $z_d = 1$ rad/nC, and $\omega = 1$ rad/ms.

with $M = 0.55\mu A$ is $T_{max}^{M} = 10.312$ ms and from (2.18) the maximum spiking time feasible by I^* is $T_{max}^{I^*} = 9.006$ ms. Therefore, in this example, any desired spiking time $T_f \in (9.006, 10.312]$ ms can be obtained with minimum power by the use of $I^*_{M,T_f>T}$. Figure 2.8(b) illustrates the bounded and unbounded optimal controls that spike the neuron at $T_f = 10$ ms, where I^* is the minimum-power stimulus when the control amplitude is not limited and $I^*_{M,T_f>T}$ is the minimum-power stimulus when $M = 0.55\mu A$. I^* drives the neuron from $\theta(0) = 0$ to $\theta(10) = 2\pi$ with $2.193\times10^{-15}A^2s$ of energy whereas $I^*_{M,T_f>T}$ requires $2.327\times10^{-15}A^2s$.

A summary of the optimal (minimum-power) spiking scenarios for a prescribed spiking time of the neuron governed by the sinusoidal phase model (2.2) is illustrated in Figure 2.9 and 2.10.

2.3.2 SNIPER Phase Model

We now consider the SNIPER phase model as in Section 1.2.4, in which $f(\theta) = \omega$ and $Z(\theta) = z_d(1 - \cos\theta)$, where $z_d > 0$ and $\omega > 0$. That is,

$$\dot{\theta} = \omega + z_d(1 - \cos\theta)I(t). \tag{2.19}$$

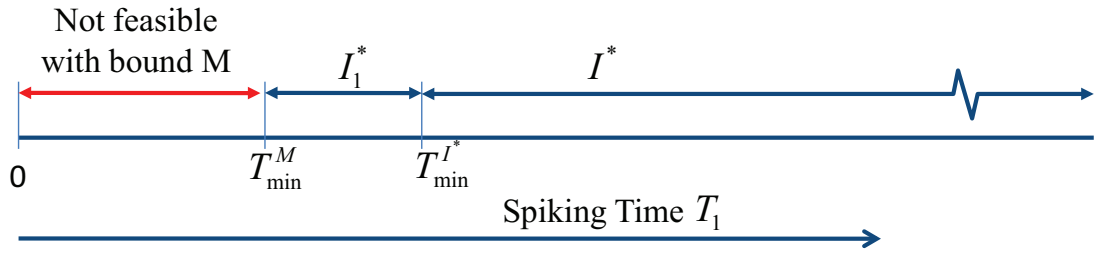

Figure 2.9: A summery of the optimal control strategies for the sinusoidal PRC neuron for $M \geq \omega/z_d$

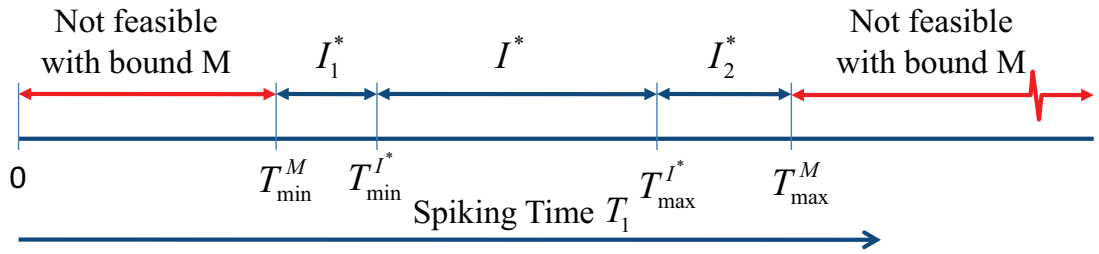

Figure 2.10: A summery of the optimal control strategies for the sinusoidal PRC neuron for $M < \omega/z_d$.

The minimum-power stimuli for spiking neurons modeled by this phase model can be easily derived with analogous analysis described previously in 2.3.1

Spiking SNIPER Neurons with Unbounded Controls

Employing the maximum principle as in A, the minimum-power stimulus that spikes the SNIPER neuron at a desired time T_f can be derived and given by

$$I^* = \frac{-\omega + \sqrt{\omega^2 - \omega\lambda_0 z_d^2(1-\cos\theta)^2}}{z_d(1-\cos\theta)}, \tag{2.20}$$

where λ_0 corresponding to the optimal trajectory is determined through the integral relation with T_f,

$$T_f = \int_0^{2\pi} \frac{1}{\sqrt{\omega^2 - \omega\lambda_0 z_d^2(1-\cos\theta)^2}} d\theta.$$

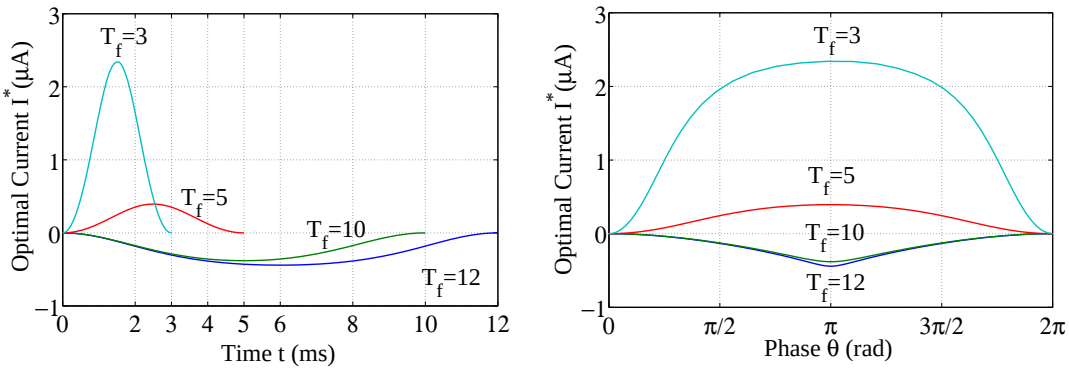

(a) (b)

Figure 2.11: (a) Optimal controls for various spiking times $T_f = 3, 5, 10, 12$ ms, and (b) variation of I^* with phase θ for SNIPER PRC model with $z_d = 1$ rad/nC and $\omega = 1$ rad/ms.

The minimum-power stimuli I^* plotted with respect to time and phase for various spiking times $T_f = 3, 5, 10, 12$ ms with parameter values z_d=1 rad/nC and $\omega = 1$ rad/ms are illustrated in Figure 2.11(a) and 2.11(b), respectively. The corresponding optimal trajectories of $\lambda(\theta)$ and $\theta(t)$ for these spiking times are displayed in Figure 2.12(a) and 2.12(b).

Spiking SNIPER Neurons with Bounded Controls

When the amplitude of the available stimulus is limited, i.e., $|I(t)| \leq M$, the control that achieves the shortest spiking time for the SNIPER phase model is given by $I^*_{Tmin} = M > 0$ for $0 \leq \theta \leq 2\pi$, since $1 - \cos\theta \geq 0$ for all $\theta \in [0, 2\pi]$. As a result, the shortest possible spiking time with this control is $T^M_{min} = 2\pi/\sqrt{\omega^2 + 2z_d\omega M}$. Also, the shortest spiking time achieved by the control I^* in (2.20) given the bound M is given by

$$T^{I^*}_{min} = \int_0^{2\pi} \frac{1}{\sqrt{\omega^2 + z_d M(z_d M + \omega)(1 - \cos\theta)^2}} d\theta. \tag{2.21}$$

Similar to the sinusoidal PRC case, the longest possible spiking time of the neuron varies with the control bound M. If $M \geq \omega/(2z_d)$, an arbitrarily large spiking time is achievable, however, if $M < \omega/(2z_d)$ there exists a maximum spiking time.

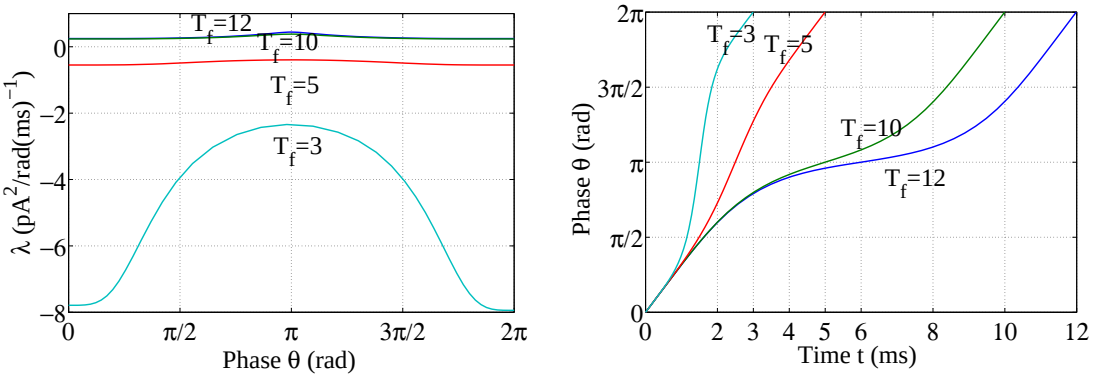

(a) (b)

Figure 2.12: (a) Variation of the optimal multiplier, λ^*, with θ, and (b) optimal phase trajectories following I^* for spiking times $T_f = 3, 5, 10, 12$ ms for SNIPER PRC model with $z_d = 1$ rad/nC and $\omega = 1$ rad/ms.

Case I: $M \geq \omega/(2z_d)$. Any spiking time $T_f \in [T^{I^*}_{min}, \infty)$ is possible with control I^* but a shorter spiking time $T_f \in [T^M_{min}, T^{I^*}_{min})$ requires switching between I^* and I^*_{Tmin}, which is characterized by two switchings,

$$I^*_{M,T_f<T} = \begin{cases} I^*, & 0 \leq \theta < \theta_1 \\ M, & \theta_1 \leq \theta \leq 2\pi - \theta_1 \\ I^*, & 2\pi - \theta_1 < \theta \leq 2\pi \end{cases} \tag{2.22}$$

where $\theta_1 = \cos^{-1}\left[1 + 2\omega M/(z_d M^2 + z_d \omega \lambda_0)\right]$. The initial value λ_0 which results in the optimal trajectory is given by,

$$T_f = \int_0^{\theta_1} \frac{2}{\sqrt{\omega^2 - \omega\lambda_0 z_d^2 (1-\cos\theta)^2}} d\theta + \int_{\theta_1}^{\pi} \frac{2}{\omega + z_d M(1-\cos\theta)} d\theta.$$

Figure 2.13(a) illustrates the relation between λ_0 and $T_f \in [T^M_{min}, T^{I^*}_{min})$ by $I^*_{M,T_f<T}$ for $M = 2\mu A$, $z_d = 1$ rad/nC, and $\omega = 1$ rad/ms. In this case, the shortest feasible spiking time is $T^M_{min} = 2.09$ ms and the shortest with the control I^* is $T^{I^*}_{min} = 3.18$ ms. Any spiking time in the interval $(2.09, 3.18]$ ms is achievable by $I^*_{M,T_f<T}$ in (2.22) with minimum-power. Figure 2.13(b) illustrates the unbounded and bounded, with $M = 2\mu A$, optimal stimuli that fire the neuron at $T_f = 3$ ms with minimum-power.

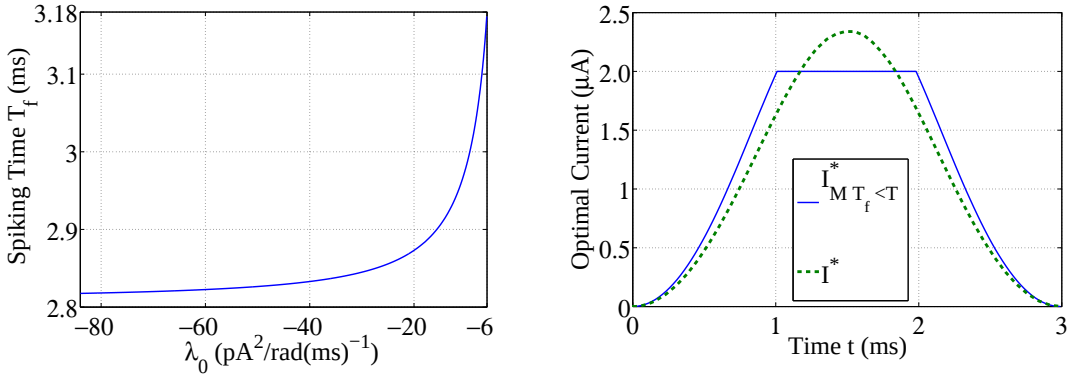

(a) (b)

Figure 2.13: (a) Variation of the spiking time $T_f \in [T_{min}, T'_{min})$ with the initial multiplier value, λ_0, for SNIPER PRC model when $M = 2\mu A$. (b) Minimum-power controls with ($M = 2\mu A$) and without a constraint on the control amplitude for SNIPER PRC model with $T_f = 3$ ms, $z_d = 1$ rad/nC, and $\omega = 1$ rad/ms.

Case II: $M < \omega/(2z_d)$. In this case there exists a longest possible spiking time (i.e., T^M_{max}) which is achieved by $I^*_{max} = -M$ for all $\theta \in [0, 2\pi]$. T^M_{max} is given by $2\pi/\sqrt{\omega^2 - 2z_d\omega M}$. The longest spiking time feasible with the control I^* as in (2.20) is given by

$$T^{I^*}_{max} = \int_0^{2\pi} \frac{1}{\sqrt{\omega^2 + z_d M(z_d M - 2\omega)(1-\cos\theta)^2}} d\theta.$$

Therefore, any spiking time $T_f \in [T^M_{min}, T^{I^*}_{min})$ for a given $M < \omega/(2z_d)$ can be achieved with the minimum-power control $I^*_{M,T_f<T}$ as given in (2.22), any $T_f \in [T^{I^*}_{min}, T^{I^*}_{max}]$ can be achieved with minimum power by I^* in (2.20), and moreover any $T_f \in (T^{I^*}_{max}, T^M_{max}]$ can be obtained by switching between I^* and I^*_{max}, that is,

$$I^*_{M,T_f>T} = \begin{cases} I^*, & 0 \le \theta < \theta_2 \\ -M, & \theta_2 \le \theta \le 2\pi - \theta_2 \\ I^*, & 2\pi - \theta_2 < \theta < 2\pi \end{cases}$$

where $\theta_2 = \cos^{-1}\left[1 - 2\omega M/(z_d M^2 + z_d\omega\lambda_0)\right]$. The λ_0 associated with the optimal trajectory is determined via the relation with the desired spiking time T_f,

$$T_f = \int_0^{\theta_1} \frac{2}{\sqrt{\omega^2 - \omega\lambda_0 z_d^2(1-\cos\theta)^2}} d\theta + \int_{\theta_1}^{\pi} \frac{2}{\omega - z_d M(1-\cos\theta)} d\theta.$$

Figure 2.14(a) illustrates the relation between λ_0 and $T_f \in (T^{I^*}_{max}, T^{M}_{max}]$ by $I^*_{M,T_f>T}$ for $M = 0.3\mu A$, $z_d = 1$ rad/nC, and $\omega = 1$ rad/ms. In this case, the longest feasible spiking time is $T^{M}_{max} = 9.935$ ms and the longest with the control I^* is $T^{I^*}_{max} = 8.596$ ms. The unbounded and bounded, with $M = 0.3\mu A$, optimal stimuli that fire the neuron at $T_f = 9.8$ ms with minimum-power are illustrated in Figure 2.14(b).

A summary of the optimal (minimum-power) spiking scenarios for a prescribed spiking time of the neuron governed by the SNIPER PRC model in (2.19) can be illustrated analogously to Figure 2.9 and 2.10 for $M \geq \omega/(2z_d)$ and $M < \omega/(2z_d)$, respectively.

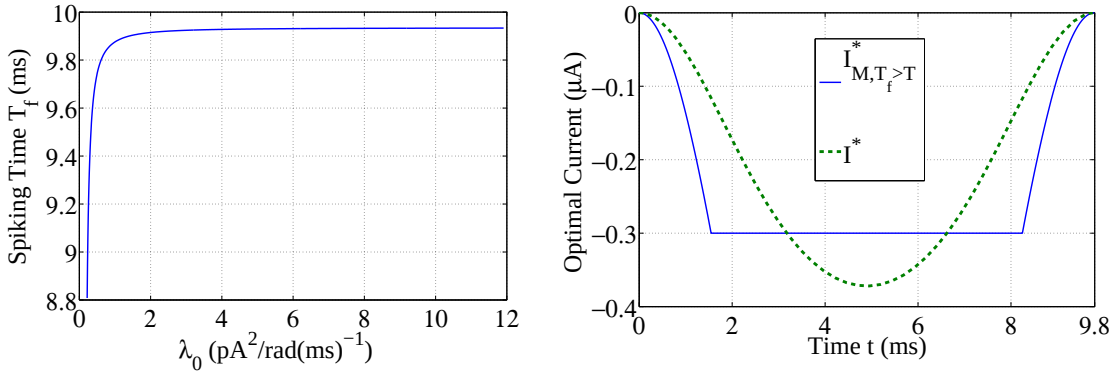

(a) (b)

Figure 2.14: (a) Variation of the spiking time $T_f \in (T'_{max}, T_{max}]$ with the initial multiplier value, λ_0, for SNIPER PRC model when $M = 0.3\mu A$. (b) Minimum-power controls with ($M = 0.3\mu A$) and without a constraint on the control amplitude for SNIPER PRC model with $T_f = 9.8$ ms, $z_d = 1$ rad/nC, and $\omega = 1$ rad/ms.

Many of experimentally determined PRC's for real neurons are not of sinusoidal or SNIPER, which are approximations arising from the study of mathematical models of neuron oscillators close to certain bifurcations. In the following, we apply the derived optimal control strategies to the Morris-Lecar PRC. Previous work has shown that the PRC for an Aplysia motoneuron, which can be experimentally observed, is extremely similar to that of a Morris-Lecar neuron [38]. As a result, we find minimum-power stimuli for Morris-Lecar neuron with 1 cm^2 membrane area to demonstrate the applicability and generality of our analytic method to practical PRC's.

2.3.3 Morris-Lecar Phase Model

The phase model of the Morris-Lecar neuron, described in Section 1.2.4, is given by

$$\dot{\theta} = \omega + Z(\theta)I(t) \tag{2.23}$$

where ω is the natural frequency of the oscillation and the PRC, $Z(\theta)$, for the system and parameters described in Section 1.1.2 is shown in Figure 1.3, calculated by XPP [29]. It has the natural period $T = 22.211$ ms and natural frequency $\omega = 0.283$ rad/ms. We can calculate the optimal controls for different spiking times following the same procedure as we explained sinusoidal PRC and SNIPER PRC in Section 2.3.1 and 2.3.2. Figure 2.15(a) and 2.15(b) show the optimal current stimuli without an amplitude constraint and the corresponding trajectories for various desired spiking times that are shorter, close, and longer than the natural spiking time.

With a bounded control amplitude, the feasible range of spiking times is limited. Figure 2.16 shows the variation of the minimum and maximum spiking time with control amplitude bound. According to the Figure 2.16 the possible range is $[19.623, 26.268]$ ms for the bound $M = 0.01\,\mu A$. Figure 2.17(a) and 2.17(b) illustrate the unbound and bounded ($M = 0.01\,\mu A$) minimum-power controls for the spiking times $T_f = 20$ ms and 25.5 ms that are shorter and longer than the natural spiking time, respectively.

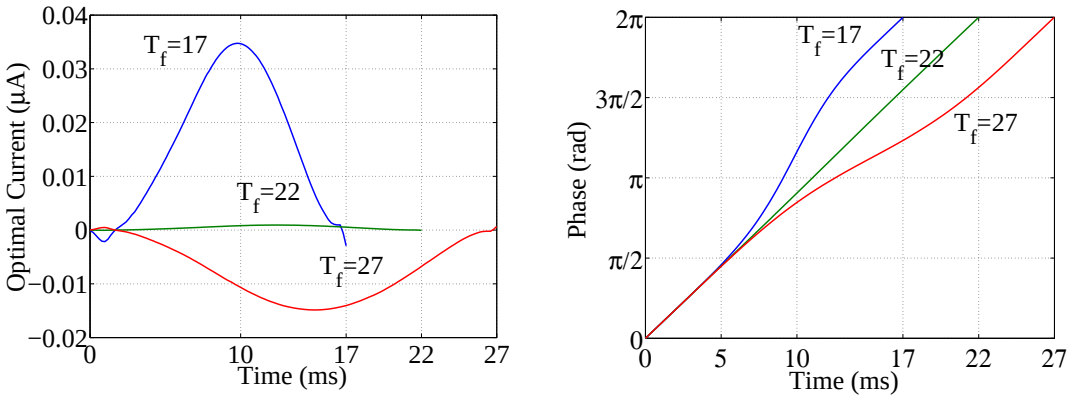

(a) (b)

Figure 2.15: (a) Optimal currents for various spiking times $T_f = 17, 22, 27$ ms for the Morris-Lecar PRC, and (b) corresponding phase trajectories under the optimal current stimuli.

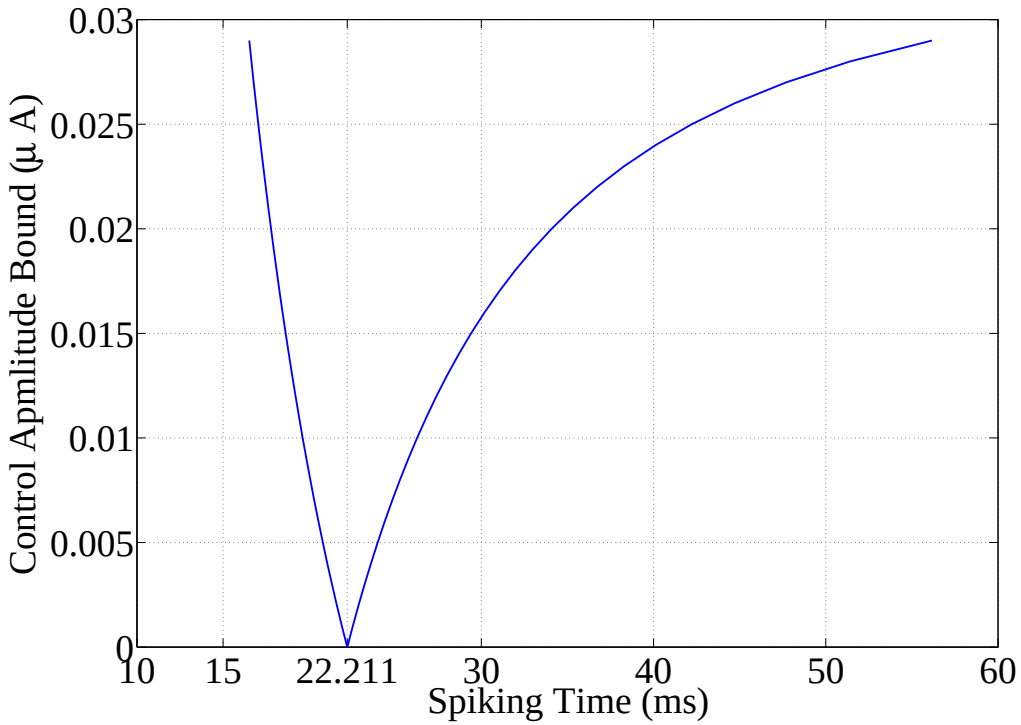

Figure 2.16: Variation of the minimum and maximum spiking time with control amplitude bound for Morris-Lecar PRC.

2.4 Minimum-Power Control for Electrochemical Oscillators

To experimentally verify the theoretical results developed in this chapter, we use an electrochemical oscillator to emulate the neuron spiking behavior.

The apparatus that we use in the experiment consists of a nickel and a platinum electrode that are submerged in sulfuric acid, as illustrated in Figure 2.18. The voltage difference between the two electrodes is controlled by a potentiostat and the control signal is superimposed on the constant voltage through a Labview interface. When constant voltage is applied between the two electrodes, the nickel wire undergoes a dissolution process which produces oscillating currents in the circuit [78]. These currents can be effectively controlled by the super imposed external voltage signal which effects the dissolution rate of the system. This system exhibits rich dynamical

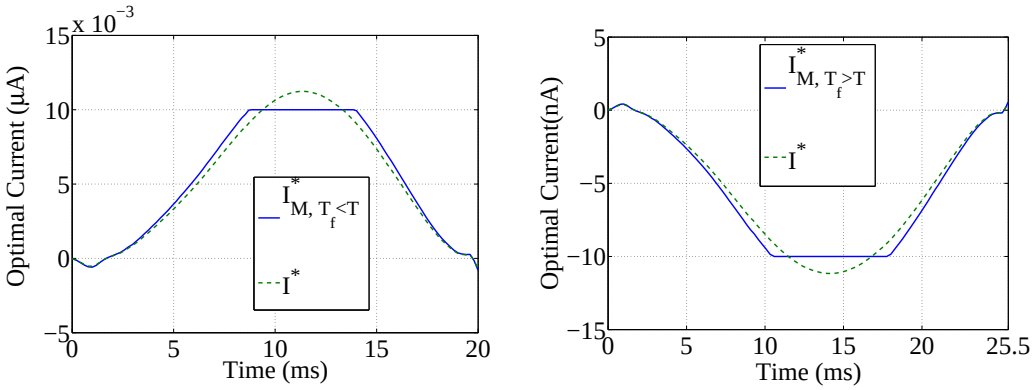

(a) (b)

Figure 2.17: (a) Unbounded and bounded minimum-power controls for $T_f = 20.0$ ms, and (b) Unbounded and bounded minimum-power controls for $T_f = 25.5$ ms for Morris-Lecar neuron with $M = 0.01\mu A$.

behavior including smooth, relaxational and chaotic oscillators [78, 134]. The phase response curve of the system has been obtained by applying narrow weak pulses at different phases to perturb the system in its limit cycle. Then the measured phase difference due to the pulsing is used to construct the phase response curve as a function of the phase at which the pulses are received. Close to the Hopf bifurcation point, where oscillations start when increasing the potentiostat voltage, the experimentally observed phase response curve is nearly sinusoidal (see Figure 2.19). For the voltages further away from the Hopf bifurcation point, the current waveform is more relaxational and the phase response curve exhibits higher harmonics.

2.4.1 Experimental Procedures and Results

We demonstrate that the phase of the nickel-sulfuric electrochemical oscillator described in Section 2.4 can be controlled to obtain current spikes at a given time instance T_f. We use the phase equation in the form of (2.23) to capture the transient dynamics of the oscillator in a quantitative manner. One experimental difficulty in the application of derived optimal control laws for an electrochemical oscillator is the lack of system information at the initial phase. This initial phase encodes the starting time of the open loop control signal. This problem has been solved by the application of a sinusoidal signal before the optimal control signal to entrain the system to a

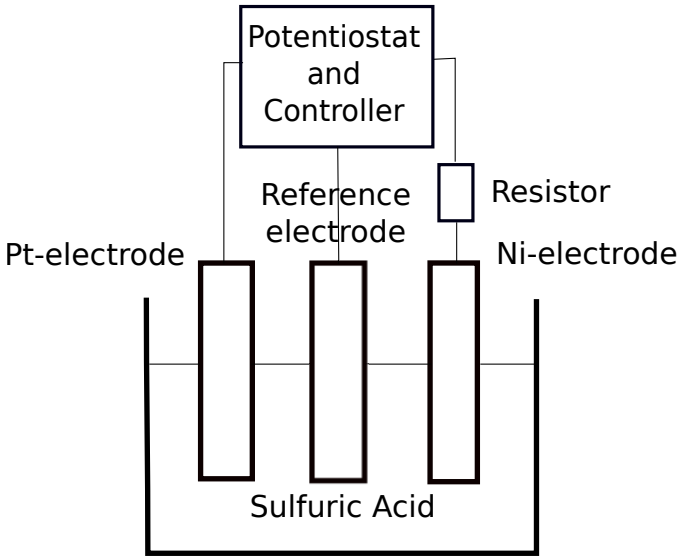

Figure 2.18: Schematic diagram of experimental setup

steady state. At the entrained state, the phase of the oscillator is slaved to the phase of the sinusoidal forcing signal. At any given time, the phase of the control signal is known, and in the entrainment state, the phase of the oscillator is approximately π rads apart from the control signal. This procedure gives a systematic way to estimate the phase of the oscillator which is not directly observable. The control signal can be conveniently switched from the sinusoidal entrainment signal to optimal control signal at the time when the phase of the forcing sinusoidal signal is equal to zero. This way, the optimal control signal can be start at the phase π of the oscillator and then, by repeating the control, we can obtain the spiking train with a desired spiking time.

The experiments thus will performed as follows.

1. First the the natural frequency of the system is measured and the phase response curve is constructed by the pulsing method.

2. Given the phase response curve $Z(\theta)$, natural frequency ω, and the target spiking time T_f we calculate the optimal control using a Matlab code.

3. Sinusoidal forcing signal with amplitude roughly the same as the optimal signal is applied for 20 cycles to entrained the system.

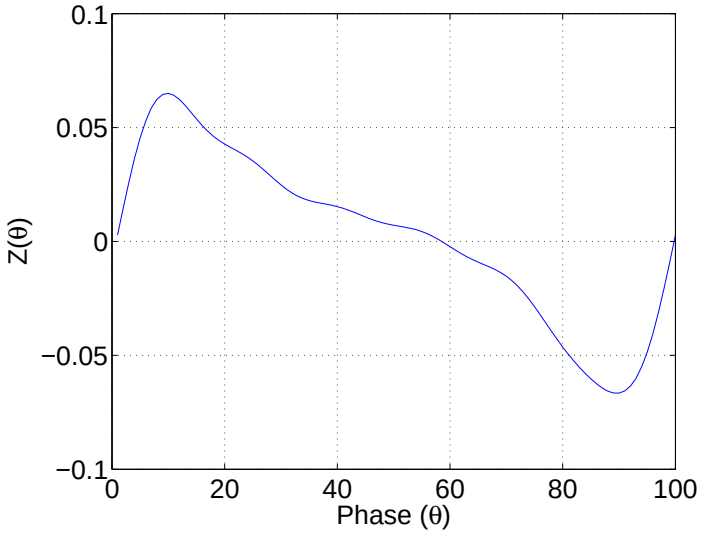

Figure 2.19: Phase response curve for Nickel-Sulfuric electro chemical oscillator with external voltage 1.1 V, R = 1 kΩ

4. After 20 cycles of sinusoidal forcing, at the π phase of the oscillator, the optimal control has been applied and continued for another ten cycles.

5. Through out step 3 and 4, the current of the electrochemical reaction is recorded by a LabView setup; and for data processing purposes we record the applied voltage signal as well.

Two target frequencies $\omega_f = 2\pi/T_f$, which are 10% lower and higher than the natural frequency, have been tested with the optimal controls for nickel-sulfuric oscillator and results are depicted in Figure 2.20 and 2.21. In these figures the black horizontal line indicates the point where the optimal control starts, and as we expected, the controls turn the frequencies of the oscillation to the desired value almost immediately.

2.5 Conclusion

In this chapter, we studied various phase-reduced models that describe the dynamics of neuron systems. We considered the design of minimum-power stimuli for spiking a neuron at a specified time instant that is different from the natural spiking time. We

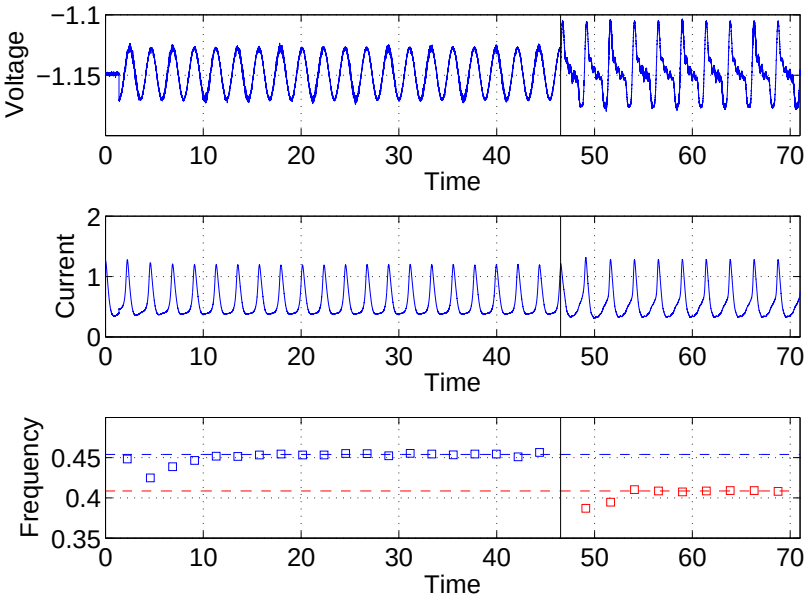

Figure 2.20: Frequency detuning from natural frequency $\omega = 0.454$ rad/s to target frequency $0.9\omega = 0.401$ rad/s of the nickel-sulfuric electro chemical oscillator.

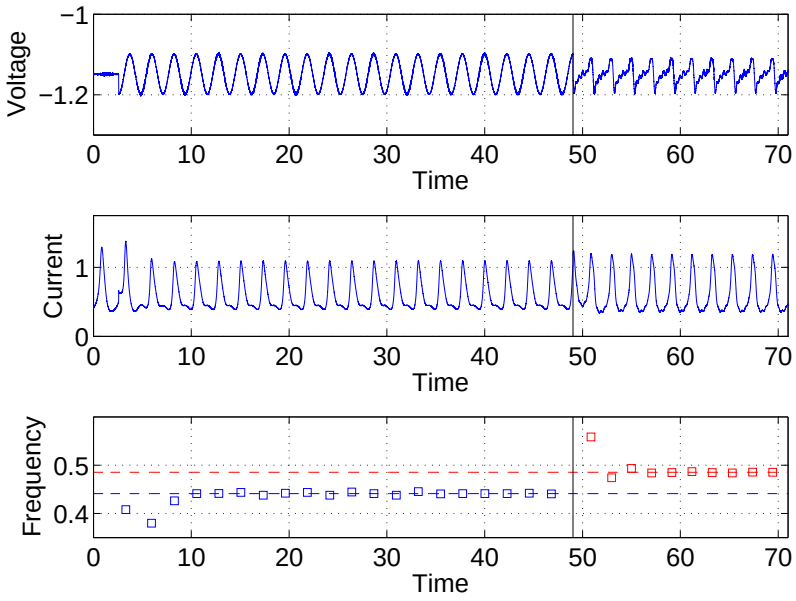

Figure 2.21: Frequency detuning from natural frequency $\omega = 0.454$ rad/s to target frequency $0.9\omega = 0.5$ rad/s of the nickel-sulfuric electro chemical oscillator.

formulated this as an optimal control problem and investigated both cases when the control amplitude is unbounded and bounded, for which we found analytic expressions of optimal feedback control laws. In particular for the bounded control case, we characterized the range of possible spiking periods in terms of the control bound. The bound can be chosen sufficiently small within the range that the PRC of a neuron is valid. We illustrated that our method can be applied not only to ideal mathematical models of neuron oscillators but also to experimentally observed PRC's, such as that of an Aplysia motoneuron. The derived feasible spiking range for Morris-Lecar phase model has shown a great qualitatively agreement with experimental results of Aplysia motoneuron [57]. We experimentally verified the derived control laws for a nickel-sulfuric oscillator which has similar phase dynamics compared to neural phase models.

The methodology derived in this chapter can be directly applied to design minimum-power control for steering any type of nonlinear oscillators that can be as in Section 1.2 between desired states. In addition practical design constraints such as the charge-balance constraint, can be readily incorporated into this framework, which is of clinical importance as in the DBS for Parkinson's disease [94]. This addition is considered in Chapter 3 and 4. Although one-dimensional phase models are reasonably accurate to describe the dynamics of neurons, studying higher dimensional models is essential for more accurate computation of optimal neural inputs.

Chapter 3

Charge-Balanced Time-Optimal Controls for Spiking Neuron Oscillators

In this chapter, we investigate the fundamental limits on how the inter-spike time of a neuron oscillator can be perturbed by the application of a bounded external control input (a current stimulus) with zero net electric charge accumulation. We use phase models to study the dynamics of neurons and derive charge-balanced controls that achieve the minimum and maximum inter-spike times for a given bound on the control amplitude. Our derivation is valid for any arbitrary shape of the phase response curve and for any value of the given control amplitude bound. In addition, we characterize the change in the structures of the charge-balanced time-optimal controls with the allowable control amplitude. We demonstrate the applicability of the derived optimal control laws by applying them to mathematically ideal and experimentally observed neuron phase models, including the widely-studied Hodgkin-Huxley phase model, and by verifying them with the corresponding original full state-space models. This work addresses a fundamental problem in the field of neural control and provides a theoretical investigation to the optimal control of oscillatory systems.

3.1 Introduction

Neurons exhibit short-lasting voltage spikes known as action potentials, which are sensitive to external current stimuli [60]. The inter-spike time interval of a neuron

characterizes its properties and can be controlled by use of external stimuli. The ability to control neuron spiking activities is fundamental to theoretical neuroscience, and the concept of effective control of such neurological behavior has led to the development of innovative therapeutic procedures [117, 4] for neurological disorders including deep brain stimulation (DBS) for Parkinson's disease and essential tremor [85, 96], where electrical pulses are used to inhibit pathological synchrony among neuron populations. In such neurological treatments and other applications such as the design of artificial cardiac pacemakers [100], it is of clinical importance to avoid long and strong electrical pulses in order to prevent the tissue from damage, as well as to maintain zero net electric charge accumulation over each stimulation cycle in order to suppress undesirable side effects. High levels of electric charge accumulation may trigger irreversible electrochemical reactions resulting in damage of neural tissues and corrosion of electrodes [88].

Motivated by these practical needs, in this chapter we study the design of time-optimal controls for spiking neurons, which lead to the minimum and maximum inter-spike times and remain charge-balanced. We study the dynamics of neuron oscillators through phase models which are simplified yet accurate models that capture essential overall properties of an oscillating neuron [60, 11], and which form a standard nonlinear control system that characterizes the evolution of an oscillating system by a single variable, namely, the phase. Phase models are conventionally used to investigate the synchronization patterns and study the dynamical responses of oscillators where the inputs to the oscillatory systems are initially defined [11, 3, 128]. Recently, control-theoretic approaches, including calculus of variations and the maximum principle, have been employed to design external stimuli for optimal manipulation of the dynamic behavior of neuron oscillators. These include the design of minimum-power controls for spiking a single neuron at specified time instances [90, 21, 23], optimal waveforms for entrainment of neuron ensembles [140, 139, 49], and open-loop controls for establishing and maintaining a desired phase configuration, such as anti-phase for two coupled neuron oscillators [122]. Work on considering stochastic effects to neuron systems such as the optimal control of neuronal spiking activity receiving a class of random synaptic inputs has also been investigated [33]. In addition, controllability of an ensemble of uncoupled neurons was explored for various mathematically ideal phase models, where an effective computational optimal control method based on pseudospectral approximations was employed to construct optimal controls that

elicit simultaneous spikes of a neuron ensemble [84, 80]. The derivation of time-optimal and spike timing controls for spiking neurons has been attempted for limited classes of control functions [95, 18], however, a complete characterization of the optimal solutions has not been provided, and an analytical and systematic approach for synthesizing the time-optimal controls has been missing.

In this chapter, we derive charge-balanced time-optimal controls for a given bound on the control amplitude and fully characterize the possible range of neuron spiking times determined by such optimal controls. Employing techniques from the optimal control theory, we are able to reveal different structures of the time-optimal controls that vary with the allowable bound of the control amplitude. Moreover, we validate these controls derived according to phase models by applying them to the corresponding original full state-space neuron models. As a demonstration, the validation is performed using the Hodgkin-Huxley equations [52], where the spiking behavior of the state-space model shows great qualitative agreement with that of the phase model and which demonstrates the applicability of our theoretical results based on the phase model. Such an important validation, which is largely lacking in the literature, allows us to explore the fundamental limits of the phase model as an approximation of state-space models.

This chapter is organized as follows. In Section 3.2, we consider the time-optimal control of a general phase oscillator and derive the charge-balanced minimum-time and maximum-time controls with constrained control amplitude by using the Pontryagin's maximum principle [107]. In Section 3.3, we apply the derived optimal control strategies to both mathematically ideal and experimentally observed phase models, including the well-known SNIPER [11], Hodgkin-Huxley, and Morris-Lecar [92] phase models, and present the simulated optimal solutions. In Section 3.4, we validate the obtained optimal controls through the Hodgkin-Huxley model.

3.2 Charge-Balanced Time-Optimal Control

Recall that, the dynamics of a periodically spiking neuron oscillator can be described by a phase model of the form [11]

$$\frac{d\theta}{dt} = \omega + Z(\theta)I(t), \tag{3.1}$$

where θ denotes the phase of the oscillation, $\omega > 0$ is neuron's natural oscillation frequency, and $I(t) \in \mathbb{R}$ is the external current stimulus (control) that is applied to perturb the phase dynamics of the neuron. The real-valued function $Z(\theta)$ is the phase response curve (PRC) that characterizes the infinitesimal change of the phase to an external control input. Conventionally, the neuron is said to spike when its phase $\theta = 2n\pi$, where $n \in \mathbb{N}$. In the absence of any input $I(t)$, the neuron spikes periodically at its natural frequency, while the spiking time may be advanced or delayed in a desired manner by the application of an appropriate weak control.

3.2.1 Charge-Balanced Minimum-Time Control

The optimal design of controls that lead to the minimum inter-spiking time of a neuron subject to a given bound on the control amplitude and the charge-balance constraint can be formulated as a time-optimal steering problem of the form

$$\begin{aligned} \min_{I(t)} \quad & T, \\ \text{s.t.} \quad & \dot{\theta} = \omega + Z(\theta)I(t), \\ & \dot{p} = I(t), \\ & |I(t)| \leq M, \quad \forall\, t \in [0, T], \\ & \theta(0) = 0, \quad \theta(T) = 2\pi, \\ & p(0) = 0, \quad p(T) = 0, \end{aligned} \tag{3.2}$$

where T is the inter-spiking time required that we wish to minimize and $M > 0$ is the bound of the control amplitude. The constraints involving the time-dependent variable $p(t)$ are equivalent to the charge-balance constraint, i.e., $p(t) = \int_0^t I(\sigma)d\sigma = 0$

with $p(0) = p(T) = 0$, guaranteeing that the charge accumulated over a spiking cycle is zero. Note that the consideration of bounded controls is of fundamental importance since the phase reduction is no longer valid when the control exceeds a level that can be considered weak.

Derivation of the Charge-Balanced Minimum-Time Control:

The Hamiltonian of the optimal control problem as in (3.2) is given by

$$H = \lambda_0 + \lambda_1(\omega + Z(\theta)I) + \lambda_2 I \tag{3.3}$$

where $\lambda_0 \geq 0,\ \lambda_1$, and λ_2 are Lagrange multipliers associated with the Lagrangian, system dynamics, and the charge-balance constraint, respectively. According to the optimality conditions of the maximum principle (see A.2), the adjoint variables λ_1 and λ_2 must satisfy the time-varying equations $\dot{\lambda}_1 = -\frac{\partial H}{\partial \theta}$ and $\dot{\lambda}_2 = -\frac{\partial H}{\partial p}$, respectively, which yields

$$\dot{\lambda_1} = \ -\lambda_1 I \tfrac{\partial Z(\theta)}{\partial \theta}, \tag{3.4}$$

$$\dot{\lambda_2} = \qquad 0, \tag{3.5}$$

and hence λ_2 is a constant. Since the Hamiltonian H is not explicitly dependent on time and the terminal time is free, we have $H \equiv 0,\ \forall\, t \in [0, T]$, along the optimal trajectory from the maximum principle.

It is straightforward to see from a rearrangement of (3.3), $H = \lambda_0 + \lambda_1\omega + (\lambda_1 Z(\theta) + \lambda_2)I$, that the control

$$I^*_{min} = \begin{cases} M, & \phi < 0 \\ -M, & \phi \geq 0 \end{cases} \tag{3.6}$$

minimizes the Hamiltonian H, where

$$\phi = \lambda_1 Z + \lambda_2 \tag{3.7}$$

is called the switching function. Hence, according to the maximum principle, I^*_{min} is a candidate of the optimal solution to the problem as in (3.2), provided $\phi = 0$ for a nonzero time period does not occur. This type of controls is known as bang-bang

controls, which takes only the extremals of the control set, e.g., $-M$ or M in this case. The switching between $-M$ and M occurs at $\phi = 0$ and the challenge is to calculate the values of the multipliers λ_1 and λ_2, which define the function ϕ and thus the optimal control sequence.

An alternative candidate of the minimum-time control may exist. If $\phi \equiv 0$ for some non-zero time interval $S = [\tau_1, \tau_2]$, then its derivatives $\dot{\phi}$, $\ddot{\phi}$, etc., will also be equal to zero over S. In this case, the bang-bang control (3.6) may not be optimal. Such a control that forces the switching function ϕ and all of its derivatives to vanish over a time period is known as a singular control [6], and it can be calculated according to the following fashion. When $\phi = 0$, $\dot{\phi} = 0$, $\ddot{\phi} = 0$, ..., for a given time interval S, we have

$$\phi = \lambda_1 Z + \lambda_2 = 0 \tag{3.8}$$

and then, by substituting from (3.1), (3.4), and (3.5), the function $\dot{\phi}$ is given by

$$\dot{\phi} = \lambda_1 \omega \frac{\partial Z}{\partial \theta} = 0 \tag{3.9}$$

which yields $\frac{\partial Z}{\partial \theta} = 0$ because $\omega > 0$ and $\lambda_1 \neq 0$. The latter is due to the non-triviality condition of the maximum principle, i.e., $(\lambda_0, \lambda_1, \lambda_2) \neq \mathbf{0}$, since $\lambda_2 = 0$ if $\lambda_1 = 0$ from (3.8), which leads to $\lambda_0 = 0$ from (3.3) as $H \equiv 0$. Therefore, $\lambda_1 \neq 0$ holds along the optimal trajectory and $\frac{\partial Z}{\partial \theta} = 0$ defines a singular trajectory, i.e., the trajectory of the system following a singular control. As in the calculation of $\dot{\phi}$, the second derivative $\ddot{\phi}$ can be obtained using (3.1) and $\frac{\partial Z}{\partial \theta} = 0$ to get

$$\ddot{\phi} = \lambda_1 \omega \frac{\partial^2 Z}{\partial \theta^2}(\omega + ZI). \tag{3.10}$$

It is clear from (3.10) that if $\frac{\partial^2 Z}{\partial \theta^2} \neq 0$, the control that makes $\ddot{\phi} = 0$ is given by $I_s = -\omega/Z$. In the case when $\frac{\partial^2 Z}{\partial \theta^2} = 0$, we need to calculate $\dddot{\phi}$ in order to get the singular control I_s. However, no matter how many derivatives are used, the singular control is given by the same form, $I_s = -\omega/Z$.

If a singular trajectory exists, then one must examine whether it is "fast" or "slow" compared to the bang-bang trajectory in order to determine the minimum-time control. Suppose that the singular control $I_s = -\omega/Z$ is admissible over a nonzero time interval $S = [\tau_1, \tau_2]$. Then, from (3.1) the phase velocity is equal to zero, i.e., $\dot{\theta} \equiv 0$,

over S by the application of I_s. This implies that the singular trajectory is slower than any feasible trajectory along which $\dot{\theta} \geq 0$ over S. Therefore, the charge-balanced control that spikes neurons in minimum time is of the bang-bang form.

Computation and Synthesis of the Charge-Balanced Minimum-Time Control:

Because the minimum spiking time of the neuron system as in (3.1) is achieved by a bang-bang control, it remains to calculate the switching points in order to synthesize this time-optimal control. Since $\phi = 0$ holds at the switching points, according to (3.8), these points are defined via the inverse function of the PRC,

$$\theta_s = Z^{-1}\left(-\frac{\lambda_2}{\lambda_1}\right). \tag{3.11}$$

In addition, with the Hamiltonian condition $H \equiv 0$, the value of the multiplier λ_1 is given by $\lambda_1 = -\frac{\lambda_0}{\omega}$ at these switching points. Without loss of generality, we let $\lambda_0 = 1$, which leads to $\lambda_1 = -\frac{1}{\omega}$. Applying this to (3.11) results in

$$\theta_s = Z^{-1}(\alpha) = Z^{-1}\left(\lambda_2 \omega\right), \tag{3.12}$$

where λ_2 and ω are both constants. Let $Z^{-1}(\alpha)$ have n solutions in the interval $(0, 2\pi)$ given by $\theta_1, \theta_2, \ldots \theta_n$, and define $\theta_0 = 0$ and $\theta_{n+1} = 2\pi$. Then, if we start with the control $I = M$, the charge-balance constraint gives rise to the condition

$$0 = \int_0^T I(t)dt = \sum_{i=0}^{i=n} \int_{\theta_i}^{\theta_{i+1}} \frac{(-1)^i M}{\omega + (-1)^i Z(\theta) M} d\theta \tag{3.13}$$

and the total time T under this bang-bang control is represented by

$$T = \sum_{i=0}^{i=n} \int_{\theta_i}^{\theta_{i+1}} \frac{1}{\omega + (-1)^i Z(\theta) M} d\theta. \tag{3.14}$$

Equation (3.13) together with the switching conditions $Z(\theta_i) = \alpha$ for $i = 1, 2, \ldots n$ define $n+1$ equations of $n+1$ variables, $\{\theta_1, \theta_2, \ldots \theta_n, \alpha\}$. This system of equations can be solved to get the set of optimal switching angles, denoted as S_M, and the constant

α. Similarly, if we start with the control $I = -M$, by substituting M with $-M$ in (3.13) we obtain the other set of solutions, denoted as S_{-M}. The bang-bang control, determined by the set of switching angles, which results in the shorter spiking time is the charge-balanced minimum-time control, while the opposite case is a candidate for the charge-balanced maximum-time control.

Alternatively, given the two sets of switching angles, the optimal switching sequence can be determined by computing $\dot{\phi}$ at the switching points. We denote the vector fields corresponding to the constant bang controls $I(t) \equiv -M$ and $I(t) \equiv M$ by $X = \omega - MZ$ and $Y = \omega + MZ$, respectively, and call the respective trajectories corresponding to them as X- and Y- trajectories. A concatenation of an X-trajectory followed by a Y-trajectory is denoted by XY, while the concatenation in the reverse order is denoted by YX. If $\dot{\phi} < 0$ at a switching point, then the X to Y switch is optimal according to the switching law (3.6), and similarly if $\dot{\phi} > 0$, then the Y to X switch is optimal. Since $\lambda_1 = -1/\omega$ at the switching points, we have

$$\dot{\phi} = \lambda_1 \omega \frac{\partial Z}{\partial \theta} = -\frac{\partial Z}{\partial \theta}. \tag{3.15}$$

Therefore, the value of $\frac{\partial Z}{\partial \theta}$ at the switching points defines the switching type. If $\frac{\partial Z}{\partial \theta} > 0$, an X to Y switch is optimal and if $\frac{\partial Z}{\partial \theta} < 0$, a Y to X switch is optimal.

3.2.2 Charge-Balanced Maximum-Time Control

(CaseI: Bang-Bang Control)

When the control amplitude is limited by $M < \min\left\{\left|\frac{\omega}{Z(\theta)}\right| : \theta \in [0, 2\pi)\right\}$, singular controls are not admissible since $I_s = -\omega/Z$ as shown in Section 3.2.1. Therefore, the maximum-time control is given by the bang-bang form

$$I^*_{max} = \begin{cases} -M, & \phi \leq 0 \\ M, & \phi > 0. \end{cases} \tag{3.16}$$

where ϕ is defined as in (3.7). The optimal switching sequence is determined between S_M and S_{-M}, whichever results in longer spiking time. Another way to determine the

optimal switching sequence is by evaluating $\frac{\partial Z}{\partial \theta}$ at the switching points as described in Section 3.2.1. When $\frac{\partial Z}{\partial \theta} > 0$ at a switching point, a Y to X switch is optimal, while when $\frac{\partial Z}{\partial \theta} < 0$, an X to Y switch is optimal.

(CaseII: Bang-Singular-Bang Control)

When singular controls are admissible, that is, when $M \geq \min\left\{\left|\frac{\omega}{Z(\theta)}\right| : \theta \in [0, 2\pi)\right\}$, the maximum-time control is a combination of bang and singular controls (see the examples in Section 3.3.1 and 3.3.2). The procedure of the optimal control synthesis is to choose a bang control that drives the system to a singular trajectory (a system trajectory following a singular control), staying on that trajectory, and then exiting at the point from which a bang control can steer the system to the desired terminal state. Examples involving the construction of charge-balanced minimum-time and maximum-time optimal controls are illustrated in Section 3.3.

3.3 Examples

We now apply the derived optimal control strategies to several commonly-used phase models characterized by various PRC's, including mathematically ideal and experimentally observed phase models. These examples demonstrate the applicability of our optimal control methods to manipulate neuron dynamics. We emphasize that these optimal controls are designed with respect to a given bound of the control amplitude, so that they can be made practical and satisfy the weak forcing assumption in the phase model.

3.3.1 SNIPER Phase Model

The SNIPER phase model is characterized by a type I PRC and is of the form [11]

$$\dot{\theta} = \omega + z_d\,(1 - \cos\theta)I, \tag{3.17}$$

where ω is the natural oscillation frequency of the neuron, z_d is a model-dependent constant, and I is the external stimulus.

Before calculating the minimum- and maximum-time spiking controls for the SNIPER phase model, we first examine the existence of singular trajectories. Recall from (3.9) that the singular trajectory is defined by $\frac{\partial Z}{\partial \theta} = 0$, which yields

$$z_d \sin\theta = 0.$$

Therefore, there exist three possible singular trajectories (in this case singular points), $\theta = 0$, $\theta = \pi$, and $\theta = 2\pi$. The points $\theta = 0$ and $\theta = 2\pi$ are infeasible singular points, at which the nonzero phase velocity, $\dot{\theta} = \omega$, immediately forces the system away from these points, Hence, $\theta_s = \pi$ is the only possible singular point, and the singular control $I = -\omega/Z(\theta_s) = -\omega/(2z_d)$ yields $\dot{\theta} = 0$ at θ_s, making the system stay at θ_s.

Charge-Balanced Minimum-Time Control for SNIPER Phase Model:

Since the charge-balanced minimum-time control takes the bang-bang form as shown in Section 3.2.1, the switching points are given from (3.12) by

$$\theta_s = \cos^{-1}\left\{1 - \frac{\omega\lambda_2}{z_d}\right\}. \tag{3.18}$$

The cosine function has two solutions in $[0, 2\pi)$ and thus there are two switching points $\theta_1 = \gamma$ and $\theta_2 = 2\pi - \gamma$ with $\gamma \in [0, \pi)$. Because $\lambda_1 = -1/\omega$ for both switching points and the derivative of the switching function $\dot{\phi} = -z_d \sin\theta < 0$ for $\theta \in (0, \pi)$, if a switch occurs on the interval $(0, \pi)$, it will be X to Y. Reversely, if a switch occurs on $(\pi, 2\pi)$, then it will be Y to X because $\dot{\phi} > 0$ for $\theta \in (\pi, 2\pi)$. It follows that an XYX trajectory is optimal for achieving the minimum inter-spike time. The parameter γ that defines the switching points is calculated using the charge-balance constraint as in (3.13) by solving $R(M, \gamma) = 0$, where

$$R(M,\gamma) = \int_0^{\gamma} \frac{-M}{\omega - z_d(1-\cos\theta)M} d\theta + \int_{\gamma}^{\pi} \frac{M}{\omega + z_d(1-\cos\theta)M} d\theta. \tag{3.19}$$

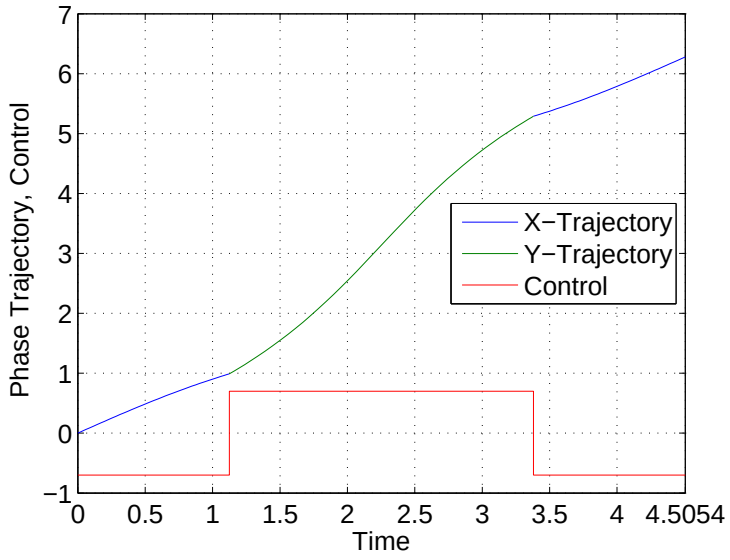

Figure 3.1: The charge-balanced minimum-time control and the corresponding phase trajectory for the SNIPER phase model with $z_d = 1$, $\omega = 1$, and $M = 0.7$.

Then, the optimal control is given by

$$I^*_{min} = \begin{cases} -M, & 0 \leq \theta < \theta_1, \\ M, & \theta_1 \leq \theta \leq \theta_2, \\ -M, & \theta_2 < \theta \leq 2\pi, \end{cases} \tag{3.20}$$

and by following (3.14) the time required to spike the neuron, namely, to reach $\theta = 2\pi$, is given by

$$T = \int_0^{\gamma} \frac{4}{\omega - z_d(1-\cos\theta)M} d\theta. \tag{3.21}$$

Figure 3.1 shows the charge-balanced minimum-time control and the corresponding phase trajectory for the SNIPER phase model with $z_d = 1$, $\omega = 1$, and $M = 0.7$.

Charge-Balanced Maximum-Time Control for SNIPER Phase Model:

There are two control scenarios for maximizing the spiking time of a SNIPER neuron depending on the control amplitude.
(*Case I:* $M < \frac{\omega}{2z_d}$) If the bound of the control amplitude $M < |\frac{\omega}{Z(\theta)}| = |\frac{\omega}{z_d(1-\cos\theta)}| < \frac{\omega}{2z_d}$, then there exist no admissible singular controls and the maximum-time control

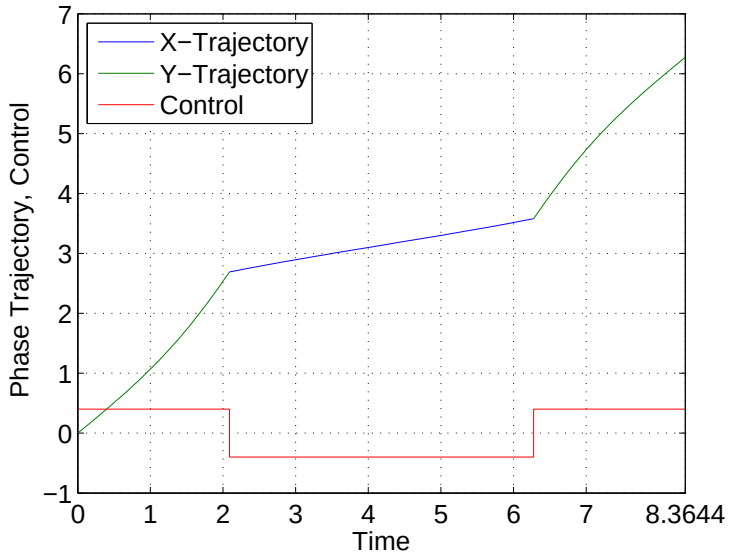

Figure 3.2: The charge-balanced maximum-time control and the corresponding phase trajectory for the SNIPER phase model with $z_d = 1$, $\omega = 1$, and $M = 0.4 < \frac{\omega}{2z_d} = 0.5$.

takes the bang-bang form as described in Section 3.2.2. In this case, there are two switches and the YXY trajectory is optimal. The maximum-time control is given by

$$I^*_{max} = \begin{cases} M, & 0 \leq \theta < \theta_1, \\ -M, & \theta_1 \leq \theta \leq \theta_2, \\ M, & \theta_2 < \theta \leq 2\pi, \end{cases} \tag{3.22}$$

where $\theta_1 = \beta$, $\theta_2 = 2\pi - \beta$, and the parameter β is obtained by solving $R(-M, \beta) = 0$ as defined in (3.19). Figure 3.2 illustrates the charge-balanced maximum-time control and the corresponding phase trajectory for the SNIPER phase model with $z_d = 1$, $\omega = 1$, and $M = 0.4 < \frac{\omega}{2z_d} = 0.5$.

(*Case II:* $M \geq \frac{\omega}{2z_d}$) In this case, the system can be driven along the singular trajectory which is optimal (slower than the bang control), and the maximum-time control takes the bang-singular-bang form. Because, for example, when $\theta \in (0, \pi)$, the derivative of the switching function $\dot{\phi} = -z_d \sin\theta < 0$, and then the YX trajectory is a candidate for optimality if a switch occurs. However, following an X-trajectory with $I = -M \leq \frac{-\omega}{2z_d}$, the singular point $\theta = \pi$ is unreachable. Hence, switching in the interval $(0, \pi)$

is not allowed, and the Y-trajectory is optimal for $\theta \in [0, \pi)$. The same reasoning applies for the regime $\theta \in (\pi, 2\pi]$, where Y-trajectory again is optimal. As a result, the optimal control is of the "Y-singular-Y" form given by

$$I^*_{max} = \begin{cases} M, & 0 \leq \theta < \pi, \\ -\frac{\omega}{2z_d}, & \theta = \pi, \\ M, & \pi < \theta \leq 2\pi. \end{cases} \tag{3.23}$$

Because $\dot{\theta} = 0$ holds along the singular trajectory (in this case the singular point $\theta_s = \pi$), the time duration over which the system stays on it is calculated according to the charge-balance constraint. Let t_1 and t_2 denote the times for which the first bang control and the singular control are applied, respectively. Since t_1 is the time that the system takes to reach $\theta_s = \pi$ by a Y-trajectory, we have

$$t_1 = \int_0^{\pi} \frac{1}{\omega + z_d(1 - \cos\theta)M} d\theta. \tag{3.24}$$

By symmetry, the amount of time that the system takes following a Y-trajectory from $\theta = \pi$ to $\theta = 2\pi$ is also t_1. Then, t_2 is given by

$$t_2 = \frac{4Mz_d t_1}{\omega}$$

in order to fulfill the charge-balance constraint. Now the charge-balanced maximum-time control can be stated in terms of time as

$$I^*_{max} = \begin{cases} M, & 0 \leq t < t_1, \\ -\frac{\omega}{2z_d}, & t_1 \leq t \leq t_1 + t_2, \\ M, & t_1 + t_2 < t \leq t_2 + 2t_1. \end{cases} \tag{3.25}$$

Figure 3.3 shows the maximum-time charge-balanced control and the corresponding phase trajectory for the SNIPER phase model with $z_d = 1$, $\omega = 1$, and $M = 0.7 \geq \frac{\omega}{2z_d} = 0.5$.

In the following, we demonstrate the robustness of our analytical method to construct optimal controls for spiking neurons of arbitrary practical PRCs through the Hodgkin-Huxley and Morris-Lecar phase models.

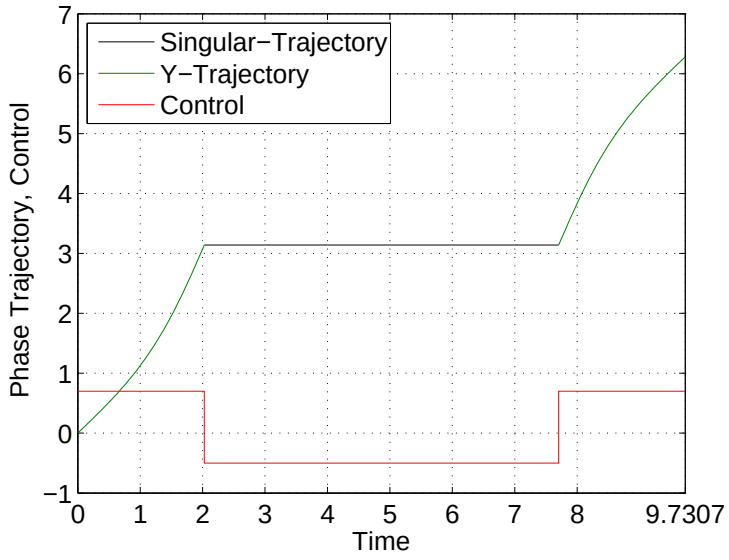

Figure 3.3: The maximum-time charge-balanced control and corresponding phase trajectory for the SNIPER phase model with $z_d = 1, \omega = 1$, and $M = 0.7$.

i	1	2	3	4	5	6	7	8
a_i	0.09176	0.07462	0.03807	0.02425	0.01747	0.006474	0.002752	0.0008111
b_i	1.002	1.996	3.002	0.5	3.747	3.747	6.228	7.651
c_i	2.609	-1.605	0.7233	0.5148	3.552	-0.7648	0.6429	-4.726

Table 3.1: The coefficients of the equation (3.26) for the Hodgkin-Huxley PRC.

3.3.2 Hodgkin-Huxley Phase Model

For the set of parameter values given in Section 1.1.1, the Hodgkin-Huxley system exhibits periodic motion with natural frequency $\omega = 0.43\, rad/ms$. Its PRC and the first and second derivatives of the PRC are depicted in Figure 3.4. To proceed the calculations, we approximate the numerically obtained PRC with eight harmonic terms given by

$$Z(\theta) = \sum_{i=1}^{8} a_i \sin(b_i\theta + c_i), \tag{3.26}$$

where the coefficients a_i, b_i and c_i are obtained by least squares fit and given in Table 3.1. In this case, there are two possible singular points, $\theta_{s,1} = 3.34$ and $\theta_{s,2} = 4.58$, satisfying $\partial Z(\theta)/\partial\theta = 0$. The charge-balanced minimum-time control, which is of the

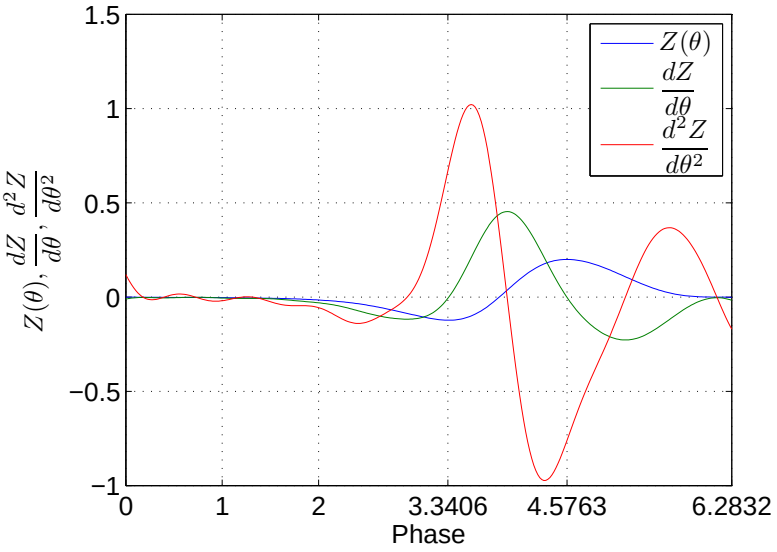

Figure 3.4: The Hodgkin-Huxley PRC $Z(\theta)$ and its derivatives, $\frac{dZ}{d\theta}$ and $\frac{d^2Z}{d\theta^2}$

YXY form, and the resulting phase trajectory for the control amplitude bound $M = 0.7\mu Acm^{-2}$ are shown in Figure 3.5. The charge-balanced maximum-time controls can take the bang-bang or the bang-sigular-bang form depending on the bound M. The cases for $M = 0.7\mu Acm^{-2}$ and $M = 3.0\mu Acm^{-2}$ are illustrated in Figures 3.6 and 3.7 respectively. The derivations of these optimal controls are given in following sections.

Charge-Balanced Minimum-Time Control for Hodgkin-Huxley Phase Model

The Hodgkin-Huxley PRC given in Figure 3.4 has at most two singular trajectories (points), $\theta_{s,1} = 3.34$ and $\theta_{s,2} = 4.58$, calculated by the condition $\frac{\partial Z(\theta)}{\partial \theta} = 0$. According to the shape of this PRC, there exist at most two switching points satisfying $Z(\theta) = \alpha$, where α is a constant defined in (3.12). Since the minimum-time control takes the bang-bang form as shown in Section 3.2.1, it requires to calculate the switching points and determine the type of the switching at these points for the optimal control synthesis. At the switching points, $\dot{\phi} = -\partial Z/\partial\theta$ is given by (3.15), and hence a Y to X switch may occur in the region $R_1 = [0, \theta_{s,1}]$ or $R_3 = [\theta_{s,2}, 2\pi]$, and an X to Y switch may occur in $R_2 = [\theta_{s,1}, \theta_{s,2}]$. This implies that bang-bang controls with one switch, such as the XY or YX form, are not feasible solutions because these controls

will violate the charge-balance constraint. Consequently, the optimal control has two switching points, and the candidate is either a YXY trajectory with one switch in the interval R_1 and one in R_2, or an XYX trajectory with one switch in R_2 and one in R_3. We can further simplify the possible intervals of switching by observing the shape of the PRC. The Hodgkin-Huxley PRC depicted in 3.4 has three zeros at $\theta_{r,1} = 0$, $\theta_{r,2} = 3.86$, and $\theta_{r,3} = 2\pi$. Therefore, for an optimal YXY trajectory the first and the second switch will occur in $[0, \theta_{s,1}]$ and $[\theta_{s,1}, \theta_{r,2}]$, respectively, and for an optimal XYX trajectory, they will occur in $[\theta_{r,2}, \theta_{s,2}]$ and $[\theta_{s,2}, 2\pi]$, respectively. The minimum-time control is then selected between these two. Note that for a given bound M, it may not be possible to have both XYX and YXY solutions. For example, if the bound is $M = 0.7$, then the only feasible optimal solution is YXY. In this case, the two switching points θ_1 and θ_2 can be calculated through

$$0 = \int_0^{\theta_1} \frac{M}{\omega + MZ(\theta)} d\theta + \int_{\theta_1}^{\theta_2} \frac{-M}{\omega - MZ(\theta)} d\theta + \int_{\theta_2}^{2\pi} \frac{M}{\omega + MZ(\theta)} d\theta, \tag{3.27}$$

$$Z(\theta_1) = Z(\theta_2), \tag{3.28}$$

and the control is then given by

$$I^*_{min} = \begin{cases} M, & 0 \le \theta \le \theta_1, \\ -M, & \theta_1 < \theta < \theta_2, \\ M, & \theta_2 \le \theta \le 2\pi. \end{cases}$$

Charge-Balanced Maximum-Time Control for Hodgkin-Huxley Phase Model

In the case of the maximum-time control, the two singular points, $\theta_{s,1}$ and $\theta_{s,2}$, are candidates for the optimal trajectory because they are slower than the bang trajectories as proved in Section 3.3.1. Letting $\dot{\theta} = 0$ in (3.1), we find the controls that keep the trajectory at the singular points are $I_{s,1} = -\frac{\omega}{Z(\theta_{s,1})} = 3.50$ and $I_{s,2} = -\frac{\omega}{Z(\theta_{s,2})} = -2.15$. There exist three cases when constructing maximum-time controls according to M and thus to the feasibility of $I_{s,1}$ and $I_{s,2}$.

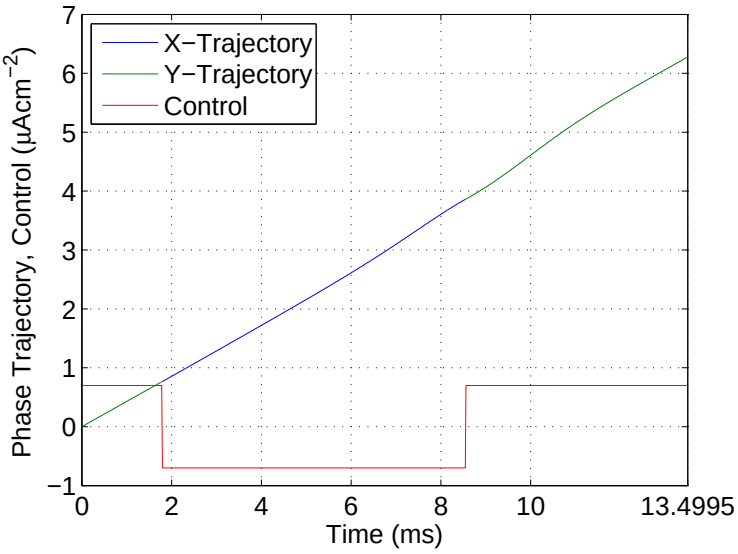

Figure 3.5: The charge-balanced minimum-time control and the corresponding phase trajectory for the Hodgkin-Huxley phase model with respect to the bound on the control amplitude $M = 0.7\ \mu Acm^{-2}$.

(Case I: $M < |I_{s,2}|$) In this case, both the singular points $\theta_{s,1}$ and $\theta_{s,2}$ are infeasible. Therefore, the optimal control is bang-bang and is in fact the opposite of the minimum-time control described above. Similar to the minimum-time case, we can calculate the corresponding XYX and YXY solutions and choose the maximum time achieved between these scenarios. For example, consider the bound $M = 0.7$, then the only solution is XYX and the two switching points are calculated by substituting M with $-M$ in (3.27) and solving (3.27) and (3.28). The optimal bang-bang control is then given by

$$I^*_{max} = \begin{cases} -M, & 0 \leq \theta < \theta_1, \\ M, & \theta_1 \leq \theta \leq \theta_2, \\ -M, & \theta_2 < \theta \leq 2\pi. \end{cases}$$

(Case II: $|I_{s,2}| \leq M < |I_{s,1}|$) In this case, $\theta_{s,2}$ is the only feasible singular trajectory (point) generated by the singular control $I_{s,2} = -2.15 < 0$. Because there are only two switching points allowed in the optimal trajectory, this together with the fact that $I_{s,2}$ is of negative charge forces the optimal control to take the "Y-singular-Y"

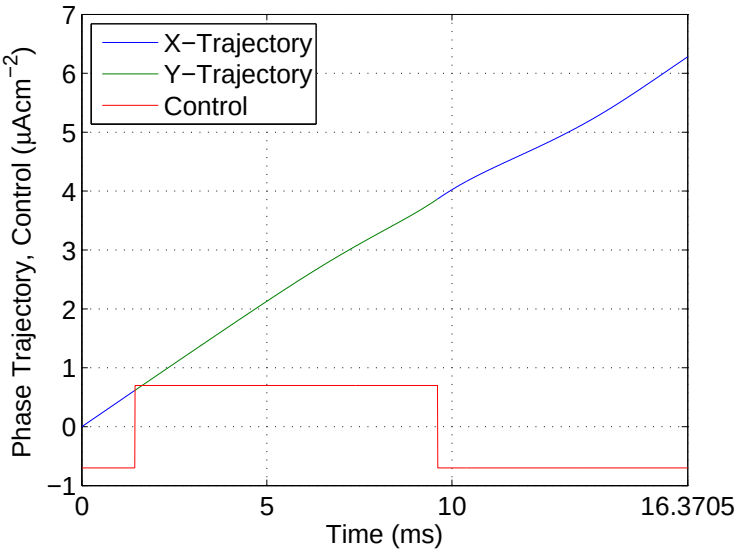

Figure 3.6: The charge-balanced maximum-time controls and the corresponding phase trajectories for $M = 0.7\ \mu Acm^{-2}$

form given by

$$I^*_{max} = \begin{cases} M, & 0 \leq \theta < \theta_{s,2}, \\ I_{s,2}, & \theta = \theta_{s,2}, \\ M, & \theta_{s,2} < \theta \leq 2\pi. \end{cases}$$

Similar to the SNIPER phase model described in Section 3.3.1, the time it takes to reach the singular point is given by,

$$t_1 = \int_0^{\theta_{s,2}} \frac{1}{\omega + Z(\theta)M} d\theta$$

and the time required to reach the target point 2π from the point $\theta_{s,2}$ is

$$t_3 = \int_{\theta_{s,2}}^{2\pi} \frac{1}{\omega + Z(\theta)M} d\theta.$$

The time during which the trajectory stays on $\theta_{s,2}$ is determined by the charge-balance constraint and is given by

$$t_2 = \left| \frac{(t_1 + t_3)M}{I_{s,2}} \right|.$$

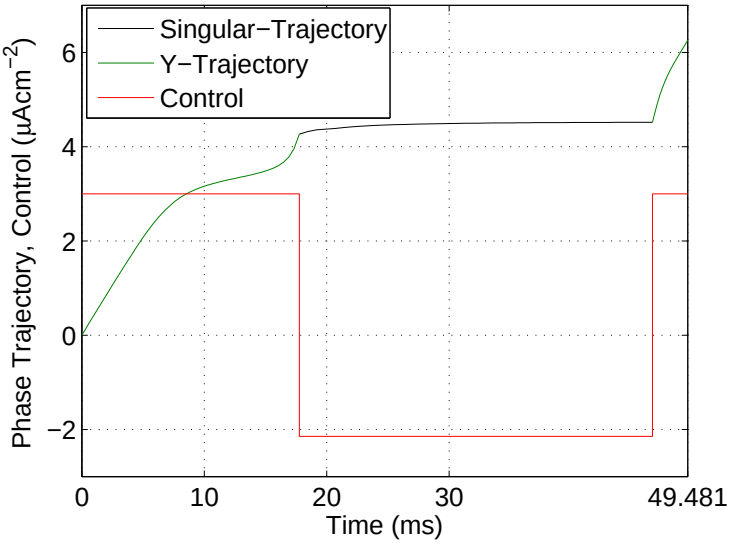

Figure 3.7: The charge-balanced maximum-time controls and the corresponding phase trajectories for $M = 3.0\ \mu Acm^{-2}$.

Now, the optimal control can be stated in terms of time as

$$I^*_{max} = \begin{cases} M, & 0 \leq t < t_1, \\ I_{s,2}, & t_1 \leq t \leq t_1 + t_2, \\ M, & t_1 + t_2 < t \leq t_1 + t_2 + t_3. \end{cases} \tag{3.29}$$

(Case III: $|I_{s,1}| \leq M$) In this case, staying on either singular point is possible by using an appropriate control. Furthermore, since the two singular controls have opposite signs, the charge-balance constraint can be preserved by staying for an appropriate time period at each singular point. As a result, the spiking time can be arbitrarily delayed, which may not be of practical interest due to the requirement of relatively high amplitude.

3.3.3 Morris-Lecar Phase Model

We consider a Morris-Lecar system with parameter values given in Section 1.1.2, which has a natural frequency $\omega = 0.283\, rad/ms$. The PRC is approximated by

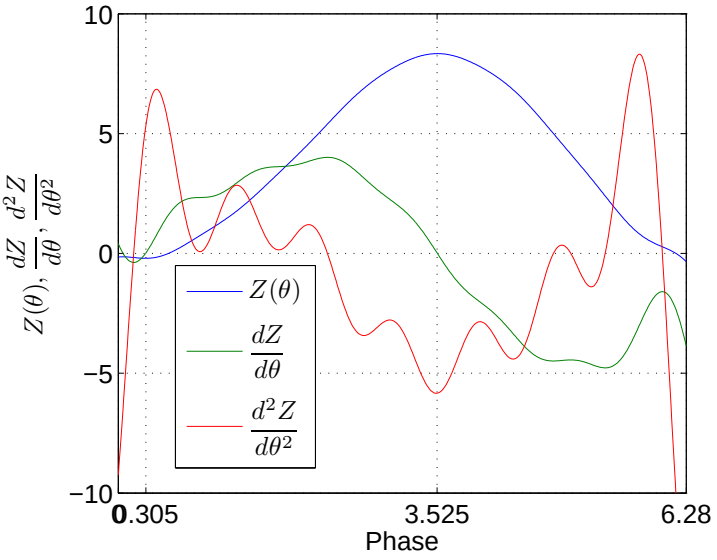

Figure 3.8: 3.8 The Morris-Lecar PRC $Z(\theta)$ and its derivatives, $\frac{dZ}{d\theta}$ and $\frac{d^2Z}{d\theta^2}$.

(3.26) with the coefficients shown in 3.2 is illustrated, with its derivatives, in Figure 3.8.

i	1	2	3	4	5	6	7	8
a_i	5.137	5.773	0.7703	1.065	0.8143	0.1028	0.09711	0.0698
b_i	0.4356	0.7105	2.185	3.09	3.362	4.876	5.829	6.525
c_i	1.005	-1.474	0.6535	1.238	3.585	2.154	2.375	3.446

Table 3.2: The coefficients of the equation (3.26) for the Morris-Lecar PRC

Three examples are made to show the different structures of the optimal controls that are associated with various values of the control amplitude M for the Morris-Lecar phase model. The charge-balanced minimum-time control and the resulting phase trajectory for $M = 0.01\ \mu Acm^{-2}$ are given in Figure 3.9. The charge-balanced maximum-time controls and the respective trajectories subject to $M = 0.005\ \mu Acm^{-2}$ and $M = 0.04\ \mu Acm^{-2}$ are given in Figures 3.10 and 3.11, respectively. The derivations of these optimal controls follow a similar procedure presented in Section 3.3.2.

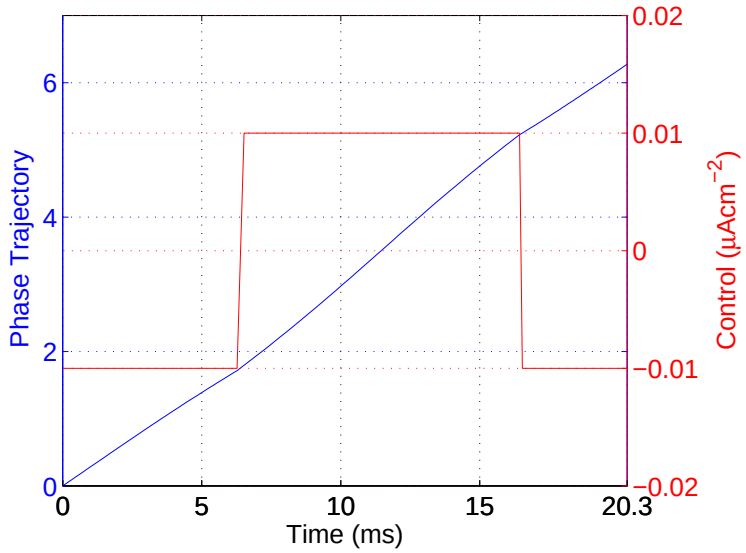

Figure 3.9: The charge-balanced minimum-time control and the corresponding phase trajectory for the Morris-Lecar phase model with respect to the bound on the control amplitude $M = 0.01\ \mu Acm^{-2}$

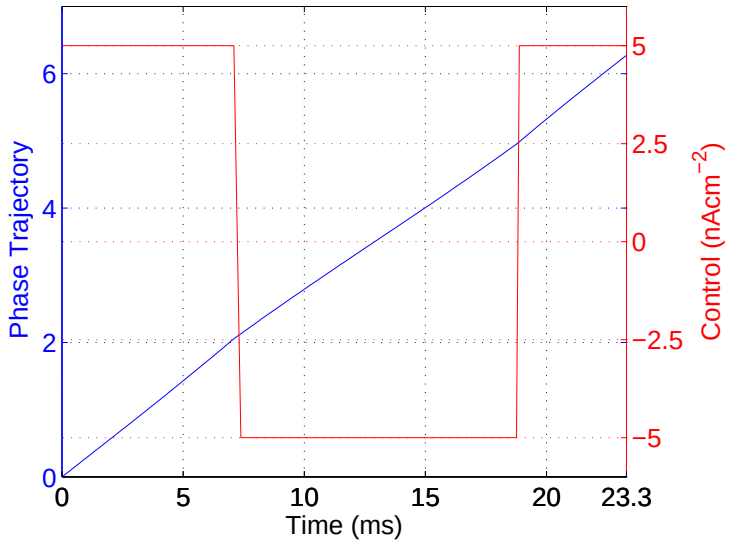

Figure 3.10: show the charge-balanced maximum-time controls and the corresponding phase trajectories with $M = 0.005\ \mu Acm^{-2}$

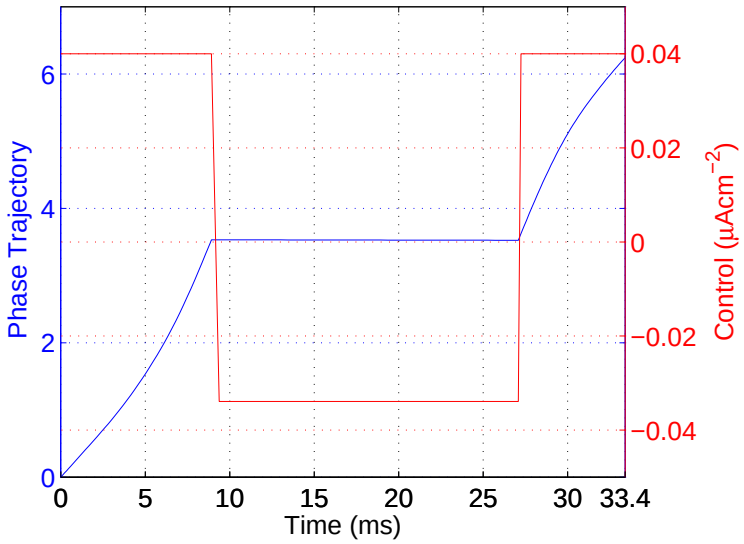

Figure 3.11: show the charge-balanced maximum-time controls and the corresponding phase trajectories with $M = 0.04\ \mu A cm^{-2}$, respectively.

3.4 Validation of Phase Model Reduction to Full State-Space Model

Because phase models of importance to applications are reductions of original higher dimensional state-space systems, we explore in this section the extent to which controls synthesized using the former can achieve the desired objectives when applied to the latter. This will provide insight into the limits of the model reduction with respect to control synthesis, and allow the relationship to be calibrated for practical applications where the weak forcing assumption must be relaxed. Such an important validation is largely lacking in the literature.

We validate our optimal control strategies derived based on the phase models with the corresponding original state-space models. Specifically, we consider the Hodgkin-Huxley model. Note that an analytical derivation of the optimal controls directly from the state-space models is in general intractable and computationally expensive. A validation of the minimum and maximum spiking times with respect to the bound on the control amplitude is depicted in Figure 3.12, where the feasible spiking times are indicated as the shaded area. Each asterisk point on this graph represents the

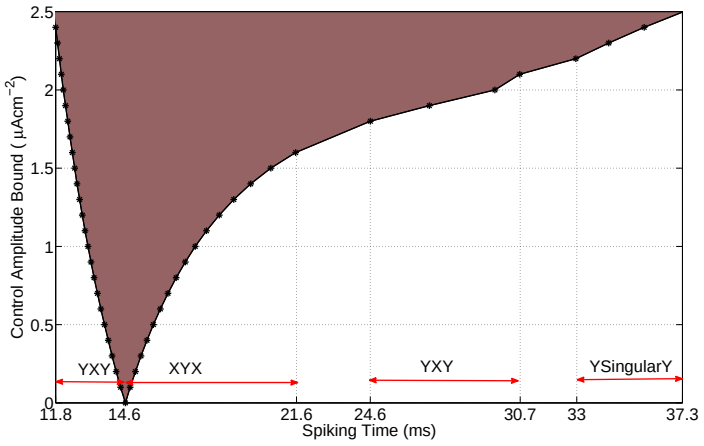

Figure 3.12: A characterization of the realizable spiking times with respect to the bound on the control amplitude, $M \in [0, 2.5]$, for the Hodgkin-Huxley phase model. The shaded region indicates the feasible spiking range resulting from the minimum- and maximum-time controls. Those minimum times (left to the natural spiking time $T_0 = 14.6\ ms$) are obtained by YXY controls and maximum-times (right to T_0) are obtained by XYX, YXY and Y-singular-Y controls depending on M.

Hodgkin-Huxley neuron spiking time achieved by a particular form of the optimal control. The points correspond to minimum spiking times, which are less than the natural spiking time $T_0 = 14.64\ ms$, are obtained by YXY controls, whereas the points correspond to maximum spiking times may be obtained by three structurally different controls, i.e., XYX, YXY, and Y-singular-Y controls. This figure illustrates the limits on possible spiking times of the Hodgkin-Huxley model, which is important to the design of practical control inputs. For example, in Chapter 4 we use the knowledge of the feasible spiking range when characterizing the minimum power controls.

The optimal controls derived based on the Hodgkin-Huxley phase model, shown in 3.5 and 3.6, are applied to the full Hodgkin-Huxley model, and a repeated application of such controls results in the desired spiking trains as displayed in 3.13 and 3.15. The respective minimum and maximum spiking times induced from these optimal controls subject to the amplitude bound $M = 0.7\ \mu Acm^{-2}$ are 13.5 ms and 16.37 ms in the phase model and 13.65 ms and 17.13 ms in the full state-space model. Such an inconsistence is due to the model reduction, however, the resulting spiking behavior of the full Hodgkin-Huxley model shows great qualitative agreement with that of the

Figure 3.13: Uncontrolled and controlled spiking trains for minimum time with amplitude $M = 0.7\ \mu Acm^{-2}$ of Hodgkin-Huxley neuron.

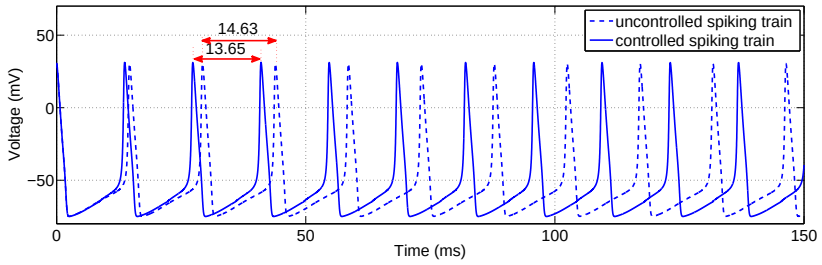

Figure 3.14: Uncontrolled and controlled spiking trains for maximum time with amplitude $M = 0.7\ \mu Acm^{-2}$ of Hodgkin-Huxley neuron.

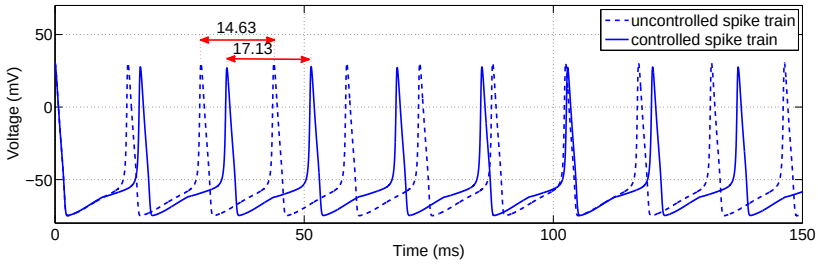

Figure 3.15: Application of derived optimal controls according to phase models to full Hodgkin-Huxley model

phase model. The variation of the absolute errors between the actual and designed spiking times is shown in 3.16, where the spiking behavior predicted based on the phase model matches better the full state-space model towards the weak forcing region.

3.5 Conclusion

In this chapter, we investigated time-optimal controls for phase models of spiking neuron oscillators. In particular, we derived charge-balanced controls that lead to the minimum and the maximum inter-spike time of a neuron for a given bound on the control amplitude. We showed that such optimal controls involve bang-bang and bang-singular-bang structures depending on the allowable control amplitude. Although the amplitude level of weak forcing in the phase model is not practically

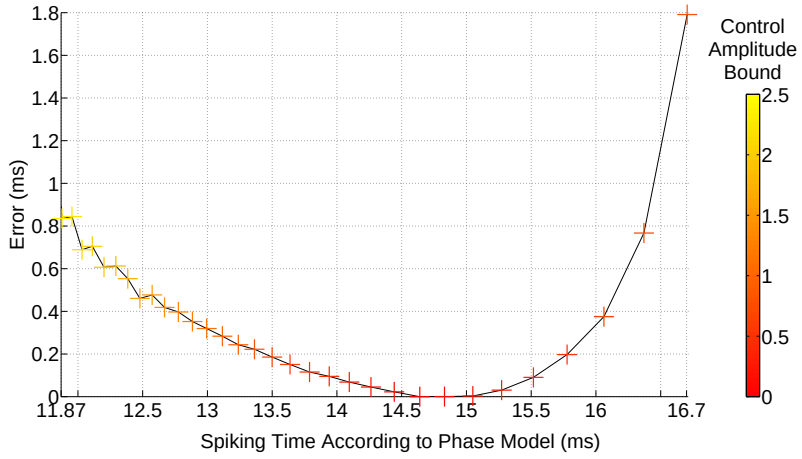

Figure 3.16: The absolute error in the spiking time when applying the charge-balanced time-optimal controls derived based on the Hodgkin-Huxley phase model to its full state-space model. The bound of the control amplitude is indicated as the color bar.

quantifiable and can be greatly dependent on the dynamics of the system, our optimal control solutions were constructed for an arbitrary choice of bounds on the control amplitude, which accounts for this practical issue. We apply the derived optimal spike timing controls to commonly-used phase models of oscillatory neurons to demonstrate their applicability to neuroscience. The methodology presented in this chapter is general and can be applied not only to oscillatory neuron systems, but also to any oscillating system that can be represented by phase models including biological, chemical, electrical, and mechanical oscillators.

The theoretical results of this work characterize the fundamental limits on neuron spiking times that can be achieved by the use of a charge-balanced bounded external input, and have potential impact on the improvement and development of innovative therapeutic procedures for neurological disorders.

Chapter 4

Charge-Balanced Minimum-Power Controls for Spiking Neuron Oscillators

In this chapter, we study the optimal control of phase models for spiking neuron oscillators. We focus on the design of minimum-power current stimuli that elicit spikes in neurons at desired times. We furthermore take the charge-balance constraint into account because in practice undesirable side effects may occur due to the accumulation of electric charge resulting from external stimuli. Charge-balanced minimum-power controls are derived for a general phase model using the maximum principle, where the cases with unbounded and bounded control amplitude are examined. The latter is of practical importance since phase models are more accurate for weak forcing. The developed optimal control strategies are then applied to both mathematically ideal and experimentally observed phase models to demonstrate their applicability, including the phase model for the widely studied Hodgkin-Huxley equations.

4.1 Introduction

The electrical activity of the nervous system and its ability to respond to external electrical signals have been long-standing subjects of active research. The resulting insights have led to the innovation of therapeutic procedures for a wide variety of neurological disorders. Deep brain stimulation is one such method, in which electrical pulses are applied to inhibit pathological synchrony among the neurons [85]

and is clinically approved in many countries for the treatment of Parkinson's disease, essential tremor, and Dystonia [4, 87]. The cardiac pace maker is another example in medical practices that employs electric pulses to stimulate nervous tissues in order to regulate a patient's heart rate [71, 72]. In these and many other neurological applications, the use of low power electrical stimuli is desired because, for example, high power stimuli are harmful to biological tissues and the reduction of power consumption in a neurological implant is essential in order to reduce its size and lengthen its lifetime. In addition, it is of clinical importance to ensure that any external inputs, e.g., currents, applied to stimulate neurons are charge-balanced. That is, the net amount of the electric charge injected into a neuron over one oscillation cycle should be kept zero, because high levels of the charge accumulation may trigger irreversible electro-chemical reactions, resulting in damage of neural tissues and corrosion of electrodes [88].

Many mathematical models have been developed to capture periodic activities of neuron oscillators [52, 109, 92, 130] and a well established example is the phase model that we explained in Section 1.2, which quantifies the asymptotic phase shift of an oscillator due to an infinitesimal perturbation of its state [11]. A phase model accurately approximates the behavior of the corresponding full state-space system in the neighborhood of its periodic orbit [60]. Due to their simplicity, phase models are very popular for modeling and analyzing the dynamics of neuron oscillators. For example, synchronization patterns resulting from the dynamics of an arbitrary network of oscillators with weak coupling have been analyzed based on phase models [3, 128]. In these studies, the inputs to the oscillatory systems were initially defined, and the dynamical responses of neuron populations were analyzed in detail. Recently, as an alternative objective, control and dynamical systems approaches have been used to manipulate neural activities in a desired way. For instance, minimum-power controls for spiking neurons at specified time instances were derived for some mathematically ideal phase models [21, 90] and charge-balanced controls were calculated using a numerical shooting method [95]. In addition, controllability of a network of neurons described by phase models has also been investigated [84].

In this chapter, we consider a general phase model and derive charge-balanced minimum-power controls for spiking a neuron oscillator at a desired time instance different from its natural spiking time. Both cases of unbounded and bounded control amplitude

are examined. The latter is of fundamental and practical importance because there exist physical limitations on medical equipment and safety margins for neural tissues and, more importantly, phase models are valid under weak forcing. We show that the bounded optimal control has switching characteristics synthesized by the unbounded optimal control and the given control bound. The developed optimal control strategies are then applied to both mathematically ideal and experimentally observed PRCs to demonstrate their applicability. Moreover, we apply the optimal controls derived from phase reduced models to the corresponding full state-space models to verify the consistency of these models through the reduction and demonstrate the robustness of our optimal control techniques. Such an important validation is missing in the literature.

This chapter is organized as follows. In Section 4.2, we present the optimal control problem of spiking a general phase oscillator. We find the charge-balanced minimum-power control for a prescribed spiking time with and without a constraint on the control amplitude by using the maximum principle [7]. In Section 4.3, we apply the derived optimal control strategies to several commonly-used phase models and present the optimal solutions and numerical simulations. In particular, we calculate optimal controls for experimentally observed PRCs including Morris-Lecar and Hodgkin-Huxley PRCs. Note that, although the theory presented in this work is motivated by neurological applications, it can be applied to broader class of oscillating systems that can be represented by phase models.

4.2 Optimal Control Problem Formulation

We consider spiking a neuron at a prescribed time with a minimum-power stimulus and, furthermore, intend to find a charge-balanced one in order to minimize the side-effects cause by the accumulation of electric charge. The design of such charge-balanced minimum-power current stimuli for spiking neurons gives rise to a

constrained optimal steering problem for a single-input nonlinear system of the form

$$\begin{aligned} \min_{I(t)} \quad & \int_0^T I(t)^2 dt, \\ \text{s.t.} \quad & \dot{\theta} = f(\theta) + g(\theta) I(t), \\ & \dot{p} = I(t), \\ & \theta(0) = 0, \quad \theta(T) = 2\pi, \\ & p(0) = 0, \quad p(T) = 0, \quad |I(t)| \leq M, \end{aligned} \tag{4.1}$$

where $M \in \mathbb{R}^+$ defines the bound of the control amplitude, and the time-dependent variable $p(t) = \int_0^t I(\sigma) d\sigma$, with boundary conditions $p(0) = p(T) = 0$, is introduced to accommodate the charge-balance constraint. In the following, we first consider the case of an unbounded control and then extend the result to the case when the control is bounded. In chapter 2, we considered some specific phase models and designed minimum-power stimuli that alter the neuron spiking time to a desired value without the charge-balance constraint. In this chapter, we generalize our method to general phase model given by $\dot{\theta} = f(\theta) + g(\theta) I(t)$ and introduce the charge-balance constraint into the optimal control problem. Consideration of charge-balance constraint significantly alter the previous optimal control problem by adding an extra dimension to the system. We were able to analytically find the minimum-power control for this two-dimensional nonlinear system by adopting the Pontryagin's maximum principle.

4.2.1 Derivation of Charge-Balanced Minimum-Power Controls

Relaxing the amplitude constraint with $|I(t)| < \infty$, we apply the maximum principle, as given in Appendix A, to characterize the extremal trajectories. The Hamiltonian of the optimal control problem presented in Section 4.2 is given by

$$H = \lambda_0 I^2 + \lambda (f(\theta) + g(\theta) I) + \mu I, \tag{4.2}$$

where λ_0, λ, and μ are Lagrange multipliers associated with the Lagrangian, system dynamics, and the charge-balance constraint, respectively. Here we consider normal extremals which are found by taking $\lambda_0 \neq 0$. Note that more specific abnormal

extremals found by letting $\lambda_0 = 0$ can be analyzed according to the expressions and properties of the functions f and g. Our derivations here are made for the general phase model, and therefore these extraordinary cases are omitted. Therefore, without loss of generality, we let $\lambda_0 = 1$. The optimality condition from the maximum principle demands that $\frac{\partial H}{\partial I} = 0$ along the optimal trajectory, which yields

$$I = -\frac{\lambda g(\theta) + \mu}{2}. \tag{4.3}$$

The adjoint variables λ and μ are solutions to the time-varying differential equations $\dot{\lambda} = -\frac{\partial H}{\partial \theta}$ and $\dot{\mu} = -\frac{\partial H}{\partial p}$. Together with (4.3) these equations can be written as

$$\dot{\lambda} = -\lambda \frac{\partial f(\theta)}{\partial \theta} + \frac{\lambda(\lambda g + \mu)}{2} \frac{\partial g(\theta)}{\partial \theta}, \tag{4.4}$$

$$\dot{\mu} = 0, \tag{4.5}$$

which implies that μ is a constant. In addition, since the Hamiltonian is not explicitly dependent on time, H is a constant along the optimal trajectory. Hence, we let $H = c$, $\forall\, t \in [0, T]$. This can be seen from the transversality condition of the maximum principle.

It follows that the optimal multiplier λ can be found from (4.2) by substituting (4.3) for I. Then, solving for λ yields

$$\lambda = \frac{-\mu g + 2f \pm 2\sqrt{f^2 - g\mu f - g^2 c}}{g^2}. \tag{4.6}$$

Here we will choose the negative square root because the positive case corresponds to a backward evaluation of the phase, which would invalidate the phase model. The phase velocity equation along the optimal trajectory can then be found by using (4.6), (4.3), and (4.1), resulting in

$$\dot{\theta} = \sqrt{f^2 - g\mu f - g^2 c}. \tag{4.7}$$

In addition, substituting (4.6) into (4.3) gives rise to the optimal control I^* in terms of the two constants μ and c,

$$I^* = \frac{-f + \sqrt{f^2 - g\mu f - g^2 c}}{g}. \tag{4.8}$$

For a given spiking time T, the constants c and μ can be determined from (4.7) by separation of variables together with the charge-balance constraint written as $\int_0^{2\pi} \frac{I^*(\theta)}{\dot{\theta}} d\theta = 0$, which yields

$$T = \int_0^{2\pi} \frac{1}{\sqrt{f^2 - g\mu f - g^2 c}} d\theta, \tag{4.9}$$

and

$$\int_0^{2\pi} \frac{-f + \sqrt{f^2 - g\mu f - g^2 c}}{g\sqrt{f^2 - g\mu f - g^2 c}} d\theta = 0. \tag{4.10}$$

Now the optimal control is completely classified by (4.8), because the constants μ and c can be found from (4.9) and (4.10) for any specified spiking time T.

Remark 1 *In the absence of the charge-balance constraint, corresponding to $\mu = 0$, it is sufficient to characterize the optimal control by* (4.8) *and* (4.9).

4.2.2 Charge-Balanced Minimum-Power Control with Constrained Amplitude

In practice, the feasible amplitude of the stimulus is limited, and phase models are valid only for weak forcing. Therefore, spiking neurons with controls of bounded amplitude is of practical importance. In this case where we assume that $|I| \leq M$, $\forall\ t \in [0, T]$, the minimum and maximum possible spiking times for a neuron system can be determined according to the procedure in [23, 22]. It is easy to see that for a given bound $M > 0$, the minimum spiking time without the charge-balanced

constraint is achieved by

$$I^*_{T_{min}} = \begin{cases} M, & g(\theta) \geq 0 \\ -M, & g(\theta) < 0, \end{cases} \tag{4.11}$$

which keeps the phase velocity at its maximum. The minimum spiking time for a given value of M, denoted by T^M_{min}, is then given by

$$T^M_{min} = \int\limits_{\theta \in \mathcal{A}} \frac{1}{f(\theta) + g(\theta)M} d\theta + \int\limits_{\theta \in \mathcal{B}} \frac{1}{f(\theta) - g(\theta)M} d\theta, \tag{4.12}$$

where $\mathcal{A} = \{\theta |\ g(\theta) \geq 0, 0 \leq \theta \leq 2\pi\}$ and $\mathcal{B} = \{\theta |\ g(\theta) < 0, 0 \leq \theta \leq 2\pi\}$. Symmetric to the minimum spiking time, the maximum spiking time, denoted T^M_{max}, for the bound M can be found by applying the opposite control $-I^*_{T_{min}}$, for $M < \min\{|\frac{f(\theta)}{g(\theta)}| : \theta \in [0, 2\pi)\}$, and it is given by $T^M_{max} = T^{-M}_{min}$. Note that, theoretically, arbitrarily large spiking times are achievable if the bound $M \geq \min\{|\frac{f(\theta)}{g(\theta)}| : \theta \in [0, 2\pi)\}$. The derivation of the minimum and maximum spiking times with both charge-balance and amplitude bound constraints is more involved and can be done according to [23, 22].

It is obvious that if $|I^*(\theta)| \leq M$, $\forall\, \theta \in [0, 2\pi)$, then the amplitude constraint is inactive and I^* as in (4.8) is the charge-balanced minimum-power control. While $|I^*| > M$ for some $\theta \in [0, 2\pi)$, it is sufficient to consider the case when $I^* > M$ because the case $I^* < -M$ is symmetric. Suppose that $I^* > M$ for $\theta \in (\theta_1, \theta_2) \subset [0, 2\pi)$, we now show that the bang control $I = M$ is optimal for $\theta \in [\theta_1, \theta_2]$. Since the Hamiltonian (4.2) is a convex function of I, $I = M$ is then the minimizer when $I^* > M$ for $\theta \in [\theta_1, \theta_2]$. In this case, we have, from (4.2), the Lagrange multiplier

$$\lambda = \frac{c - M^2 - \mu M}{f(\theta) + Mg(\theta)}, \tag{4.13}$$

which satisfies the adjoint equation (4.4), and hence $I(\theta) = M$ is optimal for $\theta \in [\theta_1, \theta_2]$. Similarly, the same approach can be used to show that $I = -M$ is optimal on the interval over which $I^* < -M$. Therefore, the charge-balanced minimum-power

control with limited control amplitude M is of the form with switching characteristic

$$I_M^*(\theta) = \begin{cases} -M, & I^*(\theta) < -M \\ I^*(\theta), & -M \leq I^*(\theta) \leq M \\ M, & I(\theta)^* > M. \end{cases} \tag{4.14}$$

The switching phases $\theta_i, \theta_j \in [0, 2\pi)$ such that $I^*(\theta_i) = -M$ and $I^*(\theta_j) = M$ can be computed (see the examples in Section 4.3) and the required parameter values μ and c can be calculated according to the specified spiking time and the charge-balance constraint from the equations

$$T = \int_0^{2\pi} \frac{1}{f(\theta) + g(\theta) I_M^*} d\theta \tag{4.15}$$

and

$$0 = \int_0^{2\pi} \frac{I_M^*}{f(\theta) + g(\theta) I_M^*} d\theta. \tag{4.16}$$

Remark 2 *Since the Hamiltonian has a linear term with respect to control I, it is possible to have admissible singular trajectories with sufficiently large control amplitudes. Such complicated scenarios are discussed for specific f and g functions in following Sections.*

4.3 Examples

We now apply our optimal control strategies to several commonly-used phase models characterized by various PRCs, including mathematically ideal models, such as SNIPER PRC, sinusoidal PRC, and theta neuron model, as well as more realistic phase models such as Hodgkin-Huxley and Morris-Lecar PRCs. These mathematically ideal phase models are approximations to full state-space models at certain bifurcation points, whereas Hodgkin-Huxley and Morris-Lecar phase models are obtained numerically by perturbing their periodic orbits using unit impulses.

4.3.1 SNIPER Phase Model

The SNIPER phase model as given in Section 1.2.4 is characterized by a type I PRC and is of the form [11],

$$\dot{\theta} = \omega + z_d(1 - \cos\theta)I, \tag{4.17}$$

where ω is the natural oscillation frequency of the system, z_d is a model-dependent constant, and I is the external stimulus. Neurons described by this phase model spike periodically with the natural period $T_0 = 2\pi/\omega$ in the absence of any external input.

Unbounded Control for SNIPER Phase Model

Substituting $f = \omega$ and $g = z_d(1 - \cos\theta)$ into (4.8), (4.9), and (4.10), the optimal control for spiking a neuron modeled by the SNIPER phase model at time T satisfying the charge-balance constraint is given by,

$$I^* = \frac{-\omega + \sqrt{\omega^2 - \mu\omega z_d(1 - \cos\theta) - cz_d^2(1 - \cos\theta)^2}}{z_d(1 - \cos\theta)}, \tag{4.18}$$

where the constants c and μ can be obtained by simultaneously solving

$$T = \int_0^{2\pi} \frac{1}{\sqrt{\omega^2 - \mu\omega z_d(1 - \cos\theta) - cz_d^2(1 - \cos\theta)^2}} d\theta, \tag{4.19}$$

$$\int_0^{2\pi} \frac{-\omega + \sqrt{\omega^2 - \mu\omega z_d(1 - \cos\theta) - cz_d^2(1 - \cos\theta)^2}}{z_d(1 - \cos\theta)\sqrt{\omega^2 - \mu\omega z_d(1 - \cos\theta) - cz_d^2(1 - \cos\theta)^2}} d\theta = 0. \tag{4.20}$$

We use a simple example to demonstrate these results. Consider a neuron with the natural oscillation frequency $\omega = 1$ and take $z_d = 1$, then the optimal controls with and without the charge-balance constraint for the desired spiking times $T = 5.3$ and $T = 7.8$, smaller and greater, respectively, than the natural spiking time $T_0 = 2\pi$ are shown in Figure 4.1. The corresponding optimal phase trajectories are depicted in Figure 4.2. Note that optimal controls without considering the charge-balance constraint are obtained by taking $\mu = 0$ in (4.18), and in this case we only need to calculate the constant c using (4.19).

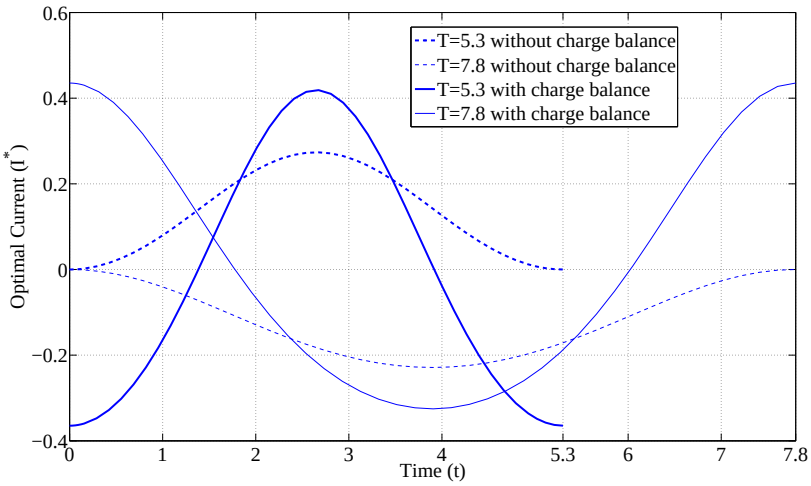

Figure 4.1: Unbounded optimal controls with and without the charge-balance constraint for spiking a SNIPER neuron with $\omega = 1$ and $z_d = 1$ at $T = 5.3$ $T = 7.8$

Remark 3 *Consider the case of abnormal extremals for the SNIPER phase model, where the multiplier* $\lambda_0 = 0$. *Then, the Hamiltonian as in* (4.2) *is given by* $H = \lambda\omega + \lambda z_d(1 - \cos\theta)I + \mu I$, *and the optimality condition of the maximum principle gives*

$$\frac{\partial H}{\partial I} = \lambda z_d(1 - \cos\theta) + \mu = 0. \tag{4.21}$$

Differentiating this equation with respect to time, we obtain

$$\lambda z_d(\sin\theta)\dot{\theta} + \dot{\lambda} z_d(1 - \cos\theta) + \dot{\mu} = 0. \tag{4.22}$$

Adjoint equation for abnormal trajectories are given by,

$$\dot{\lambda} = - z_d\lambda \sin\theta I, \tag{4.23}$$

$$\dot{\mu} = 0, \tag{4.24}$$

and substituting (4.17), (4.23), *and* (4.24) *into* (4.22) *for* $\dot{\theta}, \dot{\lambda}$, *and* $\dot{\mu}$, *respectively, yields*

$$\omega\lambda z_d \sin\theta = 0. \tag{4.25}$$

Abnormal extremals must satisfy (4.25), *and it is clear that* (4.25) *holds only when* $\lambda \equiv 0$ *if* $\theta \neq 0, \pi, 2\pi$. *This leads to* $\mu \equiv 0$ *from* (4.21), *which, together with* $\lambda \equiv 0$, *violates the nontriviality condition of the maximum principle. Therefore, only*

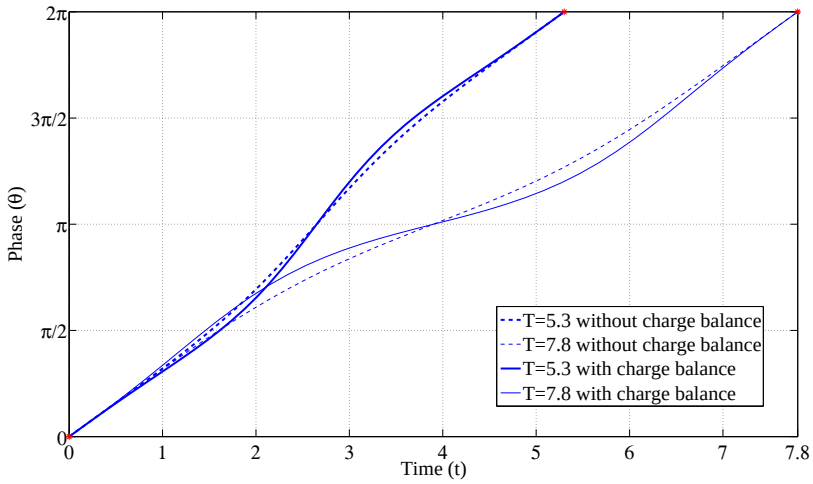

Figure 4.2: The optimal charge-balanced phase trajectories for SNIPER neuron with $\omega = 1$ and $z_d = 1$ at $T = 5.3$ $T = 7.8$.

abnormal trajectories are (in this case abnormal points), $\theta = 0$, $\theta = \pi$, and $\theta = 2\pi$. The points $\theta = 0$ and $\theta = 2\pi$ are infeasible abnormal points, at which the nonzero phase velocity, $\dot{\theta} = \omega$, immediately forces the system away from these points, Hence, $\theta_{ab} = \pi$ is the only possible abnormal point, and the control $u = -\omega/Z(\theta_{ab}) = -\omega/(2z_d)$ yields $\dot{\theta} = 0$ at θ_{ab}, making the system stay at θ_{ab}. Since $\dot{\theta}_{ab} = 0$, this point is not a candidate for optimality when decreasing the spiking time, but this trajectory is particularly interested when increasing the spiking time with bounded controls where it can be used to define the absolute maximum spiking time with the charged-balance constraint.

Bounded Control for SNIPER Phase Model

Having an amplitude constraint $|I(t)| \leq M$, $\forall\, t \in [0, T]$, the minimum and maximum possible spiking times are limited as described in Section 4.2.2 and they can explicitly calculated by the procedures described in Chapter 3 [23, 22]. For infeasible spiking times, there exist no simultaneous solutions to (4.15) and (4.16), which give valid c and μ values. Given a bound of control amplitude M, the bounded charge-balanced minimum-power control for spiking a SNIPER neuron to achieve a desired feasible spiking time can be constructed according to (4.14), (4.15) and (4.16) with $f = \omega$ and $g = z_d(1 - \cos\theta)$. More specifically, for example, consider spiking the SNIPER

neuron with $\omega = 1$ and $z_d = 1$ at $T = 5.3$ subject to $M = 0.4$. It is clear from Figure 4.1 that the spiking time $T = 5.3$ is not feasible by the unbounded charge-balanced optimal control I^* since $I^* > M$ for some time interval. This overshoot implies the existence of two switching points θ_1 and θ_2 at which $I^* = M$. This together with (4.15) and (4.16) allow us to calculate the values of θ_1, θ_2, c, and μ by solving the following equations simultaneously,

$$
\begin{aligned}
M &= \frac{-\omega + \Delta(\theta_1)}{z_d(1-\cos\theta_1)}, \\
M &= \frac{-\omega + \Delta(\theta_2)}{z_d(1-\cos\theta_2)}, \\
T &= \int_0^{\theta_1} \frac{1}{\Delta(\theta)} d\theta + \int_{\theta_1}^{\theta_2} \frac{1}{\omega + z_d(1-\cos\theta)M} d\theta + \int_{\theta_2}^{2\pi} \frac{1}{\Delta(\theta)} d\theta, \\
0 &= \int_0^{\theta_1} \frac{-\omega + \Delta(\theta)}{z_d(1-\cos\theta)\Delta(\theta)} d\theta + \int_{\theta_1}^{\theta_2} \frac{M}{\omega + z_d(1-\cos\theta)M} d\theta + \int_{\theta_2}^{2\pi} \frac{-\omega + \Delta(\theta)}{z_d(1-\cos\theta)\Delta(\theta)} d\theta,
\end{aligned}
$$

where, $\Delta(\theta) = \sqrt{\omega^2 - \mu\omega z_d(1-\cos\theta) - c z_d^2 (1-\cos\theta)^2}$. We found $\theta_1 = 2.686$, $\theta_2 = 3.597$, $c = -0.968$, and $\mu = 0.733$, and the optimal control I_M^* is given by

$$
I_M^*(\theta) = \begin{cases} \frac{-\omega + \Delta(\theta)}{z_d(1-\cos\theta)}, & 0 \le \theta \le \theta_1 \\ M, & \theta_1 \le \theta \le \theta_2 \\ \frac{-\omega + \Delta(\theta)}{z_d(1-\cos\theta)}, & \theta_2 \le \theta \le 2\pi, \end{cases} \tag{4.26}
$$

which is depicted in Figure 4.3 as a function of time. Figure 4.3 also illustrates bounded charge-balanced minimum-power controls for spiking this SNIPER neuron at other spiking times that are greater and smaller than its natural spiking period $T_0 = 2\pi$. There are three structurally different controls presented, which have four, two, and zero switches, depending on the desired spiking time.

Remark 4 *For a fixed control amplitude bound $M > 0$, when we increase the spiking time, the minimum-power controls presented in Section 4.3.1 converge to the time-optimal controls given in Section 3.3.1 [23, 22]. For control amplitudes $M > \omega/(2z_d)$ the singular trajectory given in Section 3.3.1 [23, 22] coincides with the abnormal trajectory described in Remark 3.*

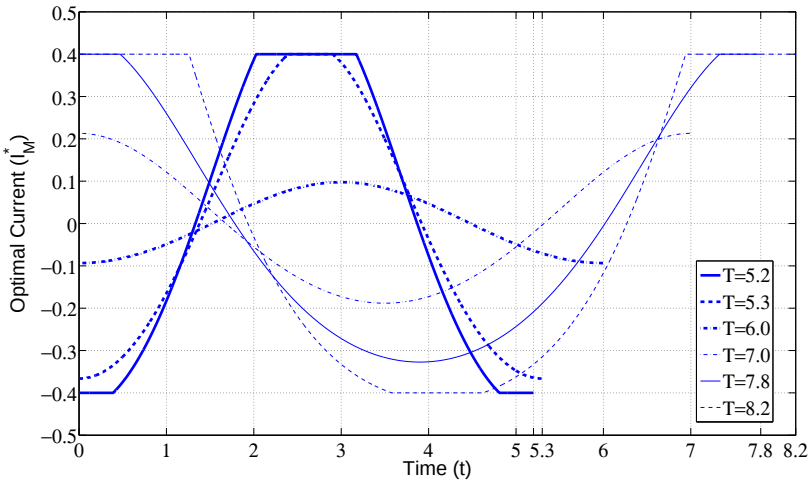

Figure 4.3: Optimal charge-balanced controls of minimum power given the control bound $M = 0.4$ for spiking a SNIPER neuron with $\omega = 1$ and $z_d = 1$ at $T = 5.2, 5.3, 6.0, 7.0, 7.8, 8.2$.

Remark 5 *Observe from* (4.8) *that for the canonical type II PRC, the sinusoidal phase model characterized by* $g(\theta) = z_d \sin\theta$ *and* $f(\theta) = \omega$ *[11],* $I^*(\theta)$ *is anti-symmetric around* $\theta = \pi$*, namely,* $I^*(\theta) = -I^*(\theta+\pi)$ *for* $0 \le \theta \le \pi$*, when the charge-balance constraint is not considered, i.e.,* $\mu = 0$*. Therefore, the minimum-power control for the sinusoidal phase model is automatically charge-balanced, and thus from* (4.8) *with* $\mu = 0$ *the optimal control is given by* $I^* = (-\omega + \sqrt{\omega^2 - cz_d^2 \sin^2\theta})/(z_d \sin\theta)$*, where* c *is specified by the desired spiking time* $T = \int_0^{2\pi} (\sqrt{\omega^2 - cz_d^2 \sin^2\theta})^{-1} d\theta$*. More detailed optimal control analysis for the sinusoidal phase model can be found in Section 2.3.1 [21].*

4.3.2 Theta Neuron Phase Model

Recall from the Section 1.2.4, the theta neuron phase model is defined by $f(\theta) = 1 + \cos\theta + (1 - \cos\theta)I_b$ and $g(\theta) = (1 - \cos\theta)$, where I_b is known as the neuron baseline current [90]. Here we focus on the case of $I_b < 0$. Similar to previous case, the unbounded and bounded charge-balanced minimum-power controls can be directly calculated by employing (4.8), (4.9), and (4.10), or (4.14), (4.15), and (4.16) in Section 4.2, respectively. Optimal controls for spiking a theta neuron with $I_b = -0.25$ and $M = 1$ are shown in Figure 4.4.

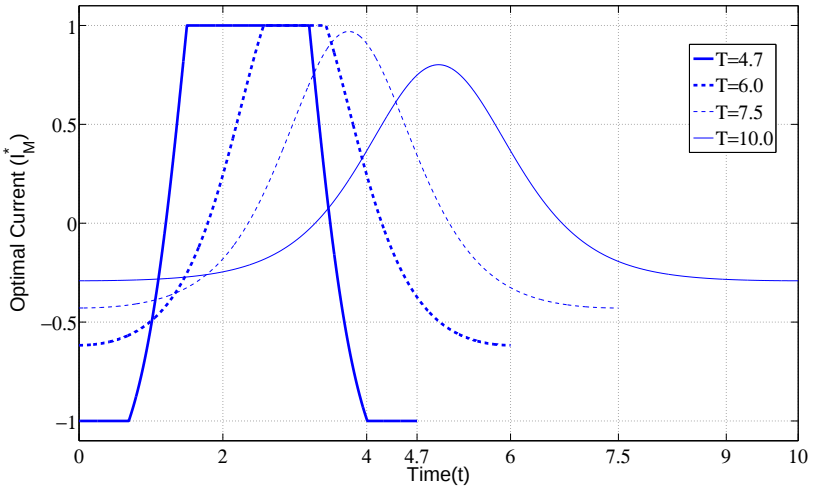

Figure 4.4: Optimal charge-balanced controls with bound $M = 1.0$ and for theta neuron model (with $I_b = -0.25$) to elicit spikes at $T = 4.7, 6.0, 7.5, 10.0$.

The above phase models, though commonly used, are ideal mathematical models of neuron oscillators. We now apply our optimal control strategies to models with experimentally observed PRC's, such as Hodgkin-Huxley and Morris-Lecar phase models, to demonstrate their applicability and generality.

4.3.3 Morris-Lecar Phase Model

The Morris-Lecar model has been extensively studied and used as a standard model for representing many different real neurons. The phase model of the Morris-Lecar neuron is given by

$$\dot{\theta} = \omega + Z(\theta)I(t), \tag{4.27}$$

where ω is the natural oscillation frequency and $Z(\theta)$ represents the PRC that can be calculated numerically from the ODE system by the software package XPP [29]. For the set of parameter values given in Section 1.1.2, the natural frequency $\omega_{ML} = 0.28\ rad/ms$ and the PRC is depicted in Figure 1.3. The charge-balanced minimum-power controls that elicit spikes for this phase model at various times are shown in Figure 4.5. Note that a truncated Fourier series is used as the Z function, which accurately approximate the PRC shown in Figure 1.3. We consider six different cases

for which the optimal controls have zero, two, and four switchings for spiking times that are longer and shorter than the natural spiking time, $T_0 = 2\pi/\omega_{ML} = 22.20\ ms$.

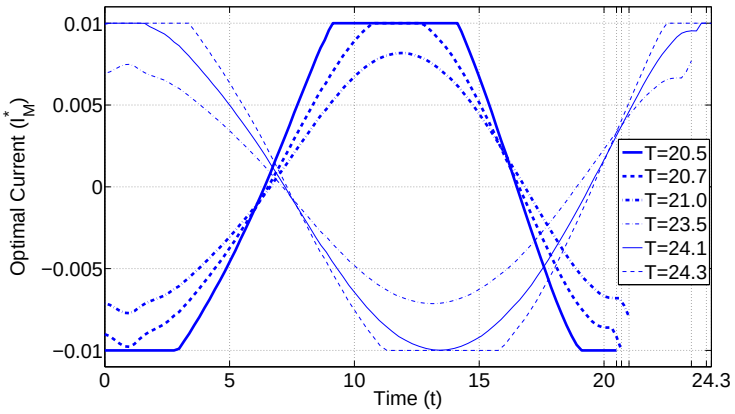

Figure 4.5: Optimal charge-balanced controls of minimum power for spiking a Morris-Lecar neuron at $T = 20.5, 20.7, 21.0, 23.5, 24.1, 24.3\ ms$ given the control bound $M = 0.01\ \mu A cm^{-2}$.

4.3.4 Hodgkin-Huxley Phase Model and Phase Model Validation

The phase model for the Hodkin-Huxley neuron oscillator is also of the form as in (4.27). For the set of parameter values given in Section 1.1.1, the system has a natural frequency ω_{HH}= $0.43\, rad/ms$ and its PRC is displayed in Figure 1.2. The charge-balanced minimum-power controls that elicit spikes at different time instances are shown in Figure 4.6.

Phase model reduction characterizes the dynamics of the underlying oscillating systems, where some of the state variables, but not all, can be observed. There is a fundamental need to explore the limits of the phase-reduced model as an approximation to the original oscillating system, because this important validation is largely lacking in the literature. The optimal controls for phase models presented so far in this work alter the spiking times of an oscillator during the course of one oscillatory cycle, so that a desired spike train can be constructed by repeating the control

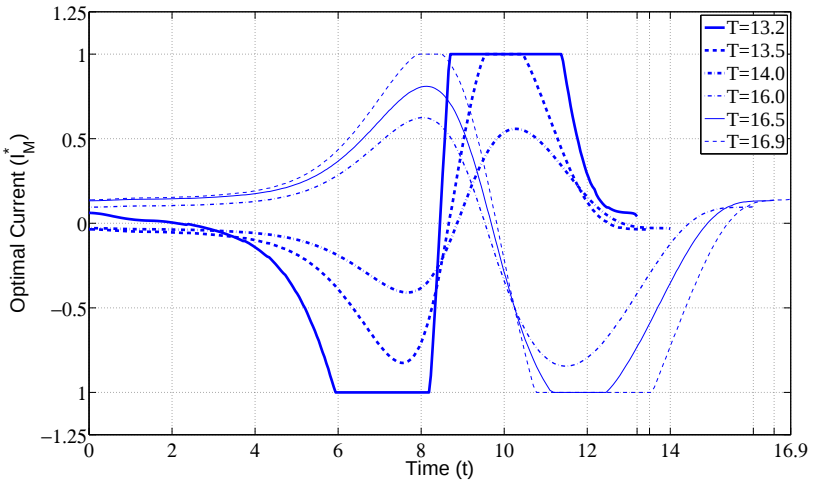

Figure 4.6: Optimal charge-balanced controls of minimum power for spiking a Hodgkin-Huxley neuron at $T = 13.2, 13.5, 14.0, 16.0, 16.5, 16.9\ ms$ given the control bound $M = 1.0\ \mu Acm^{-2}$.

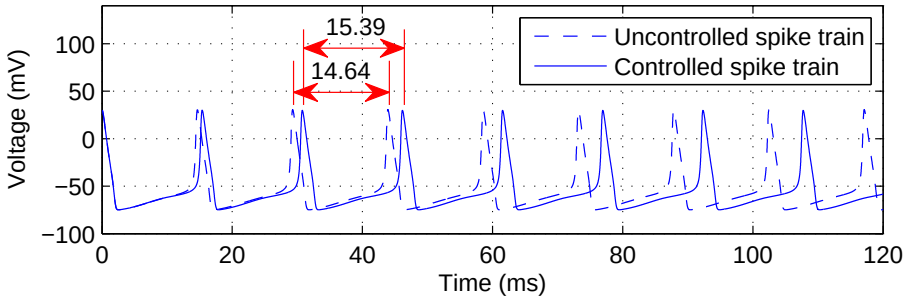

Figure 4.7: Uncontrolled and controlled spiking trains of Hodgkin-Huxley model with natural spiking time $T_0 = 14.64\ ms$. The desired spiking time $T = 1.05T_0 = 15.37\ ms$

input. We now apply the optimal controls derived according to the scalar Hodgkin-Huxley phase model to its full state-space model, which is a system of four differential equations as shown in section 1.1.1. The spike trains obtained by repeated application of the optimal controls and the uncontrolled train spiking at the natural period, $T_0 = 2\pi/\omega_{HH} = 14.64\ ms$, are illustrated in Figure 4.3.4 and 4.3.4. We present the cases for producing inter-spike times $T = 15.37\ ms$ and $T = 13.91\ ms$ that are respectively 5% longer and shorter than the natural period subject to the control amplitude bound $M = 1\ \mu Acm^{-2}$. It is seen that the corresponding optimal control delays the spiking time to 15.39 ms in the first case and advances it to 14.02 ms in the second

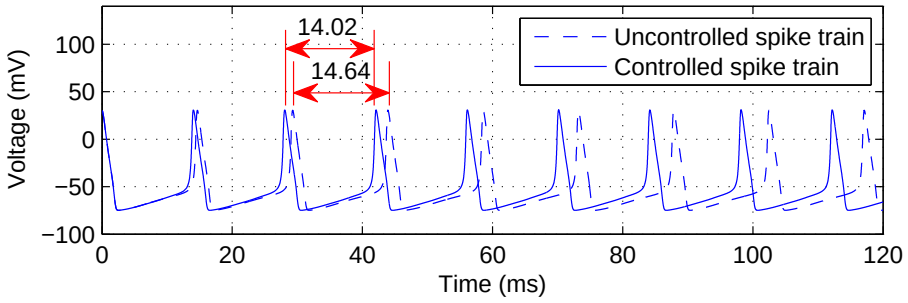

Figure 4.8: Uncontrolled and controlled spiking trains of Hodgkin-Huxley model with natural spiking time $T_0 = 14.64\ ms$.The desired spiking time $T = 0.95T_0 = 13.91\ ms$.

case in the full state-space model. These results demonstrate accurate approximations of phase reduced models to the full state-space systems under the weak forcing assumption. The variation of the absolute errors between the actual and designed spiking times is shown in Figure 4.9, where the spiking behavior predicted based on the phase model matches better the full state-space model towards the weak forcing region.

4.4 Conclusion

In this chapter, we considered the optimal control of phase models of neuron oscillators. We derived charge-balanced minimum-power current stimuli that elicit spikes of neurons at desired time instances for the cases of unbounded and bounded control amplitude. In particular, we showed that for the bounded case the optimal control has switching characteristics synthesized by the unbounded optimal control and the control bound. We implemented the resulting analytical optimal controls to various commonly used phase models, including mathematically ideal and experimentally observed models, to demonstrate their applicability. We then applied the optimal controls derived according to the phase-reduced model of Hodgkin-Huxley to the corresponding full state-space system to validate the approximation of the phase model under weak forcing. The theory presented in this work can be applied not only to neuron oscillators but also to any oscillating systems that can be represented using similar model reduction techniques such as biological, chemical, electrical, and mechanical oscillators.

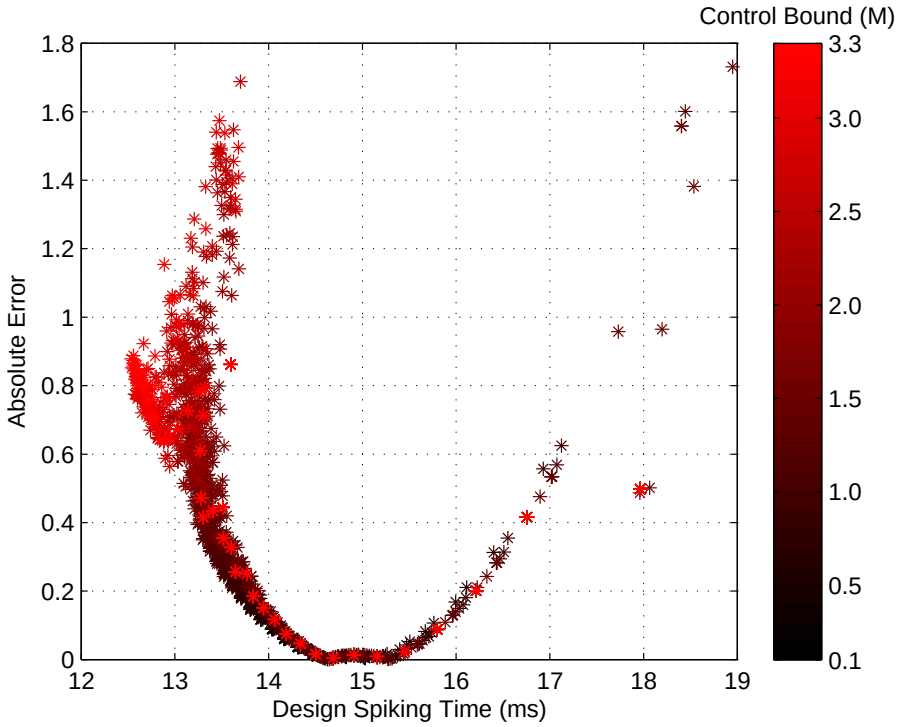

Figure 4.9: The absolute error in the spiking time when applying the charge-balanced minimum-power controls derived based on the Hodgkin-Huxley phase model to its full state-space model. The bound of the control amplitude is indicated as the color bar.

The theoretical results presented in this chapter characterize the fundamental limit of how the dynamics of neurons can be perturbed by the use of external inputs. Alternatively, they provide an insight into how the neuron dynamics determine the synaptic input necessary for eliciting spikes, which facilitates the development of optimal stimuli for neurological treatments such as deep brain stimulation for Parkinson's disease. The extension of this work to the optimal control of networks of neuron oscillators is of fundamental and practical importance. Our recent work has shown that an ensemble of uncoupled neurons is controllable, and that the minimum-power controls that spike a network of heterogeneous neurons can be found by using a multidimensional pseudospectral method [84, 80]. We extend this work to investigate the optimal control of an ensemble of neurons in Chapter 5 where we consider both coupled and uncoupled neural systems.

Chapter 5

Control of Neuron Ensembles

Oscillation is a phenomenon that occurs in many natural, social, and engineered systems. Control of population of oscillatory systems is motivated by a wide range of applications in neuroscience from neurological treatment of Parkinson's disease to the design of neurocomputers. In this chapter, we study the optimal control of an ensemble of neuron oscillators described by phase models. In particular, by employing Pontryagin's maximum principle, we analytically derive optimal controls for a two-neuron system and analyze the applicability of the derived controls to an ensemble of systems. Finally, we present a robust computational method for optimal control of spiking neurons based on homotopy perturbation techniques. This method is not limited to neural oscillators and can be applied generally to a broad class of nonlinear oscillatory systems that can be represented by phase model dynamics.

5.1 Introduction

Natural and engineered systems that consist of ensembles of isolated or interacting nonlinear dynamical components often exhibit complexities that are beyond human comprehension. Such systems, moreover, are often tremendously large which poses serious theoretical and computational challenges to modeling, guiding, controlling, or optimizing them. Developing optimal external waveforms or forcing signals that steer complex systems to desired dynamical conditions is of fundamental and practical importance in neuroscience [50, 69]. Minimum-power external stimuli that synchronize or desynchronize a network of coupled or uncoupled neurons is imperative for a wide

range of applications from neurological treatment of Parkinson's disease and epilepsy [3, 4, 117] to the design of neurocomputers [55, 54].

Various phase model-based control theoretic techniques have been proposed to design external inputs that drive oscillators to behave in a desired way or to form certain synchronization patterns. These include multi-linear feedback control methods for controlling individual phase relations between coupled oscillators [63] and phase model-based feedback approaches for efficient control of synchronization patterns in oscillator ensembles [69, 111, 138]. These synchronization engineering methods, though effective, do not explicitly address optimality in the control design process.

In this chapter, we generalize our work on optimal control of a single neuron [21, 20, 23] to consider the control and synchronization of a collection of neuron oscillators. In particular, we investigate the fundamental properties and develop optimal controls for the synchronization of such types of large-scale neuron systems. In Section 5.2, we formulate optimal control of spiking neurons as steering problems and derive analytical tools to construct minimum-power and time-optimal controls for two-neuron systems. Furthermore, in Section 5.3 we implement the homotopy perturbation method to find the optimal controls for two-neuron system and extend the method for an ensemble of neurons. Note that the derived methods are universal to the control of general nonlinear oscillators whose dynamics can be described by phase models.

5.2 Optimal Control of Neuron Ensembles

Practical applications demand minimum-power or time-optimal controls that form certain synchronization patterns for a population of oscillators, which gives rise to an optimal steering problem,

$$\begin{aligned} \min \quad & J = \varphi(T, \Theta(T)) + \int_0^T \mathcal{L}(\Theta(t), I(t))dt \\ \text{s.t.} \quad & \dot{\Theta}(t) = f(\Theta) + Z(\Theta)I(t) \\ & \Theta(0) = \Theta_0,\ \Theta(T) = \Theta_d \end{aligned} \tag{5.1}$$

where $\Theta \in \mathbb{R}^n$, $I \in \mathbb{R}$, and $\varphi : \mathbb{R} \times \mathbb{R}^n \to \mathbb{R}$ denotes the terminal cost. $\mathcal{L} : \mathbb{R}^n \times \mathbb{R} \to \mathbb{R}$ denotes the running cost, and $f, Z : \mathbb{R}^n \to \mathbb{R}^n$ are Lipschitz continuous (over the respective domains) with respect to their arguments. For spiking a neuronal population, for example, the goal is to drive the system from the initial state, $\Theta_0 = \mathbf{0}$, to a final state $\Theta_d = (2m_1\pi, 2m_2\pi, \ldots, 2m_n\pi)'$, where $m_i \in \mathbb{Z}^+$, $i = 1, \ldots, n$. Steering problems of this kind have been well studied, in particular, in the context of nonholonomic motion planning and sub-Riemannian geodesic problems [115, 91]. This class of optimal control problems in principle can be attempted by the maximum principle. However, in most cases, they are analytically intractable, especially when the system is of high dimension, e.g., greater than three. In the following, we start with two-neuron systems and develop a robust computational method for solving the challenging optimal control problems of steering an ensemble of neurons.

5.2.1 Time-Optimal Control of Uncoupled Two Neuron Oscillators

Spiking a neuron in minimum time, subject to a given control amplitude, can be solved in a straightforward manner. Consider the phase model of a single neuron as in

$$\frac{d\theta}{dt} = f(\theta) + Z(\theta)I(t). \tag{5.2}$$

It is easy to see that for a given control bound $M > 0$, the minimum spiking time is achieved by the bang-bang control

$$I_t^* = \begin{cases} M, & Z(\theta) \geq 0 \\ -M, & Z(\theta) < 0, \end{cases} \tag{5.3}$$

which keeps the phase velocity, $\dot{\theta}$, at its maximum. The minimum spiking time with respect to the control bound M, denoted by T_{min}^M, is then given by

$$T_{min}^M = \int\limits_{\theta \in \mathcal{A}} \frac{1}{f(\theta) + Z(\theta)M} d\theta + \int\limits_{\theta \in \mathcal{B}} \frac{1}{f(\theta) - Z(\theta)M} d\theta, \tag{5.4}$$

where the sets $\mathcal{A}$ and $\mathcal{B}$ are defined as

$$\mathcal{A} = \{\theta |\ Z(\theta) \geq 0, 0 \leq \theta \leq 2\pi\},$$
$$\mathcal{B} = \{\theta |\ Z(\theta) < 0, 0 \leq \theta \leq 2\pi\}.$$

Time-optimal control of spiking two neurons is more involved, and can be formulated as in (5.1) with $\varphi(T, \Theta(T)) = 0$ and $\mathcal{L}(\Theta(t), I(t)) = 1$. As an example, we consider two theta neurons, where the dynamics are given by

$$f = \begin{bmatrix} f_1 \\ f_2 \end{bmatrix} = \begin{bmatrix} \alpha_1 + \beta_1 \cos\theta_1 \\ \alpha_2 + \beta_2 \cos\theta_2 \end{bmatrix}, \quad Z = \begin{bmatrix} Z_1 \\ Z_2 \end{bmatrix} = \begin{bmatrix} 1 - \cos\theta_1 \\ 1 - \cos\theta_2 \end{bmatrix}. \tag{5.5}$$

Our objective is to drive this two-neuron system from the initial state $\Theta_0 = (0, 0)'$ to the desired final state $\Theta_d = (2m_1\pi, 2m_2\pi)'$ in minimum time, where $m_1, m_2 \in \mathbb{Z}^+$. The Hamiltonian for this optimal control problem is given by

$$H = \lambda_0 + \langle \lambda, f + ZI \rangle, \tag{5.6}$$

where $\lambda_0 \in \mathbb{R}$ and $\lambda \in \mathbb{R}^2$ are the multipliers that correspond to the Lagrangian and the system dynamics, respectively, and $\langle\ ,\ \rangle$ denotes a scalar product in the Euclidean space $\mathbb{E}^2$.

Proposition 1 *The minimum-time control that spikes two theta neurons simultaneously is bang-bang.*

Proof. The Hamiltonian in (5.6) is minimized by the control,

$$I(t) = \begin{cases} M & \text{for} \quad \phi(t) < 0, \\ -M & \text{for} \quad \phi(t) > 0, \end{cases} \tag{5.7}$$

where ϕ is the switching function defined by $\phi = \langle \lambda, Z \rangle$. If there exists no non-zero time interval over which $\phi \equiv 0$, then the optimal control is given by the bang-bang form as in (5.7), where the control switchings are defined at $\phi = 0$. We show by contradiction that maintaining $\phi = 0$ is not possible for any non-zero time interval.

Suppose that $\phi(t) = 0$ for some non-zero time interval, $t \in [\tau_1, \tau_2]$. Then we have

$$\phi = \langle \lambda, Z \rangle = 0, \tag{5.8}$$

$$\dot{\phi} = \langle \lambda, [f, Z] \rangle = 0, \tag{5.9}$$

where $[f, Z]$ denotes the Lie bracket of the vector fields f and Z. According to (5.8) and (5.9), λ is perpendicular to both vectors Z and $[f, Z]$, where

$$[f, Z] = \frac{\partial Z}{\partial \theta} f - \frac{\partial f}{\partial \theta} Z = \begin{bmatrix} 2 \sin \theta_1 \\ 2 \sin \theta_2 \end{bmatrix}.$$

Since $\lambda \neq 0$ by the non-triviality condition of the maximum principle, Z and $[f, Z]$ are linearly dependent on $t \in [\tau_1, \tau_2]$. One can easily show that these two vectors are linearly dependent either when $\theta_1 = 2n\pi$ and $\theta_2 \in \mathbb{R}$, $\theta_1 \in \mathbb{R}$ and $\theta_2 = 2n\pi$, or $\theta_1 = \theta_2 + 2n\pi$ and $\theta_2 \in \mathbb{R}$, where $n \in \mathbb{Z}$. These three families of lines represent the possible paths in the state-space where ϕ can vanish for some non-trivial time-interval. Now we show that these are not feasible phase trajectories that can be generated by a control. Suppose that $(\theta_1(\tau), \theta_2(\tau)) = (2n\pi, \alpha)$ for some $\tau > 0$ and for some $n \in \mathbb{Z}$, where $\alpha \in \mathbb{R}$. We then have $\dot{\theta}_1(\tau) = 2 \neq 0$, irrespective of any control input. Hence, the system immediately deviates from the line $\theta_1 = 2n\pi$. The same reasoning can be used for showing the case of $\theta_2 = 2n\pi$.

Similarly, if $(\theta_1(\tau), \theta_2(\tau)) = (\alpha + 2n\pi, \alpha)$ for some $\tau > 0$ and for some $n \in \mathbb{Z}$, for the system to remain on the line $(\theta_1(t), \theta_2(t)) = (\theta_2 + 2n\pi, \theta_2)$, requires that $\dot{\theta}_1(t) = \dot{\theta}_2(t)$ for $t > \tau$. However, this occurs only when $\theta_1 = 2m\pi$ and $\theta_2 = 2(n + m)\pi$, where $m \in \mathbb{Z}$, since $\dot{\theta}_1 - \dot{\theta}_2 = (I_1 - I_2)(1 - \cos \theta_1)$. Furthermore, staying on these points is impossible with any control inputs since for $\theta_1(\tau) = 2m\pi$ and $\theta_2(\tau) = 2(n+m)\pi$, the phase velocities are $\dot{\theta}_1(\tau) = \dot{\theta}_2(\tau) = 2$, which immediately forces the system away from these points. Therefore, the system cannot be driven along the path $(\theta_2 + 2n\pi, \theta_2)$. This analysis concludes that $\phi = 0$ and $\dot{\phi} = 0$ do not hold simultaneously over a non-trivial time interval. □

Now, we construct the bang-bang structure for time-optimal control of this two-neuron system and, without loss of generality, let $\lambda_0 = 1$.

Definition 1 *We denote the vector fields corresponding to the constant bang controls* $I(t) \equiv -M$ *and* $I(t) \equiv M$ *by* $X = f - MZ$ *and* $Y = f + MZ$*, respectively, and call the respective corresponding trajectories* X*- and* Y*- trajectories. The concatenation of an* X*-trajectory followed by a* Y*-trajectory is denoted by* XY*, while the concatenation in the reverse order is denoted by* YX*.*

Due to the bang-bang nature of the time-optimal control for this system, it is sufficient for us to calculate the time between consecutive switches, and then the first switching time can be determined by the end point constraint. The inter-switching time can be calculated following the procedure described in [124, 125, 120].

Let p and q be consecutive switching points, and let pq be a Y-trajectory. Without loss of generality, we assume that this trajectory passes through p at time 0 and is at q at time τ. Since p and q are switching points, the corresponding multipliers vanish against the control vector field Z at those points, i.e.,

$$\langle \lambda(0), Z(p) \rangle = \langle \lambda(\tau), Z(q) \rangle = 0. \tag{5.10}$$

Assuming that the coordinate of $p = (\theta_1, \theta_2)'$, our goal is to calculate the switching time, τ, in terms of θ_1 and θ_2. In order to achieve this, we need to compute what the relation $\langle \lambda(\tau), Z(q) \rangle = 0$ implies at time 0. This can be obtained by moving the vector $Z(q)$ along the Y-trajectory backward from q to p through the pushforward of the solution $\omega(t)$ of the variational equation along the Y-trajectory with the terminal condition $\omega(\tau) = Z(q)$ at time τ. We denote by $e^{tY}(p)$ the value of the Y-trajectory at time t that starts at the point p at time 0 and by $(e^{-tY})_*$ the backward evolution under the variational equation. Then we have

$$\omega(0) = (e^{-\tau Y})_* \, \omega(\tau) = (e^{-\tau Y})_* \, Z(q) = (e^{-\tau Y})_* \, Z(e^{\tau Y}(p)) = (e^{-\tau Y})_* \, Z \, e^{\tau Y}(p).$$

Since the "adjoint equation" of the maximum principle is precisely the adjoint equation to the variational equation, it follows that the function $t \mapsto \langle \lambda(t), \omega(t) \rangle$ is constant along the Y-trajectory. Therefore, $\langle \lambda(\tau), Z(q) \rangle = 0$ also implies that

$$\langle \lambda(0), \omega(0) \rangle = \langle \lambda(0), (e^{-\tau Y})_* \, Z \, e^{\tau Y}(p) \rangle = 0. \tag{5.11}$$

Since $\lambda(0) \neq 0$, we know from (5.10) and (5.11) that the two vectors $Z(p)$ and $(e^{-\tau Y})_* Z\, e^{\tau Y}(p)$ are linearly dependent. It follows that

$$\gamma Z(p) = (e^{-\tau Y})_* Z\, e^{\tau Y}(p), \tag{5.12}$$

where γ is a constant. We make use of the well-known Campbell-Baker-Hausdorff formula [58] to expand $(e^{-\tau Y})_* Z\, e^{\tau Y}(p)$, that is,

$$(e^{-\tau Y})_* Z\, e^{\tau Y}(p) = e^{\tau ad_Y}(Z) = \sum_{n=0}^{\infty} \frac{\tau^n}{n!} ad_Y^n Z.$$

A straightforward computation of Lie brackets gives

$$\begin{aligned} ad_Y Z &= [Y, Z] = [f + MZ, Z] = [f, Z] = 2 \begin{bmatrix} \sin\theta_1 \\ \sin\theta_2 \end{bmatrix}, \\ ad_Y^2 Z &= [Y, [Y, Z]] = 2(f - AZ), \end{aligned}$$

where $A = \text{diag}\,\{2(\alpha_1 - 2 + M), 2(\alpha_2 - 2 + M)\}$, and furthermore

$$\begin{aligned} ad_Y^{2n+1} Z &= (-1)^n 2^n (A + MI)^n [f, Z], \\ ad_Y^{2n+2} Z &= (-1)^n 2^{n+1} (A + MI)^n (f - AZ). \end{aligned}$$

Consequently, we have

$$\begin{aligned} e^{\tau ad_Y Z} =& Z + \sum_{n=0}^{\infty} \frac{\tau^{2n+1}}{(2n+1)!} (-1)^n 2^n (A + MI)^n [f, Z] \\ &+ \sum_{n=0}^{\infty} \frac{\tau^{2n+2}}{(2n+2)!} (-1)^n 2^{n+1} (A + MI)^n (f - AZ), \end{aligned}$$

which is further simplified to

$$e^{\tau ad_Y Z} = \begin{bmatrix} h(\alpha_1, \beta_1, \theta_1, M, \tau) \\ h(\alpha_2, \beta_2, \theta_2, M, \tau) \end{bmatrix},$$

where

$$h(\alpha_i,\beta_i,\theta_i,M,\tau)=\frac{M-\beta_i-(\alpha_i+M)\cos\theta_i}{2(\alpha_i-1+M)}\cos(2\tau\sqrt{\alpha_i-1+M})$$
$$+\frac{\alpha_i+M-(M-\beta_i)\cos\theta_i}{2(\alpha_i-1+M)}+\frac{\sin\theta_i}{\sqrt{\alpha_i-1+M}}\sin(2\tau\sqrt{\alpha_i-1+M}).$$

This together with (5.12) yields

$$(1-\cos\theta_2)h(\alpha_1,\beta_1,\theta_1,M,\tau)=(1-\cos\theta_1)h(\alpha_2,\beta_2,\theta_2,M,\tau). \tag{5.13}$$

This equation characterizes the inter-switching along the Y-trajectory; that is, the next switching time τ can be calculated given the previous switching point (θ_1,θ_2) for the system evolving along the Y-trajectory. Similarly, the inter-switching along the X-trajectory can be calculated by substituting $-M$ for M in (5.13).

Note that the solution to (5.13) is not unique, and some of the solutions may not be optimal, but these can be discarded in a systematic way. The idea is to identify those possible switching points calculated from (5.13) with $\phi=0$ that also have the appropriate sign for $\dot{\phi}$. We focus on the case where f and Z are linearly independent, since the case for those being linearly dependent restricts the state space to the curve

$$(\alpha_1+\beta_1\cos\theta_1)(1-\cos\theta_2)=(\alpha_2+\beta_2\cos\theta_2)(1-\cos\theta_1).$$

If f and Z are linearly independent, then $[f,Z]$ can be written as $[f,Z]=k_1f+k_2Z$, where

$$k_1=\frac{2\sin\theta_1(1-\cos\theta_2)-2\sin\theta_2(1-\cos\theta_1)}{(\alpha_1+\beta_1\cos\theta_1)(1-\cos\theta_2)-(\alpha_2+\beta_2\cos\theta_2)(1-\cos\theta_1)},$$
$$k_2=\frac{2\sin\theta_1(\alpha_1+\beta_1\cos\theta_1)-2\sin\theta_2(\alpha_2+\beta_2\cos\theta_2)}{(\alpha_1+\beta_1\cos\theta_1)(1-\cos\theta_2)-(\alpha_2+\beta_2\cos\theta_2)(1-\cos\theta_1)}.$$

As a result, we can write $\dot{\phi}=\langle\lambda,[f,Z]\rangle=k_1\langle\lambda,f\rangle+k_2\langle\lambda,Z\rangle$. Since we know that at switching points $\phi=\langle\lambda,Z\rangle=0$, the Hamiltonian, as in (5.6), $H=0$ and the choice of $\lambda_0=1$ makes $\langle\lambda,f\rangle=-1$. Therefore, at these points, we have $\dot{\phi}=-k_1$, and the type of switching can be determined according to the sign of the function k_1. If $k_1>0$, then it is an X to Y switch since $\dot{\phi}<0$, and hence ϕ changes its sign from positive to negative passing through the switching point, which corresponds to

switching the control from $-M$ to M as in (5.7). Similarly, if $k_1 < 0$, then it is a Y to X switch. Therefore the next switching time will be the minimum non-zero solution to the equation (5.13) that satisfies the above rule. For example, suppose that the system is following a Y-trajectory starting with a switching point $p_i = (\theta_1^i, \theta_2^i)'$. The possible inter-switching times $\{\tau_{i,j}\}$, $j = 1, \ldots, n$, with $\tau_{i,1} < \tau_{i,2} < \ldots < \tau_{i,n}$ can then be calculated according to (5.13) based on p_i. Thus, the next switching point is $p_r = (\theta_1^r, \theta_2^r)' = e^{\tau_{i,r} Y}(p_i)$, $\tau_{i,r} = \min\{\tau_{i,1}, \ldots, \tau_{i,n}\}$, such that $k_1(\theta_1^r, \theta_2^r) < 0$, which corresponds to an Y to X switch.

Now in order to synthesize a time-optimal control, it remains to compute the first switching time and switching point, since the consequent switching sequence can be constructed thereafter based on the procedure described above. Given an initial state $\Theta_0 = (0, 0)'$, the first switching time and point p_1 will be determined according to the target state. For example, $\Theta_d = (2m_1\pi, 2m_2\pi)'$, where $m_1, m_2 \in \mathbb{Z}^+$, in such a way that the optimal trajectory follows a bang-bang control derived based on p_1 and it will reach Θ_d. Under this construction, we may end up with a finite number of feasible trajectories starting with either an X- or Y-trajectory, which reach the desired terminal state. The minimum time trajectory is then selected among them.

Figure 5.1 illustrates an example of driving two theta neurons time-optimally from $(0, 0)'$ to $(2\pi, 4\pi)'$ with the control bound $M = 0.5$, where the natural frequencies of the oscillators are $\omega_1 = 1.1$ ($I_1 = 0.3$) and $\omega_2 = 1.9$ ($I_2 = 0.9$), corresponding to $\alpha_1 = 1.3$, $\beta_1 = 0.7$ and $\alpha_2 = 1.9$, $\beta_2 = 0.1$. In this example, the time-optimal control has two switches at $t = 1.87$ and $t = 3.56$, and the minimum time is 5.61.

5.2.2 Simultaneous Control of Neuron Oscillators

The complexity of deriving optimal controls for higher dimensional systems, i.e., more than two neurons, grows rapidly and it makes sense to find out how the control of two neurons relates to the control of many. If the trajectories of neurons with different frequencies have no crossings following a common control input, then the control designed for any two neurons guarantees to bound trajectories of all the neurons with frequencies within the range of these two nominal neurons. The trajectories of the

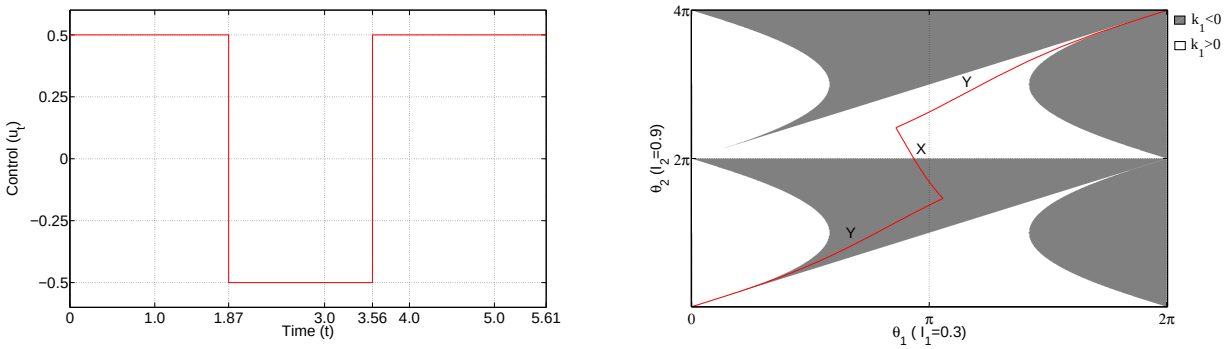

(a) (b)

Figure 5.1: (a) Time optimal control for two theta neuron system with $I_1 = 0.3$ ($\alpha_1 = 1.3$, $\beta_1 = 0.7$) and $I_2 = 0.9$ ($\alpha_2 = 1.9$, $\beta_2 = 0.1$) to reach $(2\pi, 4\pi)$ with the control bounded by $M = 0.5$ and (b) corresponding trajectories. The gray and white regions represent where k_1 is negative and positive, respectively.

two nominal neurons can then be thought of as the envelope of these other neuron trajectories. We now show that this is indeed the case.

Lemma 1 *The trajectories of any two theta neurons with positive baseline currents following a common control input have no crossing points.*

Proof. Consider two theta neurons modeled by

$$\dot{\theta_1} = (1 + I_1) + (1 - I_1)\cos\theta_1 + (1 - \cos\theta_1)I, \quad \theta_1(0) = 0, \tag{5.14}$$

$$\dot{\theta_2} = (1 + I_2) + (1 - I_2)\cos\theta_2 + (1 - \cos\theta_2)I, \quad \theta_2(0) = 0, \tag{5.15}$$

with positive baseline currents, $I_1, I_2 > 0$, and assume that $\omega_1 < \omega_2$, which implies $I_1 < I_2$ since $I_i = \frac{\omega_i^2}{4}$, $i = 1, 2$. In the absence of any control input, namely, $I = 0$, it is obvious that $\theta_1(t) < \theta_2(t)$ for all $t > 0$ since $I_1 < I_2$. Suppose that $\theta_1(t) < \theta_2(t)$ for $t \in (0, \tau)$, and that these two phase trajectories meet at time τ, i.e., $\theta_1(\tau) = \theta_2(\tau)$. Then, we have $\dot{\theta}_1(\tau) - \dot{\theta}_2(\tau) = (I_1 - I_2)(1 - \cos(\theta_1(\tau))) \leq 0$, and the equality holds only when the neurons spike at time τ, i.e., $\theta_1(\tau) = \theta_2(\tau) = 2n\pi$, $n \in \mathbb{Z}^+$. As a result, $\theta_1(\tau^+) < \theta_2(\tau^+)$, because $\theta_1(\tau) = \theta_2(\tau)$ and $\dot{\theta}_1(\tau) < \dot{\theta}_2(\tau)$, and hence there exist no crossings between the two trajectories $\theta_1(t)$ and $\theta_2(t)$. □

Note that the same result as Lemma 1 holds and can be shown in the same fashion for both sinusoidal and SNIPER phase models, as described in Section 2.3.1 and 2.3.2,

when the model-dependent constant $z_1 > z_2$ if $\omega_1 < \omega_2$, which is in general the case. For example, in the SNIPER phase model, z conventionally takes the form $z = 2/\omega$ [11].

This critical observation extremely simplifies the design of external stimuli for spiking a neuron ensemble with different oscillation frequencies, based on the design for two neurons with extremal frequencies over this ensemble. We illustrate this important result by designing optimal controls for two sinusoidal neurons, employing the Legendre pseudospectral method [80], which we outlined in Appendix B. The Legendre pseudospectral method permits a flexible framework to optimize, based on a very general cost functional subject to general constraints. We demonstrate this by solving the optimal control problem given in (5.1) by relaxing the terminal constraint $\Theta(T) = \Theta_d$. We choose

$$J = \alpha\|\Theta_d - \Theta(T)\|^2 \quad + \beta \int_0^T I^2(t)dt, \tag{5.16}$$

which minimizes the terminal error and input power scaled by the constants α and β. This scaling provides a tunable parameter that determines the trade-off between performance and input power. Figure 5.2 shows the optimized controls and corresponding trajectories for sinusoidal neuron models for $\alpha = 1$, $\beta = 0.1$, $T = 2\pi$, and ω belongs to $[1.0, 1.1]$. In this optimization, the controls are optimized over the two neuron systems with extremal frequencies, whose trajectories form an envelope, bounding the trajectories of other frequencies in between. We are able to design compensating controls for the entire frequency band solely by considering these upper and lower bounding frequencies. The controlled (black) and uncontrolled (gray) state trajectories clearly show the improvement in simultaneous spiking of the ensemble of neurons. In this case, the inclusion of the minimum power term in the cost function serves to regularize the control against high amplitude values, which makes the derived control easy to implement in practice.

This design principle greatly reduces the complexity of finding controls to spike a large number of neurons. Although the optimal control for two neurons is in general not optimal for the others, this method produces a close approximation of the optimal control.

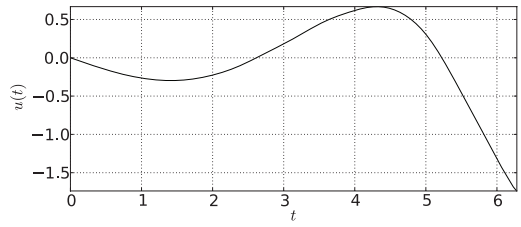

(a)

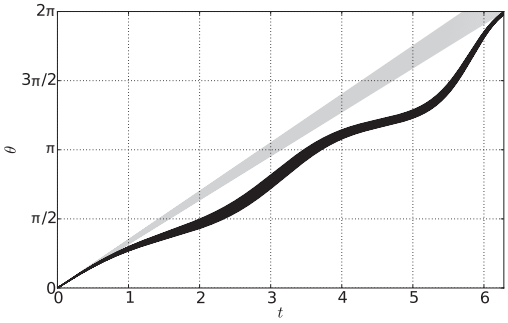

(b)

Figure 5.2: (a) The control and (b) state trajectories of the sinusoidal phase model (for $\alpha = 1$, $\beta = 0.1$, $T = 2\pi$ in (5.16)) which is optimized for $\omega \in [1.0, 1.1]$. The gray states correspond to uncontrolled state trajectories, and provide a comparison for the synchrony improvement provided by the compensating optimized ensemble control.

5.3 Homotopy Perturbation Method for Optimal Control of Neuron Ensembles

As we proceed to consider the synthesis of controls for neuron ensembles, mainly due to the large scale of the system, the analytic methods used for smaller number of neurons become intractable to use. As a result, developing computational methods to calculate optimal inputs for ensembles of neurons is of particular practical interest. Furthermore, finding an iterative optimization-free technique, that minimizes reliance on numerical optimization is compelling in order to broaden the scope and scale of the complex neural oscillator networks to which optimal control can be applied. However, implementing semi-analytical methods for the control of phase models is challenging [36], and the difficulty of achieving synchrony in certain neuron models using singular perturbations and averaging theory has been indicated [28]

A promising alternative to singular perturbation is the homotopy perturbation method (HPM) [51], which was introduced as a powerful technique for solving nonlinear boundary value problems (BVPs), and has been applied in diverse fields. Perturbation theory is applied to construct a topological homotopy that continuously deforms the solution to an initial problem into the solution of a desired BVP. This approach overcomes several limitations of singular perturbation techniques, which require the existence of a parameter that can be perturbed in a small neighborhood of its nominal value without disturbing the structure of the BVP. When multiple parameters exist, the convergence of solutions at successive singular perturbation orders is highly dependent on the choice of the perturbed parameter. As a result, an appropriate choice of singular parameter can lead to fast convergence, whereas other choices can end in failure. The validity of solutions obtained with singular perturbation techniques depends on the magnitude of the perturbation parameter, and in most cases, solutions are valid only for sufficiently small values. These requirements have restricted the application of traditional perturbation methods to BVPs with obvious small parameters. In contrast, the HPM does not require an inherent small parameter, and can be applied to a broader class of problems including, in particular, the optimal control of neuron models.

Using the (HPM), the solution to a nonlinear boundary value problem (BVP) can be obtained by using successive approximations. The procedure results in a homotopy defined for an embedding parameter that deforms the solution of an initial linear problem to the solution of the given nonlinear problem [51]. To fix the idea, we recall the definition of a homotopy.

Definition 2 *(Homotopy) Two mappings $f, g : X \to Y$ between the topological spaces X and Y are called* homotopic *if there exists a family of continuous mappings $h_p : X \to Y$ that depend continuously on a parameter $p \in [0, 1]$ such that $h_0 = f$, $h_1 = g$ [133].*

Starting from a partial solution, the method produces successive approximations that approach the solution of the BVP that satisfy the boundary conditions for all values of the embedding parameter. Consider a general boundary value problem given by

$$\dot{x} = f(x), \quad g(x(0), x(T)) = 0, \tag{5.17}$$

where $x \in \mathbb{R}^n$, $f : \mathbb{R}^n \to \mathbb{R}^n$, $g : \mathbb{R}^{2n} \to \mathbb{R}^n$ and $t \in [0, T]$. In general, the function $f(x)$ can be separated into linear and nonlinear terms of the form $f(x) = Ax + N(x)$, where $A \in \mathbb{R}^{n \times n}$, and the dynamics in (5.17) can be expressed as

$$L(x) + NL(x) = 0, \tag{5.18}$$

where $L(x) = Ax - \dot{x}$ and $NL(x)$ denote the grouped linear and nonlinear terms with respect to the variable x. We then implicitly define a homotopy that deforms the solution x_{init}, which may be arbitrary as long as the boundary conditions are satisfied, into the solution $\bar{x}$ to the full problem by

$$h_p(x) = (1 - p)(L(x) - L(x_{init})) + p(L(x) + NL(x)) = 0. \tag{5.19}$$

Here $p \in [0, 1]$ is an embedding parameter, and x_{init} is the solution to the initial linear problem that satisfies the boundary conditions. When $p = 0$, equation (5.19) simplifies to

$$h_0(x) = L(x) - L(x_{init}) = 0,$$

while at $p = 1$ equation (5.19) satisfies

$$h_1(x) = L(x) + NL(x) = 0.$$

The intention is to obtain a homotopy h_p such that when p transitions from 0 to 1, the solution x to the boundary value problem deforms continuously from initial solution x_{init} to exact solution $\bar{x}$, and the function $L(x) - L(x_{init})$ is transformed continuously to $L(x) + NL(x)$. To construct such an h_p, we choose the embedding parameter p as a perturbation parameter and expand the solution to the equation (5.18) in terms of its power series with respect to p, which is given by

$$x = \sum_{i=0}^{\infty} \bar{x}_i p^i. \tag{5.20}$$

Because the homotopy map converges to the BVP at $p = 1$, the desired solution

$$\bar{x} = \lim_{p \to 1} x = \sum_{i=0}^{\infty} \bar{x}_i \tag{5.21}$$

can be obtained by letting $p = 1$. As in the case of singular perturbation, the terms $\bar{x}_i$ in the solution of form (5.21) to the appropriate BVP are obtained by iteratively solving a sequence of ordinary differential equations corresponding to coefficients of increasing orders of the embedding parameter p. Specifically, the coefficients of p^0 are obtained from $L(\bar{x}_0) = L(x_{init})$, the coefficients of p^1 are derived from $L(\bar{x}_1) + L(x_{init}) + NL(\bar{x}_0) = 0$, and the coefficients for subsequent orders p^n follow from

$$L(\bar{x}_n) = \frac{-1}{(n-1)!} \frac{\partial^{n-1}}{\partial p^{n-1}} NL\left(\sum_{i=1}^{n-1} \bar{x}_i p^i\right)\Bigg|_{p=0}. \tag{5.22}$$

5.3.1 Minimum-Power Control of an Uncoupled Two-Neuron System

The design of the minimum-power stimuli to elicit simultaneous spikes of neurons is of clinical importance. Example applications include deep brain stimulation for a variety of neurological disorders and neurological implants of cardiac pacemakers, where mild stimulations and low energy consumption are required [4, 87]. In this section, we present the minimum-power control synthesis for a two-neuron system. This synthesis is begun by formulating the optimal control problem as in (5.1) with $\varphi(T, \Theta(T)) = 0$ and $\mathcal{L}(\Theta(t), I(t)) = I(t)^2$. As an example, we consider two sinusoidal phase models, where the dynamics are given by

$$f(\Theta) = \begin{bmatrix} f_1 \\ f_2 \end{bmatrix} = \begin{bmatrix} \omega_1 \\ \omega_2 \end{bmatrix}, \quad Z(\Theta) = \begin{bmatrix} Z_1 \\ Z_2 \end{bmatrix} = \begin{bmatrix} z_{d1} \sin\theta_1 \\ z_{d2} \sin\theta_2 \end{bmatrix}.$$

where ω_1 and ω_2 are the natural frequencies of the two neurons, and z_1 and z_2 are model-dependent constants. Our objective is to drive this two-neuron system from the initial state $\Theta_0 = (0, 0)'$ to the desired final state $\Theta_d = (2m_1\pi, 2m_2\pi)'$ with minimum power, where $m_1, m_2 \in \mathbb{Z}^+$. The Hamiltonian for this optimal control problem is given by

$$H = I^2(t) + \lambda_1(\omega_1 + z_{d1} I \sin\theta_1) + \lambda_2(\omega_2 + z_{d2} I \sin\theta_2),$$

where $\lambda_1 \in \mathbb{R}$, and $\lambda_2 \in \mathbb{R}$ are Lagrange multipliers that correspond to the system dynamics. We apply the maximum principle to transfer this problem to a two point boundary values problem. From the minimum condition of the maximum principle,

$\frac{\partial H}{\partial I} = 0$, the optimal control I satisfies

$$I = -\frac{1}{2}\left(z_{d1}\lambda_1 \sin\theta_1 - z_{d2}\lambda_2 \sin\theta_2\right). \tag{5.23}$$

By substituting (5.23) into the dynamics and the adjoint equations, $\dot{\lambda}_1 = -\frac{\partial H}{\partial \theta_1}, \dot{\lambda}_2 = -\frac{\partial H}{\partial \theta_2}$, the optimal control problem can be transferred to a boundary value problem of the following form.

$$\dot{\theta_1} = \omega_1 - \frac{z_{d1}^2\lambda_1}{2}\sin^2\theta_1 - \frac{z_{d1}z_{d2}\lambda_2}{2}\sin\theta_1\sin\theta_2, \tag{5.24}$$

$$\dot{\theta_2} = \omega_2 - \frac{z_{d2}^2\lambda_2}{2}\sin^2\theta_2 - \frac{z_{d2}z_{d1}\lambda_1}{2}\sin\theta_2\sin\theta_1, \tag{5.25}$$

$$\dot{\lambda_1} = \frac{z_{d1}^2\lambda_1^2}{2}\sin\theta_1\cos\theta_1 + \frac{z_{d1}z_{d2}\lambda_1\lambda_2}{2}\cos\theta_1\sin\theta_2, \tag{5.26}$$

$$\dot{\lambda_2} = \frac{z_{d2}^2\lambda_2^2}{2}\sin\theta_2\cos\theta_2 + \frac{z_{d2}z_{d1}\lambda_2\lambda_1}{2}\cos\theta_2\sin\theta_1, \tag{5.27}$$

where

$$\begin{aligned} &\theta_1(0) = 0, && \theta_1(T) = 2m_1\pi \\ &\theta_2(0) = 0, && \theta_2(T) = 2m_2\pi. \end{aligned}$$

Now we apply the homotopy perturbation method to solve the boundary value problem. First, we simplify the equations (5.24),(5.25),(5.26) and (5.27) by trigonometric relations and then define the homotopy map as

$$\begin{aligned} h_p(\theta_1,\theta_2,\lambda_1,\lambda_2) =& (1-p)(L(\theta_1,\theta_2,\lambda_1,\lambda_2) - L(\theta_{1,init},\theta_{2,init},\lambda_{1,init},\lambda_{2,init})) \\ &+ p(L(\theta_1,\theta_2,\lambda_1,\lambda_2) + NL(\theta_1,\theta_2,\lambda_1,\lambda_2)) = 0, \end{aligned} \tag{5.28}$$

where the linear and nonlinear part of the problem is defined by,

$$L(\theta_1,\theta_2,\lambda_1,\lambda_2) = \left[\ \dot{\theta_1} + \tfrac{z_{d1}^2\lambda_1}{4},\ \dot{\theta_2} + \tfrac{z_{d2}^2\lambda_2}{4},\ \dot{\lambda_1},\ \dot{\lambda_2}\ \right]^T$$

and

$$NL(\theta_1,\theta_2,\lambda_1,\lambda_2)=\begin{bmatrix} -\omega_1-\frac{z_{d1}^2\lambda_1\cos 2\theta_1}{4}+\frac{z_{d1}z_{d2}\lambda_2\cos(\theta_1-\theta_2)}{4}-\frac{z_{d1}z_{d2}\lambda_1\cos(\theta_1+\theta_2)}{4} \\ -\omega_2-\frac{z_{d2}^2\lambda_2\cos 2\theta_2}{4}+\frac{z_{d2}z_{d1}\lambda_1\cos(\theta_2-\theta_1)}{4}-\frac{z_{d2}z_{d1}\lambda_2\cos(\theta_1+\theta_2)}{4} \\ -\frac{z_{d1}^2\lambda_1^2\sin(2\theta_1)}{4}-\frac{z_{d1}z_{d2}\lambda_1\lambda_2\sin(\theta_1+\theta_2)}{4}+\frac{z_{d1}z_{d2}\lambda_1\lambda_2\sin(\theta_1-\theta_2)}{4} \\ -\frac{z_{d2}^2\lambda_2^2\sin(2\theta_2)}{4}-\frac{z_{d2}z_{d1}\lambda_2\lambda_1\sin(\theta_2+\theta_1)}{4}+\frac{z_{d2}z_{d1}\lambda_2\lambda_1\sin(\theta_2-\theta_1)}{4} \end{bmatrix}.$$

We substitute the variables $\theta_1, \theta_2, \lambda_1$, and λ_2 in the homotopy map $h_p(\theta_1,\theta_2,\lambda_1,\lambda_2) = 0$, with respective power series expansions:

$$\theta_1=\sum_{i=0}^{\infty}\bar{\theta}_{1,i}p^i,\quad \theta_2=\sum_{j=0}^{\infty}\bar{\theta}_{2,j}p^j,\quad \lambda_1=\sum_{k=0}^{\infty}\bar{\lambda}_{1,k}p^k,\quad \lambda_2=\sum_{l=0}^{\infty}\bar{\lambda}_{2,l}p^l,$$

and compare the powers of the p to determine the coefficients, $\bar{\theta}_{1,i}, \bar{\theta}_{2,i}, \bar{\lambda}_{1,i}$ and $\bar{\lambda}_{2,i}$. For practical purposes, we truncate this infinite series at the N^{th} power of p and implement a recursive relation to calculate the coefficients. The coefficients of the zeroth power terms of p are obtained by the equation,

$$L(\bar{\theta}_{1,0},\bar{\theta}_{2,0},\bar{\lambda}_{1,0},\bar{\lambda}_{2,0})=L(\theta_{1,init},\theta_{2,init},\lambda_{1,init},\lambda_{2,init}), \tag{5.29}$$

which shows the zeroth power coefficients are equal to the initial solution. We can freely choose the initial solution in such a way to satisfy the boundary conditions. The first order coefficients of p are obtained by solving,

$$L(\bar{\theta}_{1,1},\bar{\theta}_{2,1},\bar{\lambda}_{1,1},\bar{\lambda}_{2,1})+L(\theta_{1,init},\theta_{2,init},\lambda_{1,init},\lambda_{2,init})+NL(\bar{\theta}_{1,0},\bar{\theta}_{2,0},\bar{\lambda}_{1,0},\bar{\lambda}_{2,0})=0, \tag{5.30}$$

and the higher orders coefficients are given by,

$$L(\bar{\theta}_{1,n},\bar{\theta}_{2,n},\bar{\lambda}_{1,n},\bar{\lambda}_{2,n})=\frac{-1}{(n-1)!}\left.\frac{\partial^{n-1}NL\left(\sum_{i=0}^{n-1}\bar{\theta}_{1,i}p^i,\sum_{j=0}^{n-1}\bar{\theta}_{2,j}p^j,\sum_{k=0}^{n-1}\bar{\lambda}_{1,k}p^k,\sum_{l=0}^{n-1}\bar{\lambda}_{2,l}p^l\right)}{\partial p^{n-1}}\right|_{p=0} \tag{5.31}$$

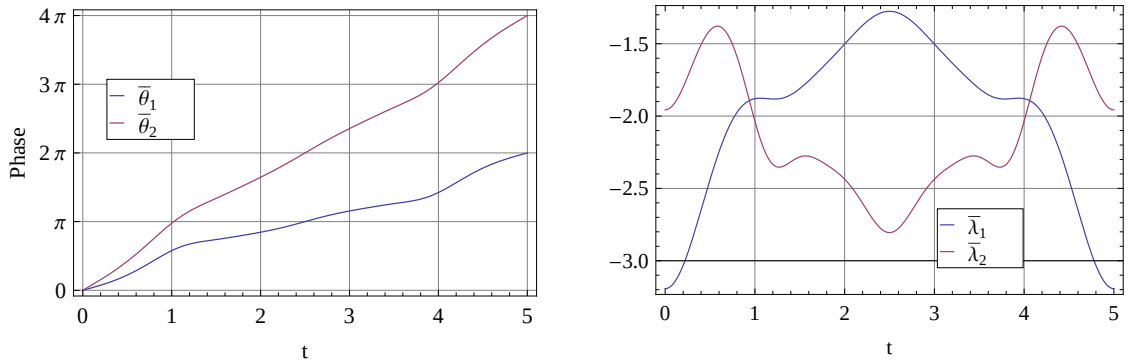

(a) (b)

Figure 5.3: (a) The θ_1, θ_2 and (b) λ_1, λ_2 trajectories for boundary value problem calculated from homotopy perturbation method.

where $n \geq 2$. This way we can calculate all the coefficients of the power series expansion for all four variables and the approximate solution is given by,

$$\bar{\theta}_1 = \sum_{i=0}^{N} \bar{\theta}_{1,i}, \quad \bar{\theta}_2 = \sum_{j=0}^{N} \bar{\theta}_{2,j}, \quad \bar{\lambda}_1 = \sum_{k=0}^{N} \bar{\lambda}_{1,k}, \quad \bar{\lambda}_2 = \sum_{l=0}^{N} \bar{\lambda}_{2,l}.$$

The approximate solution has to satisfy the initial conditions $\bar{\theta}_1(0) = 0, \bar{\theta}_2(0) = 0$ and the terminal conditions $\bar{\theta}_1(T) = 2m_1\pi, \bar{\theta}_2(T) = 2m_2\pi$ at each order of p. Therefore, we force the values of $\bar{\theta}_{1,i}$ and $\bar{\theta}_{2,j}$ to zero, at the initial time for all i, j, and at the final time for $i, j \geq 1$. The value of the the coefficients $\bar{\theta}_{1,0}(T)$ and $\bar{\theta}_{2,0}(T)$ are chosen to be $2m_1\pi$ and $2m_2\pi$ respectively to satisfy the final value:

$$\bar{\theta}_{1,i}(0) = 0 \ \forall i, \quad \bar{\theta}_{2,j}(0) = 0 \ \forall j,$$

$$\bar{\theta}_{1,0}(T) = 2m_1\pi, \quad \bar{\theta}_{2,0}(T) = 2m_2\pi, \quad \bar{\theta}_{1,i}(T) = 0 \ \forall i \geq 1, \quad \bar{\theta}_{2,j}(T) = 0 \ \forall j \geq 1.$$

For an example, consider the case where $\omega_1 = 1$, $\omega_2 = 2$, $z_{d1} = 1$, $z_{d2} = 1$, $m_1 = 1$, $m_2 = 2$ and $T = 5$. We choose the initial solutions to be $\theta_{1,init} = 2m_1\pi t/T, \theta_{2,init} = 2m_2\pi t/T, \lambda_{1,init} = 0$, and $\lambda_{2,init} = 0$; and follow the above given procedure to calculate the approximate solution. Figures 5.3(a) and 5.3(b) illustrate the approximate solutions of θ_1, θ_2 and λ_1, λ_2, if we consider up to seventh order of p. Note that by increasing the order of approximation N, we can improve the approximate solution to be arbitrarily close to the real solution.

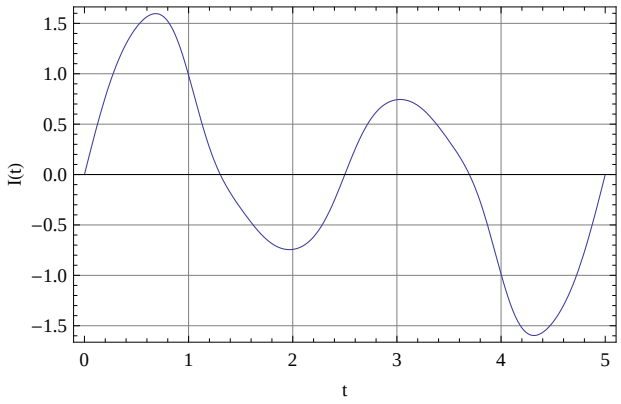

Figure 5.4: Minimum-power optimal control calculated from the homotopy perturbation method for a two-neuron system where the neurons spike simultaneously at $T = 5$.

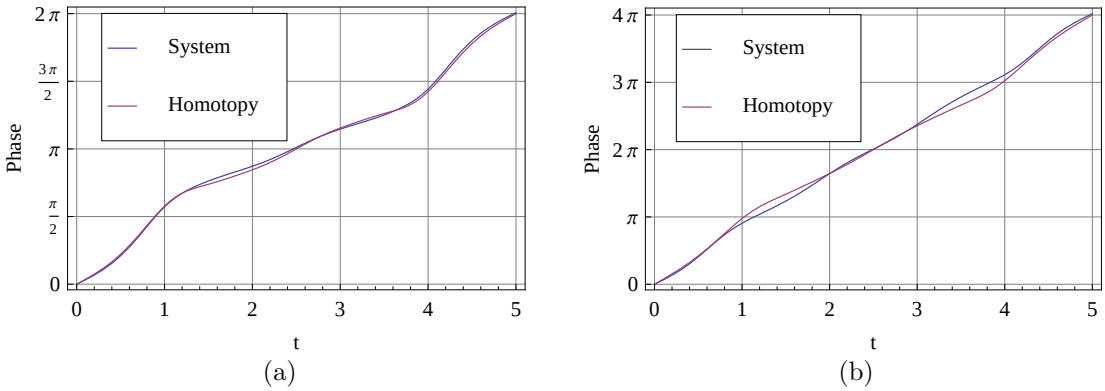

Figure 5.5: (a) Homotopy trajectory and the system trajectory under the derived optimal control for state θ_1 and (b) for state θ_2

With approximate solutions to the variable $\theta_1, \theta_2, \lambda_1$, and λ_2, we calculate the optimal control according to the equation (5.23) and it is depicted in Figure 5.4. In order to validate the derived control, we apply it back to the original system and then evolve the system forward in time. The resulted trajectories together with homotopy trajectories for state θ_1 and θ_2 are depicted in Figures 5.5(a) and 5.5(b) respectively. Homotopy trajectories and actual system trajectories under the optimal control show strong similarities, and the differences between these two kind of trajectories reduce with the order of approximation N.

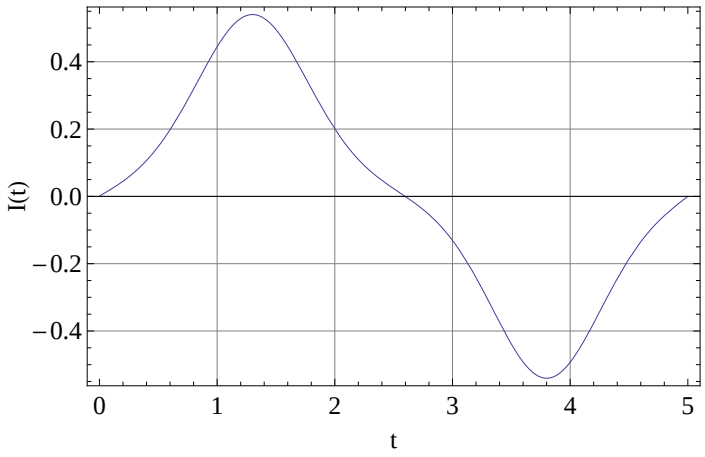

Figure 5.6: Minimum-power optimal control calculated using the homotopy perturbation method for the coupled two-neuron system with simultaneous spikes at $T = 5$.

5.3.2 Minimum-Power Control of a Coupled Two-Neuron System

Similar to Section 5.3.1, the minimum-power control of coupled neurons also can be formulated as an optimal steering problem as given in (5.1) with $\varphi(T, \Theta(T)) = 0$ and $\mathcal{L}(\Theta(t), I(t)) = I(t)^2$. We model the dynamics of coupled neurons using the following Kuramoto-like system [76]:

$$f(\Theta) = \begin{bmatrix} f_1 \\ f_2 \end{bmatrix} = \begin{bmatrix} \omega_1 + \alpha_{1,2} \sin(\theta_2 - \theta_1) \\ \omega_2 + \alpha_{2,1} \sin(\theta_1 - \theta_2) \end{bmatrix}, \quad Z(\Theta) = \begin{bmatrix} Z_1 \\ Z_2 \end{bmatrix} = \begin{bmatrix} z_{d1} \sin\theta_1 \\ z_{d2} \sin\theta_2 \end{bmatrix}.$$

where $\alpha_{1,2}$ and $\alpha_{2,1}$ denote the strength of coupling between the two neurons. Our objective is to drive this coupled two-neuron system from the initial state $\Theta_0 = (0, 0)'$ to the desired final state $\Theta_d = (2m_1\pi, 2m_2\pi)'$ with minimum power, where $m_1, m_2 \in \mathbb{Z}^+$. As in Section 5.3.1, we also use the homotopy perturbation method to solve this problem, and the result is give in Figure 5.6 for the parameter values $\omega_1 = 1, \omega_2 = 1.1, \alpha_{1,2} = 0.1, \alpha_{1,1} = -0.1, z_{d1} = 1, z_{d2} = 1, m_1 = 1, m_2 = 2$ and $T = 5$. Figure 5.7(a) and 5.7(b) illustrate the resulting trajectories for θ_1 and θ_2, where blue, red, and brown trajectories represent the system trajectory under the derived control, the homotopy trajectory and the reference trajectory without the control, respectively.

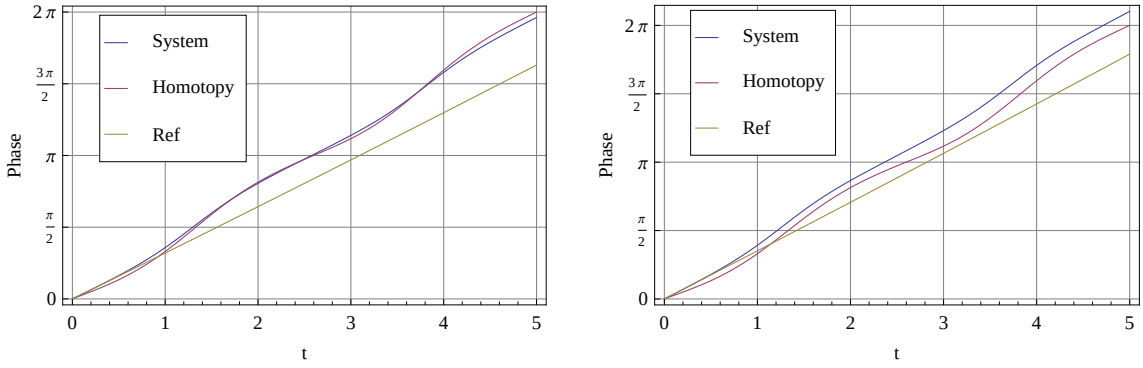

Figure 5.7: Homotopy trajectory, system trajectory under the derived optimal control, and the uncontrolled reference trajectory (a) for state θ_1 and (b) for state θ_2.

5.3.3 Minimum-Power Control of a Neuron Ensemble

In Figure 5.8, we demonstrate the flexibility of the homotopy perturbation method to drive multiple sinusoidal neurons to desired targets. In particular we seek to simultaneously spike five frequencies with widely dispersed frequency values at a time T different from their natural period. In this figure, we consider the frequencies $(\omega_1, \omega_2, \omega_3, \omega_4, \omega_5) = (1, 2, 3, 4, 5)$ and design the unbounded controls to drive these systems to $(2\pi, 4\pi, 6\pi, 8\pi, 10\pi)$, respectively, at a time $T = 2\pi - 0.5$. Controls for minimum energy ($\alpha = 0$, $\beta = 1$) transfer can be designed where the state trajectories and spike sequence follow the same general pattern. The spike train shows that the controls are able to advance the firing of each neuron so that all five spike simultaneously at the desired terminal time. Note that in this example, we just use the order approximation $N = 4$ and calculate the first five terms of the power series expansion.

This same example also can be solved in similar fashion using pseudospectral method. In Figures 5.9(a) and 5.9(b) we present results obtained from the pseudospectral method, which shows strong agreement with results obtained by the homotopy perturbation method in Figures 5.8(a) and 5.8(b).

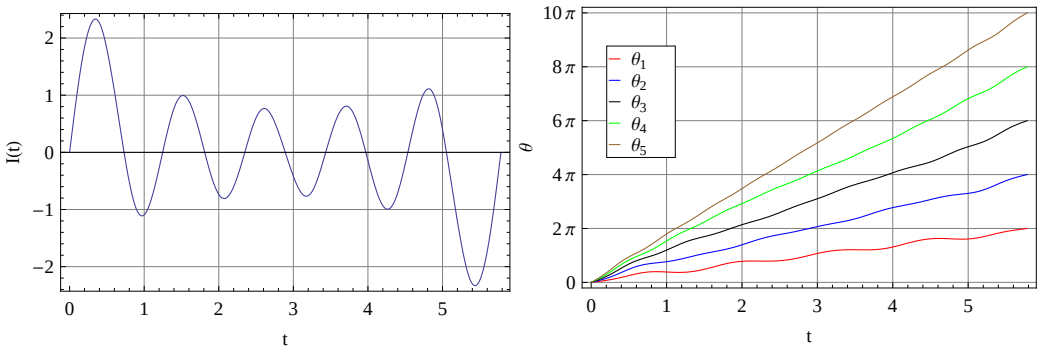

(a) (b)

Figure 5.8: (a) The controls of a sinusoidal PRC neuron model driving five frequencies, $(\omega_1, \omega_2, \omega_3, \omega_4, \omega_5) = (1, 2, 3, 4, 5)$, to the desired targets $\theta(T) = (2\pi, 4\pi, 6\pi, 8\pi, 10\pi)$ when $T = 2\pi - 0.5$ and (b) their state trajectories obtained obtained form homotopy perturbation technique.

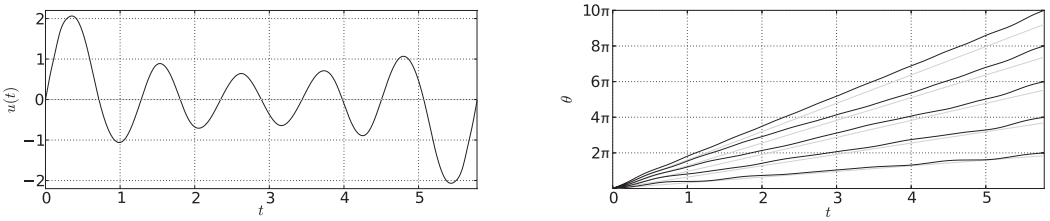

(a) (b)

Figure 5.9: (a) The controls of a sinusoidal PRC neuron model driving five frequencies, $(\omega_1, \omega_2, \omega_3, \omega_4, \omega_5) = (1, 2, 3, 4, 5)$, to the desired targets $\theta(T) = (2\pi, 4\pi, 6\pi, 8\pi, 10\pi)$ when $T = 2\pi - 0.5$ and (b) their state trajectories

5.4 Conclusion

In this Chapter, we considered the optimal control of a heterogenous neuron ensemble described by phase models. In particular, the synthesis of minimum-power and time-optimal controls that achieve coordinated spiking in neuron ensembles was described. The ability to manipulate phase oscillators is of theoretical significance in neuroscience, and is of practical importance for the development of therapeutic procedures such as deep brain stimulation for clinical treatment of Parkinson's disease and epilepsy. Our technique can be used to control oscillating systems that arise in diverse fields including biology, chemistry, semiconductor electronics, and mechanical vibrating systems.

Chapter 6

Conclusion

In this dissertation we study a series of optimal control problems involving nonlinear oscillators. We represent the dynamics of oscillators by their phase models and derive the optimal control laws that optimize various given cost functionals. The methodologies presented in the dissertation are generic for all oscillatory systems whose dynamics can be described by phase models. Our work has broad impact on various areas, where the ability to manipulate dynamic structures such as synchronization, is fundamental. These include the control of voltage-controlled phase-lock loops in electrical engineering, suppression of vibrations in mechanical systems, control of circadian rhythms in biological systems, and formation of social groups in social networks. In the past, researchers have used phase models to perform qualitative analyses of the oscillatory systems, however there are only a handful of works on quantitative control. Our novel contribution in this dissertation is to establish a control-theoretic framework that provides analytically and numerically tractable methods for optimal control of weakly forced nonlinear oscillators.

We design minimum-power controls that lead to a desired spiking time of neuron oscillators. We consider a bound on the control amplitude and characterize the range of possible spiking times determined by this bound. We show that, for a given bound, the corresponding feasible spiking times are optimally achieved by piecewise continuous controls. We test these bounded controls in the full state-space model to quantitatively verify and illustrate the weak forcing assumption. We present analytical expressions with numerical simulations of the minimum-power stimuli for several phase models including the sinusoidal, SNIPER, and Morris-Lecar phase models. We

demonstrate the practicality and applicability of our method by successful experimental realizations of the derived optimal controls in electrochemical oscillators.

In addition, we derive charge-balanced minimum-power as well as charge-balanced time-optimal controls. The latter determines the minimum and maximum spiking time of a neuron oscillator. The derived optimal controls are applied to both mathematically ideal and experimentally observed phase models. This work addresses a fundamental problem in the field of neural control and provides a theoretical investigation of the optimal controls of oscillatory systems subject to a constrained control set. We develop a systematic computation procedure for the synthesis of these optimal controls and completely characterize the different structures of these controls with respect to the allowable bound on the control amplitude. Our consideration of bounded controls is of fundamental importance because the phase model reduction is valid for weak forcing. These optimal control designs have potential impact on the improvement and development of innovative therapeutic procedures for neurological disorders, where accumulation of electrical charge has undesirable side effects. The qualitative performance that we observed from the controls derived from the phase models when applying them to the underlying full state-space models is highly promising in practical applications such as clinical therapy.

Furthermore, we investigate the optimal control of a neuron ensemble. The optimal control of a single neuron system studied in this work provides a guide line that enables us to study optimal control of spiking neuron populations. Our recent work proved the controllability of a neural population described by phase models [84]. It assures the existence of a control law that causes simultaneous spikes of a network of neurons. We examine the optimal control of an ensemble of coupled and uncoupled neuron oscillators that have variation in the frequency. We analytically derive the time-optimal control for spiking two neuron oscillators and propose an optimization-free and iterative computational method based on homotopy perturbation techniques to construct optimal controls for spiking neuron ensemble. This computational method is not only robust to optimal control problems of neuron oscillators, but also applicable to solve a broad class of optimal control problems, such as optimal control of nuclear spin dynamics in nuclear magnetic resonance spectroscopy and imaging. The derived methods by this dissertation work are universal to any nonlinear oscillator whose dynamics can be described by phase models.

Appendix A

Pontryagin's Maximum Principle

A.1 General Form of the Maximum Principle

The maximum principle[116, 107] was developed by a group of mathematicians, namely L.S. Pontryagin, V.G. Boltyanskii, R.V. Gamkrelidze and E.F. Mishchenko, in the 1950s. In this section, we briefly summarize the Maximum principle and relevant definitions. Consider the optimal control problem in the following form.

$$\begin{aligned} \min \quad & J(u) = \int_{t_0}^{T} \mathcal{L}(t, x(s), u(s))ds + \varphi(x(T), T) \\ \text{s.t.} \quad & \dot{x} = f(t, x, u) \\ & \psi(T, x(T)) = 0. \end{aligned} \tag{A.1}$$

where $x \in M$ is the state of the system and $u \in U$ is the control variable. Note that open and connected $M \subset \mathbb{R}^n$ and $U \subset \mathbb{R}^m$ are used to denote the state-space and control set, respectively. The variable t is used to denote time and t_0 and T correspond to the initial and the final times. Function $\mathcal{L} : \mathbb{R} \times M \times U \to \mathbb{R}$ is known as the Lagrangian, and the integral of it gives the running cost for the objective. Function $\varphi : \mathbb{R}^{n+1} \to \mathbb{R}$ defines the terminal cost. The dynamics of the system is given by the function $f : \mathbb{R} \times M \times U \to \mathbb{R}^n$. We assume the time-varying vector field defined by function f is continuous in (t, x, u), and differentiable in x for fixed (t, u). We also assume that the partial derivatives of f are exist and are continuous in all variables. The terminal set is given by $k-$ dimensional embedded submanifold N in $\mathbb{R} \times M$. More specifically, N is given by $N = \{(t, x) \in \mathbb{R} \times M : \psi(t, x) = 0\}$.

Definition 3 *The control hamiltonian H of the above given optimal control problem is defined as*

$$H(t, \lambda_0, \lambda, x, u) = \lambda_0 L(t, x, u) + \lambda f(t, x, u),$$

where

$$H : \mathbb{R} \times [0, \infty] \times (\mathbb{R}^n) \times \mathbb{R}^n \times \mathbb{R}^m \to \mathbb{R}.$$

Theorem 1 ***(Pontryagin's Maximum Principle)****[116, 107] Let (x_*, u_*) be a controlled trajectory defined over the interval $[t_0, T]$, and suppose the control u_* is piecewise continuous. If (x_*, u_*) is optimal, then there exist a constant $\lambda_0 \geq 0$ and a co-vector $\lambda : [t_0, T] \to (\mathbb{R}^n)^*$, the so-called adjoint variable, such that the following conditions are satisfied:*

1. *Nontriviality of the multipliers: $(\lambda_0, \lambda(t)) \neq 0 \ \forall \ t \in [t_0, T]$.*

2. *Adjoint equation: the adjoint variable λ is a solution to the time-varying linear differential equation*

$$\dot{\lambda}(t) = -\lambda_0 \mathcal{L}_x(t, x_*(s), u_*(s)) - \lambda(t)\{_x(t, x_*(s), u_*(s)).$$

3. *Minimum Condition: every where in $[t_0, T]$, we have that*

$$H(t, \lambda_0, \lambda(t), x_*(t), u_*(t) = \min_{u \in U} H(t, \lambda_0, \lambda(t), x_*(t), u(t)).$$

   If the Lagrangian $\mathcal{L}$ and the dynamics f are continuously differentiable in t, then the function

$$h : t \to H(t, \lambda_0, \lambda(t), x_*(t), u_*(t))$$

   is continuously differentiable with derivative given by

$$\dot{h}(t) = \frac{dh}{dt}(t) = \frac{\partial H}{\partial t}(t, \lambda_0, \lambda(t), x_*(t), u_*(t)).$$

4. *Transversality condition: at the endpoint of the controlled trajectory, the covector*

$$(H + \lambda_0 \varphi_t, -\lambda + \lambda_0 \varphi_x).$$

is orthogonal to the terminal constant N, i.e. there exists a multiplier $\nu \in (\mathbb{R}^{n+1-k})^*$ such that

$$H + \lambda_0 \varphi_t + \nu D_t \psi = 0, \quad \lambda = \lambda_0 \varphi_x + \nu D_x \psi \quad at \quad (T, x_*(T))$$

A.2 Maximum Principle for Time-Optimal Control Problems

Theorem 2 (Time-Optimal Control [107]) *Let $(x_*(t), u_*(t))$ be a time-optimal controlled trajectory that transfers the initial condition $x(0) = x_0$ into the terminal state $x(T) = x_T$. Then, it is a necessary condition for optimality that there exist a constant $\lambda_0 \geq 0$ and a nonzero, absolutely continuous row vector function $\lambda(t)$ such that:*

1. *λ satisfies the so-called adjoint equation*

$$\dot{\lambda}(t) = -\frac{\partial H}{\partial x}(\lambda_0, \lambda(t), x_*(t), u_*(t)).$$

2. *For $0 \leq t \leq T$ the function $u \mapsto H(\lambda_0, \lambda(t), x_*(t), u)$ attains its minimum over the control set U at $u = u_*(t)$.*

3. *$H(\lambda_0, \lambda(t), x_*(t), u_*(t)) \equiv 0$.*

Appendix B

Computation of Optimal Controls for a Neuron Ensemble By a Pseudospectral Method

The pseudospectral method is a spectral collocation method originally developed to solve partial differential equations, and has recently been adapted to solve optimal control problems [110, 82, 113, 83, 43, 27]. In this approach, the differential equations that relate the states and the controls are discretized at specific collocation nodes, which result in a discrete optimization problem. All continuous-time functions are rescaled to the time domain of [-1,1] and expanded by an orthogonal polynomial basis based on a set of selected quadrature nodes [27]. Here, we use the Legendre-Gauss-Lobatto(LGL) nodes and can then write the N^{th} order interpolating approximations of the state and control functions

$$\Theta(t) \approx I_N\Theta(t) = \sum_{k=0}^{N} \bar{\Theta}_k \ell_k(t), \tag{B.1}$$
$$u(t) \approx I_N u(t) = \sum_{k=0}^{N} \bar{u}_k \ell_k(t),$$

where

$$\ell_k(t) = \prod_{i=0, i\neq k}^{N} \frac{t - t_i}{t_k - t_i}, \quad k = 0, 1, \ldots, N,$$

are the Lagrange polynomials with $\ell_k(t_i) = \delta_{ki}$, which is the Kronecker delta function. The derivative of $I_N\Theta(t)$ at the LGL node t_j, $j = 0, 1, \ldots, N$, is given by

$$\frac{d}{dt} I_N\Theta(t_j) = \sum_{k=0}^{N} \bar{\Theta}_k \dot{\ell}_k(t_j) = \sum_{k=0}^{N} D_{jk}\bar{\Theta}_k,$$

where D_{jk} are elements of the constant $(N+1) \times (N+1)$ differentiation matrix

$$D_{jk} = \begin{cases} \frac{L_N(t_j)}{L_N(t_k)} \frac{1}{t_j - t_k} & j \neq k \\ -\frac{N(N+1)}{4} & j = k = 0 \\ \frac{N(N+1)}{4} & j = k = N \\ 0 & \text{otherwise.} \end{cases}$$

The integral cost functional of the optimal control problem as in (5.1) can be accurately approximated by the Gauss-Lobatto integration rule. Thus, the pseudospectral discretization of the optimal control problem (5.1) gives rise to a finite-dimensional constrained nonlinear minimization problem of the form,

$$\begin{aligned} &\min\ \varphi(T, \bar{\Theta}_N) + \frac{T}{2} \sum_{j=0}^{N} \mathcal{L}(\bar{\Theta}_j, \bar{u}_j) w_j \\ &\text{s.t.} \quad \sum_{k=0}^{N} D_{jk}\bar{\Theta}_k = \frac{T}{2}\Big[f(\bar{\Theta}_j) + \bar{u}_j\, Z(\bar{\Theta}_j) \Big], \\ &\qquad \bar{\Theta}_0 = 0, \\ &\qquad \bar{\Theta}_N = \Theta_d, \quad \forall\ j \in \{0, 1, \ldots, N\}, \end{aligned} \tag{B.2}$$

where $\Theta_d = (2m_1\pi, 2m_2\pi, \ldots, 2m_n\pi)'$, $m_i \in \mathbb{Z}^+$, $i = 1, \ldots, n$, is the target state and w_j are the LGL weights given by

$$w_j = \frac{2}{N(N+1)} \frac{1}{(L_N(t_j))^2},$$

in which L_N is the N^{th} order Legendre polynomial. This type of constrained nonlinear programs are straightforward to implement and can be solved with many of the commercially available nonlinear solves. We implement it in the AMPL language [39] and use a third party nonlinear programming solver, KNITRO [14], to solve this optimization problem. Note that the Legendre pseudospectral method also can

be used as a direct method to verify the previously presented analytical results in Chapters 2,3,4 and 5.

Remark 6 (Extension to an infinite ensemble of neuron systems) *The pseudospectral method can be extended to discretize optimal control problems related to infinite collection of neurons, for example a population of neurons with the frequency distribution over a closed interval,* $\omega \in [\omega_a, \omega_b] \subset \mathbb{R}^+$*. In such a case, the parameterized state trajectory can be approximated by a two-dimensional interpolating polynomial, namely,* $\Theta(t, \omega) \approx I_{N \times N_\omega} \Theta(t, \omega)$*, according to the LGL nodes in the time* t *and the parameter* ω*. Similar to having only a finite number of neurons, the dynamics of the state can be expressed as an algebraic constraint in the nonlinear program and a corresponding minimization problem can be constructed accordingly [113].*

References

[1] J. A. Acebron, L. L. Bonilla, C. J. P. Vicente, F. Ritort, and R. Spigler. The Kuramoto model: A simple paradigm for synchronization phenomena. *Reviews Of Modern Physics*, 77(1):137–185, 2005.

[2] T. Aprille and T. Trick. A computer algorithm to determine the steady-state response of nonlinear oscillators. *IEEE Transactions on Circuit Theory*, 19(4):354–360, 1972.

[3] P. Ashwin and J. Swift. The dynamics of n weakly coupled identical oscillators. *J. Nonlinear Sci.*, 2:69–108, 1992.

[4] A. L. Benabid and P. Pollak. Long-term suppression of tremor by chronic stimulation of the ventral intermediate thalamic nucleus. *The Lancet*, 337:403–406, 1991.

[5] I. Blekhman. *Synchronization in science and technology*. ASME Press translations, New York, 1988.

[6] B. Bonnard and M. Chyba. *Singular Trajectory and their Role in Control Theory*. Springer-Verlag, New York, 2003.

[7] U. Boscain and B. Piccoli. *Optimal Syntheses for Control Systems on 2-D Manifolds*. Springer-Verlag, 2004.

[8] R. Brette. Dynamics of one-dimensional spiking neuron models. *J. Math. Biol.*, 48:38–56, 2004.

[9] R. Brockett. Nonlinear systems and differential geometry. *Proceedings of the IEEE*, 64(1):61–72, 1976.

[10] Eric Brown, Philip Holmes, and Jeff Moehlis. Globally coupled oscillator networks. In *In: Perspectives and Problems in Nonlinear Science: A Celebratory Volume in Honor of Larry Sirovich*, pages 183–215. Springer, 2003.

[11] Eric Brown, Jeff Moehlis, and Philip Holmes. On the phase reduction and response dynamics of neural oscillator populations. *Neural Comput.*, 16(4):673–715, 2004.

[12] Nicolas Brunel and Mark C. W. van Rossum. Lapicques 1907 paper: from frogs to integrate-and-re. *Biol. Cybern*, 97:337–339, 2007.

[13] A. E. Bryson, Jr., and Y. C. Ho. *Applied Optimal Control*. Taylor & Francis Group, New York, 1979.

[14] R. Byrd, M. E. Hribar, and Nocedal J. An interior point method for large scale nonlinear programming. *SIAM J. Optimization*, 9:877–900, 1999.

[15] C Canuto, M Y Hussaini, A Quarteroni, and T A Zang. *Spectral Methods*. Springer, Berlin, 2006.

[16] A. H. Cohen, P. J. Holmes, and R. H. Rand. The nature of the coupling between segmental oscillators of the lamprey spinal generator for locomotion: a methematical model. *J. Math. Biology*, 13:345–369, 1982.

[17] S. Coombes and P. Bressloff. Mode locking and arnold tongues in integrate-and-fire neural oscillators. *Physical Review E*, 60(2):2086–2096, 1999.

[18] P. Danzl and J. Moehlis. Spike timing control of oscillatory neuron models using impulsive and quasi-impulsive charge-balanced inputs. In *Proc. American Control Conference, Seattle, Washington, USA, 2008*. IEEE, June 2008.

[19] Per Danzl, Ali Nabi, and Jeff Moehlis. Charge-balanced spike timing control for phase models of spiking neurons. *Discrete and Continuous Dynamical Systems*, 28(4):1413–1435, Dec 2010.

[20] I. Dasanayake and J.-S. Li. Constrained minimum-power control of spiking neuron oscillators. In *50th IEEE Conference on Decision and Control*, Orlando, FL, December 2011.

[21] I. Dasanayake and J.-S. Li. Optimal design of minimum-power stimuli for phase models of neuron oscillators. *Phy. Rev. E*, 83:061916, 2011.

[22] I. Dasanayake and J.-S. Li. Charge-balanced time-optimal control for spiking neuron oscillators. In *Proc.* 51^{th} *IEEE Conference on Decision and Control*, Maui, HI, USA, Dec 2012. IEEE.

[23] I. Dasanayake and J.-S. Li. Design of charge-balanced time-optimal stimuli for spiking neuron oscillators. arXiv:1211.4549, 2012.

[24] M. Ding, E. Ding, W. L. Ditto, B. Gluckman, V. In, J. Peng, M. L. Spano, and W. Yang. Control and synchronization of chaos in high dimensional systems: Review of some recent results. *Chaos*, 7(4):644–652, 1997.

[25] D. Efimov and T. Raissi. Phase resetting control based on direct phase response curve. In *Preprints of the 8th IFAC Symposium on Nonlinear Control Systems*, pages 332–337, Bologna, September 2010.

[26] D. Efimov, P. Sacré, and R. Sepulchre. Controlling the phase of an oscillator: A phase response curve approach. In *Joint 48th Conference on Decision and Control*, pages 7692–7697, Shanghai, December 2009.

[27] G. Elnagar, M. A. Kazemi, and M. Razzaghi. The pseudospectral legendre method for discretizing optimal control problems. 40:1793–1796, Oct 1995.

[28] G.B. Ermentrout. Type I membranes, phase resetting curves, and synchrony. *Neural Comput.*, 8:979–1001, 1996.

[29] G.B Ermentrout. *Stimulating, Analyzing, and Animating Dynamical Systems*. SIAM, Philadelphia, 2002.

[30] G.B. Ermentrout and J. Rinzel. Beyond a pacemaker's entrainment limit: phase walk-through. *American Journal of Physiology - Regulatory, Integrative and Comparative Physiology*, 246(1), 1984.

[31] G.B. Ermentrout and David H. Terman. *Mathematical Foundation of Neuroscience*. Springer, 2010.

[32] F Fahroo and IM Ross. Costate estimation by a Legendre pseudospectral method. *Journal of Guidance, Control, and Dynamics*, 24(2):270–277, 2001.

[33] J. Feng and H. C. Tuckwell. Optimal control of neuronal activity. *Phy. Rev. Lett.*, 91(1):018101, 2003.

[34] I. Fischer, Y. Liu, and P. Davis. Synchronization of chaotic semiconductor laser dynamics on subnanosecond time scales and its potential for chaos communication. *Physical Review A*, 62, 2000.

[35] R. FitzHugh. Impulses and physiological states in theoretical models of nerve membrane. *Biophysical J.*, 1:445–466.

[36] D. B. Forger and D. Paydarfar. Starting, stopping and resetting biological oscillators: In search of optimal perturbation. *J. Theor. Biol.*, 230:521–535, 2004.

[37] B. Fornberg. *A Practical Guide to Pseudospectral Methods*. Cambridge University Press, 1998.

[38] J Foss and John Milton. Multistability in recurrent neural loops arising from delay. *J. Neurophysiol.*, 84:975–985, 2000.

[39] D. M. Gay. Hooking your solver to ampl. Technical report, Bell Laboratories, Lucent Technologies, Murray Hill, NY 07974, 1993.

[40] W. Gerstner, V. Hemman, and J.Cowan. What matters in neural locking. *Neural Comput.*, 8:1653–1676, 1996.

[41] R. M. Ghigliazza and P. Holmes. A minimal model of a central pattern generator and motoneuros for insect loco-motion. *SIAM J. Appl. Dyn. Syst.*, 3(4):671–700, 2004.

[42] L. Glass. Cardiac arrhythmias and circle maps-a classical problem. *Chaos*, 1(1):13–19, 1991.

[43] Q. Gong, W. Kang, and I. M. Ross. A pseudospectral method for the optimal control of constrained feedback linearizable systems. *IEEE transactions on automatic control*, 51(7):1115–1129, 2006.

[44] L. B. Good, S. Sabesan, S.T. Marsh, K. Tsakalis, D. Treiman, and L. Lasemidis. Control of synchronization of brain dynamics leads to control of epileptic seizures in rodents. *International Journal of Neural Systems*, 19:173–196, 2009.

[45] David Gottlieb, M Yousuff Hussaini, and Steven A. Orszag. Theory and applications of spectral methods. In *Spectral Methods for PDE's*. SIAM, Philadelphia, 1984.

[46] W. Govaerts and B. Sautois. Computation of the phase response curve: A direct numerical approach. *Neural Computation*, 18(4):817–847, 2006.

[47] D. Hansel, G. Mato, and C. Meunier. Phase dynamics for weakly coupled hodgking-huxley neurons. *Europhys. Lett.*, 25(5):367–372, 1993.

[48] F. Hanson. Comparative studies of firefly pacemakers. *Federation proceedings*, 38(8):2158–2164, 1978.

[49] Takahiro Harada, Hisa-Aki Tanaka, Michael J. Hankins, and István Z. Kiss. Optimal waveform for the entrainment of a weakly forced oscillator. *Phys. Rev. Lett.*, 105(8):088301, Aug 2010.

[50] Takahiro Harada, Hisa-Aki Tanaka, Michael J. Hankins, and Istvan Z. Kiss. Optimal waveform for the entrainment of a weakly forced oscillator. *Phys. Rev. Lett.*, 105(8):088301, 2010.

[51] Ji-Huan He. Homotopy perturbation technique. *Comput. Methods Appl. mech. Engrg.*, 178:257–262, 1999.

[52] A. L. Hodgkin and A. F. Huxley. A quantitative description of membrane current and its application to conduction and excitation in never. *J. Physiol.*, 117:500–544, 1952.

[53] F. Hoppensteadt and E. Izhikevich. *Weakly connected neural networks*. Springer-Verlag, New Jersey, 1997.

[54] F. C. Hoppensteadt and E. M. Izhikevich. Synchronization of laser oscillators, associative memory, and optical neurocomputing. *Physical Review E*, 62(3):4010–4013, 2000.

[55] F. C. Hoppensteadt and E. M. Izhikevich. Synchronization of mems resonators and mechanical neurocomputing. *IEEE Transactions On Circuits And Systems I-Fundamental Theory And Applications*, 48(2):133–138, 2001.

[56] Frank C. Hoppensteadt and Eugene M. Izhikevich. Oscillatory neurocomputers with dynamic connectivity. *Phys. Rev. Lett.*, 82(14):2983–2986, Apr 1999.

[57] J. D. Hunter and J. G. Milton. Amplitude and frequency dependence of spike timing: Implications for dynamic regulation. *J. Neurophysiol*, 90:387–394, 2003.

[58] A. Isidodri. *Nonlinear Control Systems*. Springer, London, 1995.

[59] E. Izhikevich and Y. Kuramoto. Weakly coupled oscillators. In *Encyclopedia of mathematical physics*. Elsevier, 2006.

[60] I. E. Izhikevich. *Dynamical Systems in Neuroscience*. The MIT Press, Cambridge, Massachusetts, 2007.

[61] Saso Jezernik, Thomas Sinkjaer, and Manfred Morari. Charge and enegy minimization in electrical/magnetic stimulation of nervous tissue. *J. Neural Eng.*, 7(4):046004, 2010.

[62] V. Jurdjevic. *Geometric Control Theory*. Cambridge University Press, Cambridge, 1997.

[63] T. Kano and S. Kinoshita. Control of individual phase relationship between coupled oscillators using multilinear feedback. *Phys. Rev. E*, 81(2):026206, Feb 2010.

[64] J. Keener and J. Sneyd. *Mathematical Physiology*. Springer-Verlag, New York, 1998.

[65] W. Kelley and A. Peterson. *The Theory of Differential Equations, Classical and Qualitative*. Pearson, 2004.

[66] H. Khalil. *Nonlinear Systems*. Prentice Hall, 3 edition, 2002.

[67] Navin Khaneja. Problems in control of quantum systems. In *Feedback Control of MEMS to Atoms*, pages 321–363. Springer US, 2012.

[68] I. Kiss, I. Zhai, and J. Hudson. Emerging coherence in a population of chemical oscillators. *Science*, 296:1676–1678, 2002.

[69] I. Z. Kiss, C. G. Rusin, H. Kori, and J. L. Hudson. Engineering complex dynamical structures: Sequential patterns and desynchronization. *Science*, 316(5833):1886–1889, 2007.

[70] I. Z. Kiss, Y. M. Zhai, and J. L. Hudson. Predicting mutual entrainment of oscillators with experiment-based phase models. *Physical Review Letters*, 94(24):248301, 2005.

[71] R. D. Klafter. An optimally energized cardiac pacemaker. *IEEE Tran. Biomed. Eng.*, 20:350–356, 1973.

[72] R. D. Klafter and L. Hrebien. An *in-vivo* study of cardiac pacemaker optimization by pulse shape modification. *IEEE Tran. Biomed. Eng.*, 23:233–239, 1976.

[73] N. Kopell and G. B. Ermentrout. Phase transitions and other phenomena in chains of coupled oscillators. *J. Math. Biol.*, 50:1014–1052, 1990.

[74] I. Kornfeld, S. Fomin, and Y. Sinai. *Ergodic theory: Differentiable Dynamical Systems*, volume 245 of *Grundlehren der mathematischen Wissenschaften*. Springer-Verlag, 1982.

[75] A. Krener. A generalization of chows theorem and the bang-bang theorem to nonlinear control problems. *SIAM J. Contr.*, 12(1):43–52, 1974.

[76] Y. Kuramoto. *Chemical Oscillations, Waves, and Turbulence*. Springer, New York, 1984.

[77] L. Lapicque. Recherches quantitative sur I'excitation électrique desnerfs traitée comme une polarization. *J. Physiol. Pathol. Gen.*, 9:620–635, 1907.

[78] O. Lev, A. Wolfberg, L. M. Pismen, and M. Sheintuch. The structure of complex behavior in anodic nickel dissolution. *Journal of Physical Chemistry*, 93:1661–1666, 1981.

[79] B. M. Levitan and V. V. Zhikov. *Almost periodic functions and differential equations*. Cambridge University Press, Cambridge, 1982.

[80] J.-S. Li, I.Dasanayake, and J. Ruths. Control and synchronization of neuron ensembles. arXiv:1111.6306v2, January 2012.

[81] J.-S. Li and N. Khaneja. Control of inhomogeneous quantum ensembles. *Physical Review A*, 73:030302, 2006.

[82] J. S. Li, J. Ruths, and Stefanatos D. A pseudospectral method for optimal control of open quantum systems. *J. Chem. Phys.*, 131:164110, 2009.

[83] J.-S. Li, J. Ruths, T.-Y. Yu, H. Arthanari, and G. Wagner. Optimal pulse design in quantum control: A unified computational method. *Proc. Natl. Acad. Sci.*, 108(5):1879–1884, 2011.

[84] Jr-Shin Li. Control of a network of spiking neuron. In *Proc. 8th IFAC Symposium on Nonlinear Control Systems, Bologna, Italy, 2010.* IFAC, Sep 2010.

[85] A.M. Lozano and H. Eltahawy. How does dbs work? *Suppl. Clin. Neurophysiol.*, 57:733–736, 2004.

[86] I. Malkin. *Methods of Poincare and Liapunov in the theory of nonlinear oscillations*. Gostexizdat, Moscow, 1949.

[87] W.J. Marks. Deep brain stimulation for dystonia. *Curr. Treat. Options Neurol.*, pages 237–243, 2005.

[88] D. R. Merril, M Bikson, and J. G. R. Jefferys. Electrical stimulation of excitable tissue: design of efficacious and safe protocols. *Journal of Neuroscience Methods*, 141:717–198, 2005.

[89] R. Mirollo and S. Strogatz. Synchronization of pulse-coupled biological oscillators. *SIAM Journal on Applied Mathematics*, 50(6):1645–1662, 1990.

[90] Jeff Moehlis, Eric Shea-Brown, and Herschel Rabitz. Optimal inputs for phase models of spiking neurons. *J. Comput. Nonlinear Dynam.*, 1(4):358–367, 2006.

[91] R. Montgomery. Optimal control of deformable bodies, isoholonomic problems and sub-riemannian geometry. In *Technical Report 05324-89, Mathematical Sciences Research Institute*, 1989.

[92] C Morris and H Lecar. Voltage oscillations in the barnacle giant muscle fiber. *Biophys. J.*, 35(1):193–213, 1981.

[93] Ali Nabi, Mohammaad Mirzadeh, Frederic Gibou, and Jeff Moehlis. Minimum energy desynchronizing control for coupled neurons. *J. Comput. Neurosci*, pages 1–13, 2012.

[94] Ali Nabi and Jeff Moehlis. Charge-balanced optimal input for phase models of spiking neurons. In *Proc. ASME Dynamic System and Control Conference*. ASME, Oct 2009.

[95] Ali Nabi and Jeff Moehlis. Charge-balanced optimal input for phase models of spiking neurons. *Discrete and Continuous Dynamical Systems*, 28(4), 2010.

[96] Ali Nabi and Jeff Moehlis. Single input optimal control for globally coupled neuron networks. *J. Neural Eng.*, 8:065008, 2011.

[97] Ali Nabi and Jeff Moehlis. Time optimal control of spiking neurons. *J. Math. Biol.*, 7(6):2466–2470, 2011.

[98] J. Nagumo, S. Arimoto, and S. Yoshizawa. An active pulse transmission line simulating nerve axon. *Proc. IRE*, 50:2061–2070, 1962.

[99] Takashi Nishikawa, Natali Gulbahce, and Adilson E. Motter. Spontaneous reaction silencing in metabolic optimization. *PLoS Computational Biology*, 4(12):e1000236, 2008.

[100] M. Ortmanns. Charge balancing in functional electrical stimulation: A comparative study. In *Proc. of IEEE International Symposium on Circuits and Systems*. IEEE, May 2007.

[101] G. V. Osipov, J. Kurths, and C. Zhou. *Synchronization in Oscillatory Networks*. Springer-Verlag, Berlin, 2007.

[102] E. Ott, J. H. Platig, T. M. Antonsen, and M. Girvan. Echo phenomena in large systems of coupled oscillators. *Chaos*, 18:037115, 2008.

[103] C. Park, R. M. Worth, and L. L. Rubchinsky. Neural dynamics in parkinsonian brain: The boundary between synchronized and nonsynchronized dynamics. *Physical Review E*, 83:042901, 2011.

[104] A. Peressini, F. Sullivan, and J. Uhl. *Mathematics of Nonlinear Programming*. Springer, 2000.

[105] L. Perko. *Differential equations and dynamical systems*. Texts in applied mathematics. Springer, New York, 2 edition, 1991.

[106] A. Pikovsky, M. Rosenblum, and J. Kurths. *Synchronization: A Universal Concept in Nonlinear Science*. Cambridge University Press, 2001.

[107] L. S. Pontryagin, V. G. Boltyanskii, R. V. Gamkrelidze, and E. F. Mishchenko. *The Mathematical Theory of Optimal Processes*. John Wiley & Sons, Inc., 1962.

[108] A. J. Preyer and R. J. Butera. Neuronal oscillators in aplysia californica that demonstrate weak coupling in vitro. *Physical Review Letters*, 95(13):4, 2005.

[109] R Rose and J Haindmarsh. The assembly of ionic currents in a thalamic neuron i. the three-dimensional model. *Proc. R. Soc. Lond. B*, 237:267–28, 1989.

[110] I. Ross and Fariba Fahroo. Legendre pseudospectral approximations of optimal control problems. In Wei Kang, Carlos Borges, and Mingqing Xiao, editors, *New Trends in Nonlinear Dynamics and Control and their Applications*, volume 295 of *Lecture Notes in Control and Information Sciences*, pages 327–342. Springer Berlin / Heidelberg, 2003.

[111] C. G. Rusin, H. Kori, I. Z. Kiss, and J. L. Hudson. Synchronization engineering: tuning the phase relationship between dissimilar oscillators using nonlinear feedback. *Philosophical Transactions of the Royal Society A-Mathematical Physical And Engineering Sciences*, 368(1918):2189–2204, 2010.

[112] J Ruths and J.-S. Li. Optimal control of inhomogeneous ensembles. *IEEE Transactions on Automatic Control: Special Issue on Control of Quantum Mechanical Systems (in press)*.

[113] J. Ruths and J.-S. Li. A multidimensional pseudospectral method for optimal control of quantum ensembles. *Journal of Chemical Physics*, 134:044128, 2011.

[114] J. Ruths, A. Zlotnik, and J.-S. Li. Convergence of a pseudospectral method for optimal control of complex dynamical systems. In *50th IEEE Conference on Decision and Control*, Orlando, FL, December 2011.

[115] S. Sastry and R. Montgomery. The structure of optimal controls for a steering problem. In *Proc. IFAC Symposium on Nonlinear Control Systems*, 1992.

[116] S. Schattler and U. Ledzewicz. *Geometric Optimal Control*, volume 38 of *Interdisciplinary Applied Mathematics*. Springer, 1 edition, 2012.

[117] Steven J. Schiff, Kristin Jerger, Duc H. Duong, Taeun Chang, Mark L. Spano, and William L. Ditto. Controlling chaos in the brain. *Nature*, 370:615–620, 1994.

[118] D. Shanno and P. Kettler. Optimal conditioning of quasi-newton methods. *Mathematics of Computation*, 24(111):657–664, 1970.

[119] SJ Smith. Lebesgue constants in polynomial interpolation. *Annales Mathematicae et Informaticae*, 33(109-123):1787–5021, 2006.

[120] D. Stefanatos, H. Schaettler, and J.-S. Li. Minimum-time frictionless atom cooling in harmonic traps. *SIAM Journal on Control and Optimization*, 49(6):2440–2462, 2011.

[121] Dionisis Stefanatos and Jr-Shin Li. Constrained minimum-energy optimal control of the dissipative bloch equations. *Systems & Control Letters*, 59(10):601–607, 2010.

[122] Dionisis Stefanatos and Jr-Shin Li. Antiphase synchronization of phase-reduced oscillators using open-loop control. *Phys. Rev. E*, 85:037201, Mar 2012.

[123] S. Strogatz. *Nonlinear Dynamics And Chaos: With Applications To Physics, Biology, Chemistry, And Engineering*. Studies in nonlinearity. Westview Press, 1 edition, 2001.

[124] H. J. Sussmann. *Time-Optimal Control in the Plane, in Feedback Control of Linear and Non-linear Systems, Lecture Notes in Control and Information Sciences*. Springer-Verlag, Berlin, 1982.

[125] H. J. Sussmann. The structure of time-optimal trajectories for single-input systems in the plane: The c^∞ nonsingular case. *SIAM J. Control Optim.*, 25:433–465, 2004.

[126] Gabor Szego. *Orthogonal Polynomials*. American Mathematical Society, New York, 1959.

[127] J. C. Bettencourt T. I. Netoff, C. D. Acker and J. A. White. Beyond two-cell networks: experimental measurement of neuronal responses to multiple synaptic inputs. *Journal Of Computational Neuroscience*, 18(3):287–295, 2005.

[128] P. A. Tass. *Phase Resetting in Medicine and Biology*. Springer, New York, 1999.

[129] P. A. Tass. A model of desynchronizing deep brain stimulation with a demand-controlled coordinated reset of neural subpopulations. *Biological Cybernetics*, 89:81–88, 2003.

[130] David Taylor and Philip Holmes. Simple models for excitable and oscillatory neural networks. *J. Math. Biol.*, 37:419–446, 1998.

[131] H. Tuckwell and J. Feng. Optimal control of neuronal activity. *Phys. Rev. Lett.*, 91:018101, 2003.

[132] P. J. Uhlhaas and W. Singer. Neural synchrony in brain disoders: Relevance for cognitive dysfunctions and pathophysiology. *Neuron*, 52:155–168, 2006.

[133] G. W. Whitehead. *Elements of homotopy theory*. Springer, 1978.

[134] M. Wickramasinghe and I. Z. Kiss.

[135] A. Winfree. *The Geometry of Biological Time*. Springer, New York, 2 edition, 2001.

[136] A. T. Winfree. *The Geometry of Biological Time*. Springer-Verlag, New York, 1980.

[137] T. Wyckhuys, P. J. Geerts, R. Raedt, K. Vonck, W. Wadman, and P. Boon. Deep brain stimulation for epilepsy: knowledge gained from experimental animal models. *Acta Neurol. Belg.*, 109:62–80, 2009.

[138] Y. Zhai, I. Z. Kiss, and J. L. Hudson. Control of complex dynamics with time-delayed feedback in populations of chemical oscillators: Desynchronization and clustering. *Ind. & Eng. Chem. Res.*, 47(10):3502–3514, 2008.

[139] A. Zlotnik and J.-S. Li. Optimal asymptotic entrainment of phase-reduced oscillators. In *Proc. ASME Dynamic Systems and Control Conf. (Arlington, VA)*, pages 479–84. ASME, 2011.

[140] A. Zlotnik and J.-S. Li. Optimal entrainment of neural oscillator ensembles. *J. Neural Eng.*, 9:046015, 2012.

Vita

Isuru Sammana Dasanayake

Degrees

Ph.D. Electrical and Systems Engineering, Washington University in St. Louis, USA, May 2013
M.Sc. Systems Science and Mathematics, Washington University in St. Louis, USA, May 2009
B.Sc.Eng Electrical & Electronic Engineering, University of Peradeniya, Sri Lanka, January 2006

Professional Societies

Student Member IEEE
Member IEEE Control Society

Journal Publications

I. Dasanayake and J.-S. Li, Design of Charge-Balanced Time-Optimal Stimuli for Spiking Neuron Oscillators, *Journal of Neural Engineering (under review).*

I. Dasanayake and J.-S. Li, Charge-Balanced Minimum-Power Controls for Spiking Neuron Oscillators, *IEEE Transaction on Automatic Control (first revision under review).*

J.-S. Li, **I. Dasanayake** and J. Ruths, Control and Synchronization of Neuron Ensembles, *IEEE Transaction on Automatic Control (accepted).*

I. Dasanayake and J.-S. Li, Optimal design of minimum-power stimuli for phase models of neuron oscillators, *Physical Review E*, 83 pp. 061916, 2011.

A. Nanayakkara and **I. Dasanayake**, Analytic semiclassical energy expansions of general polynomial potentials, *Physics Letter A*, 294 pp. 158-162, 2002.

Refereed Conference Publications

I. Dasanayake and A. Zlotnik and W. Zhang and J.-S. Li, Optimal Control of Neurons Using the Homotopy Perturbation Method, 52^{th} *IEEE Conference on Decision and Control*, December 10-13, 2013, Florence, Italy *(under review).*

I. Dasanayake and J.-S. Li, Charge-Balanced Time-Optimal

Control for Spiking Neuron Oscillators, 51^{th} *IEEE Conference on Decision and Control*, December 10-13, 2012, Maui, Hawaii, USA.

I. Dasanayake, J.-S. Li, Constrained Minimum-Power Control of Spiking Neuron Oscillators, 50^{th} *IEEE Conference on Decision and Control*, December 12-15, 2011, Orlando, Florida, USA.

I. Dasanayake, I.E. Naqa, J.-S. Li, Constrained Kalman Filter- ing for IMRT Optimization, 49^{th} *IEEE Conference on Decision and Control*, December 15-17, 2010, Atlanta, Georgia, USA.

I. Dasanayake, I.E. Naqa, J.-S. Li, Dynamic System Approach for Real-Time IMRT Optimization, 52^{nd} *Annual Meeting of the American Association of Physicists in Medicine*, July 18 - 22, 2010 ,Philadelphia, Pennsylvania, USA.

I. Dasanayake, H.M.P.P. Kummara, L.A.D.S.D. Thelisinghe, P.I. Muthukumarana, Single Phase Digital Power Meter, *The Institution of Engineers, Sri Lanka* 99^{th} *Annual Sessions* ,Oct. 2005, Sri Lanka.

J.V. Wijayakulasooriya, **D.M.I.S. Dasanayake**, P.I. Muthukumarana, H.M.P.P. Kummara, L.A.D.S.D. Thelisinghe, Remotely Accessible Single Phase Energy Measuring System, *First International Conference on Industrial and Information System*, August 2006, Peradeniya, Sri Lanka.

May 2013